

© 2007 by Steven Kyle McKay. All rights reserved.

LATERAL PREDICTION OF DEPTH-AVERAGED VELOCITY IN  
COMPOUND OPEN CHANNELS

BY

STEVEN KYLE MCKAY

B.S., Colorado State University, 2005

THESIS

Submitted in partial fulfillment of the requirements  
for the degree of Master of Science in Civil Engineering  
in the Graduate College of the  
University of Illinois at Urbana-Champaign, 2007

Urbana, Illinois

## ABSTRACT

Although flow in compound channels is three-dimensional, most engineering applications treat the flow as one-dimensional, neglecting the non-uniform distribution of velocity in the cross section. If spatial variation of velocity within a cross-section is accounted for, it is often by using correction coefficients (e.g., the Coriolis and Boussinesq coefficients,  $\alpha$  and  $\beta$ ), which are not easily quantified. Two-dimensional depth-averaged models for compound channels (developed using the continuity and momentum equations), while available, are not practicable for widespread use. Therefore, a simple to use model for predicting the lateral distribution of depth-averaged velocity would be beneficial to many aspects of science and engineering (e.g., flow measurement; stream restoration; sediment transport; etc.). Herein, dimensional analysis and experimental data from previous studies are used to develop two models for predicting depth-averaged velocity distributions across the width of straight, compound channels with uniform roughness. The first model requires velocity data to calibrate model coefficients, whereas the second model relies on prescribed relations for coefficients. The first model reproduced 95% of depth-averaged velocities within 10% of observed values, and the second model reproduced 78% of predicted values within 10% of observed depth-averaged velocities when the model was applied to the data with which it was calibrated. The second model was applied to experimental conditions beyond the calibration limits and was found to reasonably reproduce the velocity distribution for channels near to calibration conditions and poorly reproduce the velocity distribution for channels very different than those used in calibration. For this reason, the first model is recommended when sufficient depth-

averaged velocity data exist, and caution should be exercised in extrapolation of the second model beyond the calibration range. Application of the second model to discharge prediction provided an accurate, physically-based tool for index velocity rating that required no calibration. The second model was also applied to examination of compound channel flow structure and was found to be practicable for qualitatively assessing the location and width of the shear layer.

## ACKNOWLEDGEMENTS

The following work presents my maiden voyage into the realm of research. The research process has been very stimulating and has challenged me in ways that I did not know existed. Outside of the mental stimulus, the process has been very personally rewarding because of the many wonderful individuals with whom I have had the pleasure of working and playing. Without the contributions of these people and many others, this work could not have come to fruition. I would therefore like to acknowledge those who have directly or indirectly contributed to this work.

As my advisor, Professor Arthur Schmidt has guided me through much this research. Through his patience, knowledge of the field, and willingness to spend time working with me, he has helped me arrive at my goal. His ability to continually push me and force me to think on my own has provided me a strong foundation in water resources research. Thank you, Dr. Schmidt.

As my co-advisor, Professor Gregory Wilkerson has also been critically involved in this work, and I am very grateful for his involvement. This research is inspired by a paper of Dr. Wilkerson's, and his participation in this project was both crucial and enjoyable. His willingness to take time and discuss many of the important aspects of the research will not soon be forgotten. Thank you Dr. Wilkerson. Dr. Wilkerson is affiliated with the STC Program of the National Science Foundation via the National Center for Earth-surface Dynamics (NCED) under agreement number EAR-0120914, and I would like to thank NCED for Dr. Wilkerson's time.

My academic journey to the completion of this thesis has been facilitated by many influential educators. My professors at Colorado State University encouraged me to

attend graduate school and helped me form a basic understanding of water resources engineering which has proven very valuable in this process. Professors at the University of Illinois extended this basic understanding in leaps and bounds. Many thanks are due to these patient, wonderful individuals involved in my education.

Many universities, agencies, and individuals have provided data for this thesis. Without the abundant amount of experimentation in compound channel flow, the empirically based approach used in this work could not have been utilized. The team of researchers working in the Flood Channel Facility at the University of Birmingham has been very cooperative in providing much of the data for this thesis on their website. Among these researchers I would especially like to thank Drs. Donald Knight, Koji Shiono, Peter Wormleaton, Alan Ervine, Robert Myers, and Galip Seckin. Steve Maynard of the Army Corps of Engineers and Kirk Thibodeaux of the United States Geological Survey were instrumental in locating the Collins and Flynn (1977) large scale compound channel experiments. Without their assistance, this data set may have gone unnoticed.

I have been endlessly blessed by the kind, friendly, intelligent group of peers in the Ven Te Chow Hydrosystems Laboratory. In particular I'd like to thank my office mates Nils Oberg, Francisco Pedocchi, Blake Landry, Robert Haydel, Octavio Sequeiros, and Ezequiel Martin for the many lively discussions and fun office atmosphere. I would also like to thank all of the students working in Dr. Schmidt's research group: Matt Hoy, Josh Cantone, Dan Hollander, Corrie Bondar, Dan Christensen, Dan Gambill, cLaudia Crosar, and the undergraduate researchers. This research group made my time in Illinois a pleasure both inside and outside of the office. There are too many others in the lab to

thank, but everyone has been instrumental in making my graduate experience wonderful.

Thank you all!

I would especially like to thank Dan Christensen for helping me deposit my thesis remotely. With you I'm not sure how I would have deposited. Thanks!

Finally I'd like to thank my family and friends who have supported me in all of my endeavors inside and outside of the classroom. My Mom, Sandra Knight, and Dad, Jim McKay, have given me never-ending support and encouragement in all of my endeavors. These two people have served as parents, role models, mentors, and friends, and I thank you for always being there for me. Many thanks are also due to my girlfriend, Amy Walker, for her role as my companion throughout this process. She has been patient with me while I worked on this project, provided an outlet for me when I needed to vent, and stood by me every step of the way. Thank you, Amy. Many more friends and family have provided support and encouragement for me, and I thank you all for your time and love.

# TABLE OF CONTENTS

LIST OF FIGURES .....	x
LIST OF TABLES .....	xii
LIST OF SYMBOLS .....	xiii
1 INTRODUCTION .....	1
1.1 <i>Introductory Remarks</i> .....	1
1.2 <i>Literature Review</i> .....	3
1.2.1 Theoretical Considerations of Open Channel Flow .....	3
1.2.2 Prediction of Velocity in Open Channels .....	8
1.2.3 Flow Structure of Compound Channels .....	12
1.2.4 Experimental Investigation of Compound Channel Flow .....	13
1.2.5 Overview of Compound Channel Analysis .....	21
1.2.6 Beyond Straight compound channels .....	31
1.3 <i>Objectives and Scope of Research</i> .....	33
2 MODEL DEVELOPMENT .....	35
2.1 <i>Dimensional Analysis</i> .....	37
2.1.1 Parameter Selection .....	37
2.1.2 Analysis of Flow in a Compound Channel .....	41
2.1.3 Simplification of the Compound Channel Flow Problem .....	42
2.2 <i>Mathematical Model</i> .....	43
3 DATA USED IN MODEL DEVELOPMENT .....	47
4 DATA ANALYSES AND RESULTS .....	52
4.1 <i>General, Calibratable Model</i> .....	52
4.2 <i>Continuously-Varying Parameter Model</i> .....	56
4.2.1 Application of Continuously Varying Model to Calibration Data .....	62
4.2.2 Validation of Continuously Varying Model .....	64
4.2.3 Extension Beyond Model Calibration Range .....	65
4.3 <i>Model Comparison</i> .....	74
4.4 <i>Discussion</i> .....	76
5 APPLICATION I – DISCHARGE PREDICTION .....	78
5.1 <i>Use of the Continuously Varying Model for Predicting Discharge</i> .....	79
5.1.1 Model Application to Calibration Range .....	80
5.1.2 Extension beyond Model Calibration Range .....	83
5.2 <i>Discussion of Discharge Prediction</i> .....	84



6	APPLICATION II – PREDICTION OF SHEAR LAYER LOCATION AND	
	WIDTH IN COMPOUND CHANNELS.....	86
6.1	<i>Derivation of a Model for Shear Layer Width and Location.....</i>	87
6.2	<i>Estimation of Shear Layer Width and Location.....</i>	90
7	SUMMARY AND RECOMMENDATIONS.....	94
7.1	<i>Summary .....</i>	94
7.2	<i>Recommendations .....</i>	96
7.2.1	Model Improvement.....	96
7.2.2	Applications of Model .....	98
	BIBLIOGRAPHY .....	99
	APPENDIX A: MODEL RESULTS .....	114

# LIST OF FIGURES

Figure 1.1. The “Floodplain Syndrome” (from Knight, 2006a) .....	1
Figure 1.2. Flow Structure in a Compound Channel (Shiono and Knight, 1991) .....	2
Figure 1.3. Vector Definition of Flow in Open Channels.....	6
Figure 1.4. Discharge adjustment factors for Compound Channel (Ackers, 1993).....	25
Figure 2.1. “Typical” depth-averaged velocity distributions in Compound Channels (Figure titles and labels refer to series and test labels explained in Chapter 3).....	36
Figure 2.2. Zonal approach to modeling depth-averaged velocity in Compound Channels.....	36
Figure 2.3. Schematic of Compound Channel geometry .....	39
Figure 4.1. Development of Compound Channel wide floodplain criteria.....	53
Figure 4.2. Depth-averaged velocity distribution predicted by Equation 2.9 for test case FCF-020501 .....	54
Figure 4.3. Results of Equation 2.9 as displayed observed and predicted velocities .....	55
Figure 4.4. Exponential model of coefficient $a_1$ with relative depth, $D_r$ .....	58
Figure 4.5. Residuals resulting from Equation 4.1 .....	58
Figure 4.6. Boxplot of coefficients $a_2$ and $a_3$ .....	60
Figure 4.7. Model of coefficient $a_4$ with relative depth, $D_r$ .....	61
Figure 4.8. Residuals resulting from Equation 4.2 .....	61
Figure 4.9. Continuously varying model results for data used in calibration .....	63
Figure 4.10. Continuously varying parameter model results for validation data.....	64
Figure 4.11. Results of the continuously-varying parameter model as applied to channels of low main channel aspect ratio .....	66
Figure 4.12. Depth-averaged velocity distribution as predicted by the CV and general models for JB-02-A-02 ( $R^2 = 0.574$ and $0.988$ , respectively) .....	66
Figure 4.13. Results of the continuously varying parameter model as applied to channels with narrow floodplains .....	67
Figure 4.14. Depth-averaged velocity distribution as predicted by the CV and general models for S-03-240 ( $R^2 = 0.876$ and $0.999$ , respectively).....	68
Figure 4.15. Results of the CV model as applied to large, vegetated channels .....	69
Figure 4.16. Depth-averaged velocity distribution as predicted by the CV and general models for CF-206-10, ( $R^2 = 0.203$ and $0.896$ , respectively).....	69
Figure 4.17. Comparison of prescribed model coefficient $a_1$ to data beyond the project scope .....	71
Figure 4.18. Comparison of prescribed model coefficient $a_2$ to data beyond the project scope .....	72
Figure 4.19. Comparison of prescribed model coefficient $a_3$ to data beyond the project scope .....	72
Figure 4.20. Comparison of the prescribed model coefficient $a_4$ to data beyond the project scope .....	73
Figure 4.21. Depth-averaged velocity distribution of FCF-020402 as computed by different methods .....	75
Figure 4.22. Results of various models for predicting depth-averaged velocity distributions (test case FCF-020402).....	75

Figure 5.1. Results of prediction of cross-sectional mean velocity by multiple velocity rating models.....	81
Figure 5.2. Absolute error of multiple index velocity relations.....	82
Figure 5.3. Results of the CV model as applied to data beyond the project scope.....	84
Figure 6.1. Compound channel shear layer schematic .....	86
Figure 6.2. Results of application of the CV Model to estimation of shear layer location and width.....	91
Figure 6.3. Relative location of shear layer .....	92
Figure 6.4. Dimensionless shear layer width, $\delta b_{top}$ .....	93
Figure A.1. Depth-averaged velocity distribution for S-03-221.....	116
Figure A.2. Depth-averaged velocity distribution for S-03-224.....	116
Figure A.3. Depth-averaged velocity distribution for S-03-227.....	117
Figure A.4. Depth-averaged velocity distribution for S-03-230.....	117
Figure A.5. Depth-averaged velocity distribution for FCF-010201 .....	118
Figure A.6. Depth-averaged velocity distribution for FCF-010301 .....	118
Figure A.7. Depth-averaged velocity distribution for FCF-010401 .....	119
Figure A.8. Depth-averaged velocity distribution for FCF-010501 .....	119
Figure A.9. Depth-averaged velocity distribution for FCF-010601 .....	120
Figure A.10. Depth-averaged velocity distribution for FCF-010701 .....	120
Figure A.11. Depth-averaged velocity distribution for FCF-020201 .....	121
Figure A.12. Depth-averaged velocity distribution for FCF-020301 .....	121
Figure A.13. Depth-averaged velocity distribution for FCF-020401 .....	122
Figure A.14. Depth-averaged velocity distribution for FCF-020501 .....	122
Figure A.15. Depth-averaged velocity distribution for FCF-020601 .....	123
Figure A.16. Depth-averaged velocity distribution for FCF-020701 .....	123
Figure A.17. Depth-averaged velocity distribution for FCF-020801 .....	124
Figure A.18. Depth-averaged velocity distribution for FCF-030201 .....	124
Figure A.19. Depth-averaged velocity distribution for FCF-030301 .....	125
Figure A.20. Depth-averaged velocity distribution for FCF-030401 .....	125
Figure A.21. Depth-averaged velocity distribution for FCF-030501 .....	126
Figure A.22. Depth-averaged velocity distribution for FCF-080201 .....	126
Figure A.23. Depth-averaged velocity distribution for FCF-080301 .....	127
Figure A.24. Depth-averaged velocity distribution for FCF-080401 .....	127
Figure A.25. Depth-averaged velocity distribution for FCF-080501 .....	128
Figure A.26. Depth-averaged velocity distribution for FCF-080601 .....	128
Figure A.27. Depth-averaged velocity distribution for FCF-080701 .....	129
Figure A.28. Depth-averaged velocity distribution for FCF-100201 .....	129
Figure A.29. Depth-averaged velocity distribution for FCF-100301 .....	130
Figure A.30. Depth-averaged velocity distribution for FCF-100401 .....	130
Figure A.31. Depth-averaged velocity distribution for FCF-100501 .....	131
Figure A.32. Depth-averaged velocity distribution for FCF-100601 .....	131
Figure A.33. Depth-averaged velocity distribution for FCF-100701 .....	132
Figure A.34. Depth-averaged velocity distribution for FCF-100801 .....	132
Figure A.35. Depth-averaged velocity distribution for FCF-010602 .....	133
Figure A.36. Depth-averaged velocity distribution for FCF-020402 .....	134

## LIST OF TABLES

Table 1.1. Summary of Pioneer Studies of Straight Compound Channels.....	14
Table 1.2. Summary of Small Scale (Flume Width < 2m) Laboratory Investigation of Straight Compound Channels.....	16
Table 1.3. Summary of Large Scale (Flume Width = 10m) Laboratory Investigation of Straight Compound Channels.....	18
Table 1.4. Summary of Field Measurement of Straight Compound Channels.....	19
Table 1.5. Summary of Divided Channel Methods (DCM).....	24
Table 1.6. Summary of Elder Formulations for Eddy Viscosity Models used in the Lateral Distribution Method in Compound Channels.....	29
Table 1.7. Summary of other Eddy Viscosity Models applied to Compound Channels ..	30
Table 1.8. Summary of alternative Compound Channel studies .....	31
Table 2.1. Flow properties .....	38
Table 2.2. Fluid properties .....	38
Table 2.3. Channel geometry and channel properties.....	40
Table 3.1. Laboratory Data Used in this Study.....	47
Table 3.2. Geometric properties of tests used in this study .....	49
Table 3.3. Dimensionless properties of tests used in this study.....	50
Table 3.4 Dimensionless properties of data available for model calibration.....	51
Table 4.1. Data sets used in validation of Equation 2.9.....	54
Table 4.2. Data sets used in calibration of the continuously varying model .....	57
Table 5.1. Error in prediction of cross-sectional mean velocity for multiple velocity indexing models.....	83
Table A.1. Depth-averaged velocity distribution statistics for calibration data .....	115
Table A.2. Depth-averaged velocity distribution statistics for validation data.....	133

## LIST OF SYMBOLS

$a_i$	Model coefficients for the logistic model developed in this study
$A$	Total cross-sectional area
$b_i$	Model coefficients for the model of Wilkerson and McGahan (2005)
$b_{ch}$	Main channel half width to toe of main channel slope
$b_{fp}$	Width of floodplain
$b_{top}$	Distance from channel centerline to top of main channel bank
$B$	Channel half width to toe of floodplain slope
$c_i$	Coefficients of empirical index velocity relations
COH	Coherence used in Ackers Method
CV	Continuously varying parameter model
$C_z$	Chezy resistance coefficient
DCM	Divided Channel Method
DISADF	Discharge Adjustment Factor used in Ackers Method
$D_r$	Relative depth $(= (h_{tot} - h_{ch}) / h_{tot})$
EPSRC	Engineering and Physical Science Research Council
$f$	Darcy-Weisbach resistance coefficient
$f_1(z)$	Logistic function developed in this study
$f_2(z)$	Wilkerson and McGahan (2005) function adapted to this study
FCF	Flood Channel Facility
$F_r$	Froude number
$g$	Acceleration due to gravity
$g_i$	Gravitational acceleration vector
$h_{ch}$	Bankfull height of main channel
$h_{fp}$	Depth of flow on the floodplain
HIF	Hydrologic Instrumentation Facility of the USGS
$h_{tot}$	Depth of flow in main channel
$k$	Turbulent kinetic energy
$k_n$	Manning's unit conversion factor (1 for SI units, 1.486 for English units)
$k_s$	Roughness height
LDM	Lateral Distribution Method
$M$	Measure of entropy in model of Chiu et al. (1987, 1989)
$n$	Manning resistance coefficient
$P$	Total wetted perimeter of cross-section
$Q$	Volumetric rate of discharge
$R$	Hydraulic radius $(= A/P)$
$R^2$	Coefficient of determination
RANS	Reynolds Averaged Navier-Stokes Equations
$Re$	Reynolds number
$s_{ch}$	Main channel side slope (1: $s_{ch}$ , vertical: horizontal)
$s_{fp}$	Floodplain side slope (1: $s_{fp}$ , vertical: horizontal)
SCM	Single Channel Method
SERC	Science and Engineering Research Council
SKM	Shiono and Knight Method
$S_0$	Longitudinal bed slope

$S_{0z}$	Lateral bed slope
$S_w$	Longitudinal surface water slope
$T_{ij}$	Depth-averaged turbulent stress
$u'$	Turbulent perturbations of the streamwise velocity to the mean
$u_i'$	Turbulent perturbations of the velocity to the mean in the i-direction
$u_{max}$	Maximum point velocity in channel
$U$	Temporally averaged streamwise component of velocity
$U_d(z)$	Depth-averaged/depth-mean velocity at lateral location $z$
$U_i$	Temporally averaged component of velocity in the i-direction
$U_{index}$	Index depth-averaged velocity
USGS	United States Geological Survey
$U_0$	Cross-section averaged velocity
$U_{0,fp}$	Cross-section averaged velocity of the floodplain only
$v'$	Turbulent perturbations of the vertical velocity to the mean
$V$	Temporally averaged vertical component of velocity
$w'$	Turbulent perturbations of the lateral velocity to the mean
$W$	Temporally averaged lateral component of velocity
$W_e$	Weber number
$x$	Streamwise/longitudinal coordinate
$x_i$	Channel coordinate in the i-direction
$y$	Vertical coordinate
$z$	Lateral/transverse coordinate
$z_{a,WM}$	Lateral location of the asymptotic solution of the Wilkerson and McGahan (2005) model
$z_c$	Critical breakpoint between the two functions utilized in this study
$z_{ib}$	Lateral location of the inner bound of the shear layer
$z_{ob}$	Lateral location of the outer bound of the shear layer
$\alpha$	Coriolis coefficient
$\beta$	Boussinesq coefficient
$\delta$	Shear layer width
$\delta_{ij}$	Kronecker matrix
$\varepsilon$	Defect in depth-averaged velocity profile from asymptotic value
$\gamma$	Specific weight of water
$\lambda$	Dimensionless eddy viscosity
$\mu$	Dynamic viscosity of water
$\nu$	Kinematic viscosity of water
$\nu_t$	Eddy viscosity
$\rho$	Density of water
$\tau_b$	Bed shear stress
$\tau_{ij}$	Stress tensor
$Y$	Surface tension of water
$\Omega$	Dimensionless planform shape factor
$\xi$	Independent variable of Chiu et al. (1987, 1989)

# 1 INTRODUCTION

## 1.1 *Introductory Remarks*

Rivers serve as lifelines for modern civilization due to the many benefits they offer people, namely: water for consumptive purposes (household, irrigation, industrial, etc.), cost effective transportation and trade routes, environmentally friendly power sources, and rich biological life. Thus, societies have developed close to rivers, many times directly in their floodplains. As these settlements have grown, they have continued to develop the area which previously served as a buffer for flow events exceeding a river's banks (overbank discharges or floods); this has been dubbed the "Floodplain Syndrome" (Knight, 2006a).

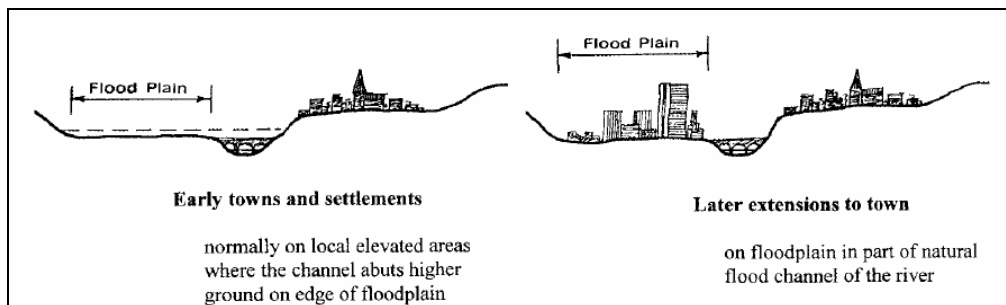


**Figure 1.1. The "Floodplain Syndrome" (from Knight, 2006a)**

In recent years, floods are responsible for almost a third of all natural disasters by quantity and economic loss, and more importantly they are to blame for over half of the lives lost (Berz, 2000). Consequently, river scientists are often charged with alleviating and/or predicting the impacts of floods. Large flow events, however, are a natural process of the hydrologic flow regime and cannot be avoided. Therefore, the task of the river engineer is to obtain a greater understanding of the processes driving the flow so that reliable warning systems can be put in place and damages minimized.

Although overbank flow is fundamentally governed by the same mechanisms that govern the flow of water within the banks of the river, the geometric complexities associated with a compound (or two-stage) channel drastically increase the difficulty in assessing the flow of water over a floodplain. During inbank flows, the streamwise velocity is primarily affected by the roughness exerted on the flow by the banks and the bed. As illustrated in Figure 1.2, the complex geometry associated with compound channels induces more complex processes that alter the streamwise velocity profile, namely, mass and momentum transfer between the channel and floodplain, large scale vortices from the shear between two streams of differential velocity, secondary currents, and different roughness scales in the floodplain and main channel.

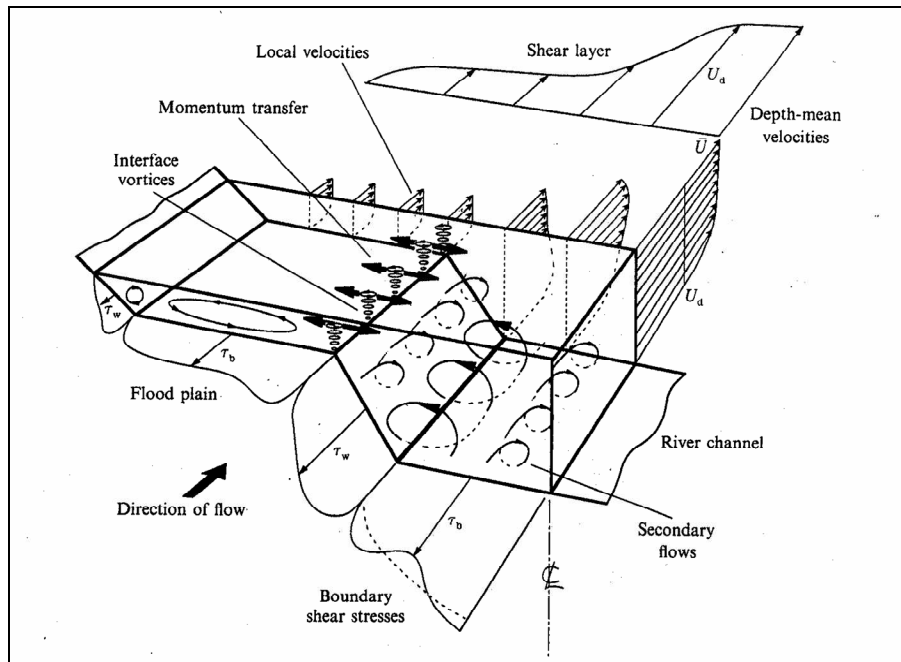


**Figure 1.2. Flow Structure in a Compound Channel (Shiono and Knight, 1991)**

Accurate information about the distribution of velocity in open channels is of great use in many hydraulic analyses. Ideally prediction of the complete three-dimensional velocity vector at any point in the flow would be the most useful source of



information and would most accurately define the velocity distribution in the channel, but this is impractical due to computational difficulties, time limitations, cost, and difficulty of use in basic engineering analyses. It will be demonstrated that a simple model for the lateral prediction of streamwise depth-averaged velocity would provide a useful tool for numerous hydraulic analyses.

## ***1.2 Literature Review***

The section reviews the literature describing the current state-of-the-art in understanding compound channel flow. This review intends to: review the basic theoretical considerations of open channel flow, explore current models for prediction of velocity in open channels, outline the mechanisms driving the complex flow structure of straight, compound channels, review a brief history of compound channel hydraulics and experimentation, and analyze current approaches for modeling velocity in compound channels. This review is intended to present a framework for the research presented in this document, not to be a comprehensive review of the literature. However, if the reader is interested in a complete review of open channel, and more specifically compound channel, hydraulics, Knight and Shiono (1996) and Knight (2006b), present extensive reviews of the literature.

### **1.2.1 Theoretical Considerations of Open Channel Flow**

This section reviews the governing equations of fluid flows in one, two, and three dimensions.

### Three-dimensional Flow

The Navier-Stokes equations for incompressible flow provide an instantaneous description of the flow of fluid with a constant density and viscosity. The momentum and continuity equations are expressed in tensor notation as:

$$\frac{\partial u_i}{\partial t} + u_j \frac{\partial u_i}{\partial x_j} = -\frac{1}{\rho} \frac{\partial p}{\partial x_i} + \nu \frac{\partial^2 u_i}{\partial x_j \partial x_j} + g_i$$

**Equation 1.1**

$$\frac{\partial u_i}{\partial x_i} = 0$$

**Equation 1.2**

Where  $u_i$  is the component of velocity in the  $i$ -direction,  $x_i$  is the coordinate in the  $i$ -direction,  $\rho$  is the density of the fluid,  $\nu$  is the kinematic viscosity of the fluid, and  $g_i$  is the gravitational acceleration vector (Refer to Figure 1.3).

These equations provide an exact, instantaneous solution to the fluid flow, but turbulent fluctuations in the flow make an exact solution difficult to use. Therefore the momentum and continuity equations are averaged over the turbulent fluctuations ( $u_i = U_i + u'_i$ ) to obtain the three-dimensional (3-D) Reynolds-Averaged Navier-Stokes equations (RANS).

$$\frac{\partial U_i}{\partial t} + U_j \frac{\partial U_i}{\partial x_j} + \frac{\partial \overline{u'_i u'_j}}{\partial x_j} = \frac{1}{\rho} \frac{\partial \tau_{ij}}{\partial x_i} + g_i$$

**Equation 1.3**

$$\frac{\partial U_i}{\partial x_i} = 0$$

**Equation 1.4**

Where  $U_i$  is the temporally averaged component of velocity in the i-direction,  $u'_i$  is the turbulent fluctuation of velocity about this temporal mean, and  $\tau_{ij}$  is the stress tensor accounting for both the pressure and viscosity terms of the Navier-Stokes equations.

This equation can be resolved in physical terms as:

$$\text{Inertia of Flow} = \text{Forces acting on Flow}$$

or

$$\text{Temporal Acceleration} + \text{Local Acceleration} + \text{Turbulent (Reynolds) Stresses} = \text{Stress} \\ \text{(due to pressure and viscosity)} + \text{Gravitational Effects}$$

In many applications, such as rivers, the resolution of the three-dimensional velocity vector is not necessary, and the streamwise components of momentum may be the only components of concern. The RANS model for longitudinal momentum combines with the continuity equation to produce:

$$\frac{\partial U}{\partial t} + V \frac{\partial U}{\partial y} + W \frac{\partial U}{\partial z} + \frac{\partial \overline{u'v'}}{\partial y} + \frac{\partial \overline{u'w'}}{\partial z} = \frac{1}{\rho} \left( \frac{\partial \tau_{xx}}{\partial x} + \frac{\partial \tau_{xy}}{\partial y} + \frac{\partial \tau_{xz}}{\partial z} \right) + gS_0$$

**Equation 1.5**

Where  $x$ ,  $y$ , and  $z$  are the streamwise, vertical, and lateral directions, respectively,  $U$ ,  $V$ , and  $W$  are the temporally averaged components of velocity in the  $x$ ,  $y$ , and  $z$  directions, and  $u'$ ,  $v'$ , and  $w'$  are the turbulent fluctuations of velocity in the  $x$ ,  $y$ , and  $z$  directions, respectively (Refer to Figure 1.3).

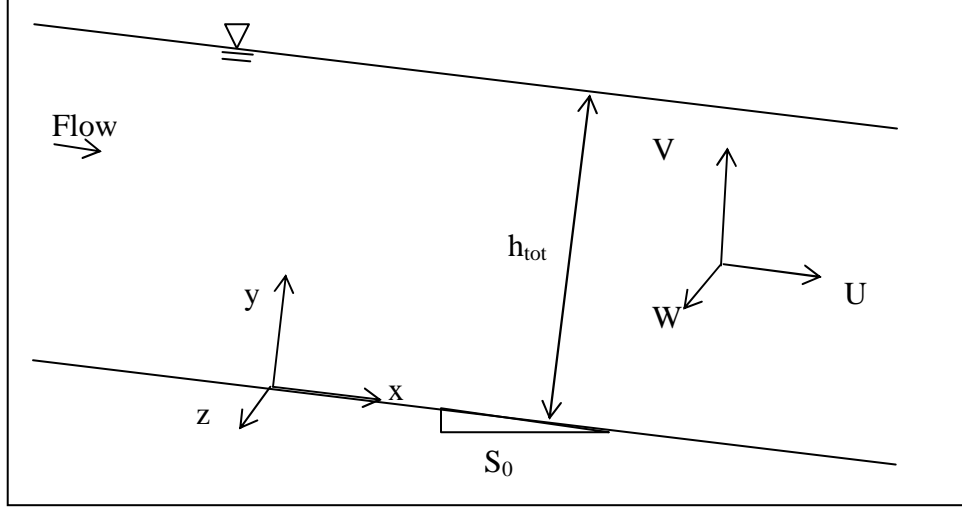


**Figure 1.3. Vector Definition of Flow in Open Channels**

This equation models the streamwise flow in three dimensions; however, difficulties arise in implementation of this equation for even the simplest of flow scenarios. In many applications of interest, the assumption of steady, uniform flow where turbulent stresses dominate is appropriate. This further simplifies Equation 1.5 to the following:

$$\rho \left( \frac{\partial UV}{\partial y} + \frac{\partial UW}{\partial z} + \frac{\partial \overline{u'v'}}{\partial y} + \frac{\partial \overline{u'w'}}{\partial z} \right) = \rho g S_0$$

**Equation 1.6**

Although the complete Navier-Stokes equations have been greatly simplified, this equation is still difficult to solve, and the resolution of the velocity profile for most engineering applications could be expressed by simpler one or two dimensional models.

### **Two-dimensional Flow**

If the lateral distribution of velocity is of concern, the model must be integrated over the depth to obtain a more useful format. By depth-averaging Equation 1.6 in the

direction normal to the bed,  $y$ , an even more simplified model is obtained for steady, uniform flow (Bousmar and Zech, 2004).

$$\rho g h_{tot} S_0 + \frac{\partial h_{tot} T_{xz}}{\partial z} - \tau_b \sqrt{1 + S_{0z}^2} = \frac{\partial}{\partial z} \int_{h_{tot}} \rho U W dy$$

**Equation 1.7**

Where  $h_{tot}$  is the depth of flow,  $T_{xz}$  is the depth-averaged turbulent shear stress,  $\tau_b$  is the bed shear stress, and  $S_{0z}$  is the lateral slope of the bed.

This equation can be resolved in physical terms as:

Gravitational Forces + Turbulent Stresses – Resistive Forces = Secondary Currents.

The turbulent (or Reynolds) stresses are commonly modeled with various eddy viscosity models explained later in section 1.2.5.

### **One-dimensional Flow**

If Equation 1.6 is integrated over the area instead of the depth, the problem simplifies to a one-dimensional equation with a single parameter accounting for all resistance. Commonly applied 1-D equations for steady, uniform flow are: Chezy, Manning, and Darcy-Weisbach equations (Equation 1.8-Equation 1.10, respectively):

$$U_0 = C_z \sqrt{R S_0}$$

**Equation 1.8**

$$U_0 = \frac{k_n}{n_m} R^{2/3} S_0^{1/2}$$

**Equation 1.9**

$$U_0 = \left( \frac{8g}{f} \right)^{1/2} \sqrt{RS_0}$$

**Equation 1.10**

In which  $C_z$ ,  $n_m$ , and  $f$  are all resistance coefficients,  $k_n$  is a unit correctional factor (1 for S.I. units, 1.486 for English units),  $R$  is the hydraulic radius ( $A/P$ ),  $A$  is the cross-sectional area, and  $P$  is the wetted perimeter.

Although these equations coarsely represent the entire resistance to flow as one lumped parameter, they provide quick estimates of velocity for use in practical engineering applications.

### **1.2.2 Prediction of Velocity in Open Channels**

The governing equations describing flow velocity in open channels have been presented in the previous section. Solution of these equations provides the distribution of velocity in open channels; however, as will be displayed in the following section, these equations do not offer the only method of determining the distribution of velocity in open channels.

#### **Empirical Approximation of Velocity in Channels of Simplified Geometry**

There exist many methods of determining the vertical distribution of velocity in “wide” open channels (width/depth ratio is greater than approximately 5 – 10, Yalin, 1971; Chow, 1959) from logarithmic and power laws (Streeter and Wylie, 1975). The resolution of the vertical distribution of velocity is useful in approximating the flow in open channels, but many channels are not “wide” and effects of side boundaries are pronounced. Therefore, methods exist to resolve the lateral distribution of depth-

averaged velocity in open channels with geometric approximations of cross-sectional shape (rectangular, trapezoidal, parabolic, etc.).

Channels are often assumed to have rectangular geometry. The lateral distribution of velocity in these channels can be approximated as constant throughout the lateral domain,  $U_d \cong U_0$  (Wilkerson, 2007). This approximation is generally applicable except in the region very near the side boundaries. This relation would work acceptably in “wide” channels, where wall effects are not of concern. However, this equation is not likely to represent the flow well in “narrow” channels.

Natural channels are also commonly assumed to have trapezoidal cross-sectional geometry. The distribution of depth-averaged velocity in such channels was investigated by Wilkerson and McGahan (2005). They made use of dimensional analysis and experimental data to develop a set of empirical models of depth-averaged velocity in trapezoidal channels where effects of the channel side slope are pronounced. Their study suggests the use of two nonlinear asymptotic models: one that is general and requires velocity data for parameter calibration (Equation 1.11) and one that has prescribed coefficients and does not require calibration (Equation 1.12). These models define the velocity distribution in a trapezoidal channel by assuming symmetry in the velocity distribution.

$$\frac{U_d(z)}{U_0} = b_0 - b_1 \exp\left(b_2 \frac{z - b_{ch}}{h_{tot} s_{ch}}\right)$$

**Equation 1.11**

$$\frac{U_d(z)}{U_0} = (1 + 0.104 s_{ch}) - (0.125 s_{ch}) \exp\left(2.24 s_{ch}^{-0.582} \frac{z - b_{ch}}{h_{tot} s_{ch}}\right)$$

**Equation 1.12**

Where  $z$  is the lateral location in the channel as measured from the channel centerline,  $U_d(z)$  is depth-averaged velocity at any lateral point  $z$ ,  $b_{ch}$  is the lateral distance of the toe of the bank slope from the channel centerline,  $h_{tot}$  is the total depth of flow,  $s_{ch}$  is the cotangent of the bank slope, and  $b_i$  are constants.

In the context of this report, Equation 1.12 is used in the following form:

$$\frac{U_d(z)}{U_{ref}} = 1 - \frac{0.125s_{ch}}{1 + 0.104s_{ch}} \exp\left(2.24s_{ch}^{-0.582} \frac{z - b_{ch}}{h_{tot}s_{ch}}\right)$$

**Equation 1.13**

Where  $U_{ref} = U_0(1 + 0.104s_{ch})$  and represents the asymptotic depth-averaged velocity toward the center of a trapezoidal channel.

Wilkerson and McGahan (2005) report results from the first model (Equation 1.11) of having high agreement with experimental data with coefficients of determination ( $R^2$ ) from 0.84 to 0.90. The second model (Equation 1.12) also yielded high correlation coefficients ( $R^2=0.86$ ). The authors recommend using the first model whenever velocity data are available for calibration.

## Entropy Approach

Another approach to estimating the distribution of streamwise velocity is the entropy maximization approach of Chiu et al. (1987, 1988, 1989, 1991). Chiu et al. (1987, 1989) present the following equation for solution of the velocity distribution in a channel cross-section:

$$u = \frac{u_{max}}{M} \ln \left[ 1 + (e^M - 1) \frac{\xi - \xi_0}{\xi_{max} - \xi_0} \right]$$

**Equation 1.14**



Where  $u$  is the velocity at  $\xi$ ,  $\xi$  is an independent variable which develops with  $u$ ,  $\xi_0$  and  $\xi_{max}$  are the minimum and maximum values of  $\xi$  that correspond to  $u = 0$  and  $u = u_{max}$ , respectively, and  $M$  is a measure of entropy.

This method of velocity prediction has proven to produce accurate results on multiple occasions (Chiu et al. 1987, 1988, 1989, 1991, 1996) and has been utilized in applications such as sediment transport (Chiu et al., 2000).

### **Energy Transport through Relative Minimum Distance**

Another model for velocity distribution prediction is that of Yang and Lim (1997) whose model is based on the concept of “energy transportation through a minimum relative distance toward the nearest boundary” (Yang et al., 2004). This model presents an analytical solution to the velocity and shear stress. The model has been adapted to compound channels and approximations have been determined to account for discontinuities as the channel exceeds its banks (Yang et al., 2004).

### **Summary**

As presented, models exist to predict the distribution of velocity in open channels other than the solution of the complete Navier-Stokes equations. In many cases these models have been developed with simplicity in mind and can be quickly used to estimate velocity in open channels. Some of these models have been adapted to compound channels, but in doing so either the complexity in application increases or the resolution of velocity decreases. Therefore, a simple model for prediction of the lateral velocity distribution in compound channels is needed.

### 1.2.3 Flow Structure of Compound Channels

The previous sections have outlined some of the methods of assessing the distribution of velocity in a channel through analytical and empirical methods. When a river overtops its banks, the geometry of the river and the complexity of the flow increase dramatically, causing many of the conventional approaches to fail. Expansion onto the floodplains increases the wetted perimeter and therefore the amount of water in contact with roughness elements. Furthermore, in many natural systems the floodplains are significantly rougher than the main channel (e.g. forested banks of a sand bed river). This increase in roughness causes a velocity differential between the main channel and floodplain regions. This difference in velocity causes a strong lateral shear across the region around the main channel and floodplain interface (Figure 1.2).

The shear created by these velocity differentials cause many forms of turbulence and further increases the friction within the flow (Zheleznyakov, 1965). This shear also generates large vertical vortices along the interface between the main channel and floodplain and induces an imbalance in the Reynolds stresses which leads to secondary flows in the channel (Sellin, 1964; Deuller, Toebe, and Udeozo, 1967; Udeozo, 1967). All of these factors combine to produce mass and momentum exchange across the main channel-floodplain interface (Figure 1.2).

The combination of secondary flows, large scale vortices, increased roughness, and mass and momentum exchange lead to a reduction in the discharge capacity of the channel. Zheleznyakov (1965) termed this reduction the “kinematic effect.”

All of these mechanisms of motion have been described for straight, compound channels. Obviously with increased complexity in planform geometry (e.g.,

meandering), lateral flow mechanisms introduce further complexity. This review will, therefore, focus on straight compound channels.

#### **1.2.4 Experimental Investigation of Compound Channel Flow**

As displayed, compound channel flow is complex. Quantification of these complex processes is of utmost importance to improve compound channel design; therefore the flow mechanisms of compound channels have been studied at great detail. The following section reviews some of the significant efforts in quantifying the mechanisms of flow in straight, compound channels in both the laboratory and the field.

##### **Pioneering Investigations**

Initial investigations of compound channels were not as concerned with the distribution of velocity in the channels, but instead the influence of this channel geometry on backwater computation (Lansford and Mitchell, 1949). Following these investigations, a flurry of concurrent research was conducted into the discharge capacity of compound channels.

Initial investigations of discharge capacity of channels with compound cross-sections were conducted in the U.S.S.R. in the late 1940's and 1950's. These studies were conducted by Zheleznyakov in 1947-1948 in both laboratory and field settings. He found that there was a reduction in discharge capacity as channels exceeded their banks. Agasieva and Barekryan confirmed Zheleznyakov's findings in their 1958-1959 experiments (Zheleznyakov, 1965).

At the same time, key experimental observations of compound channel flow structure were being made in laboratory facilities in Northern Ireland (Sellin, 1964). By

adding aluminum powder to a compound channel flume, Sellin was able to photographically record planform vortices between the main channel and floodplain. Sellin attributed these vortices to differences in floodplain and main channel velocity and believed there to be strong secondary current influence on the flow.

Whilst the experiments in Russia and England were being conducted, experiments at Purdue University were initiated (Udeozo, 1967). These experiments were conducted in a laboratory model of a compound channel with rectangular, compound geometry and varying roughness conditions. Working independently of the previously mentioned researchers, Udeozo also notes the presence of vertical vortices and secondary currents.

These three sets of independent laboratory studies all concluded that there was a reduction in discharge capacity as stage exceeded the banks of the river. They also all noted the importance of shear induced secondary currents in two-stage channels. The following sections provide an overview of compound channel research to quantify these mechanisms at multiple laboratory scales and in the field.

**Table 1.1. Summary of Pioneer Studies of Straight Compound Channels**

<b>Author</b>	<b>Year</b>	<b>Comment</b>
Lansford and Mitchell	1949	Investigated the backwater effects of compound channels in the laboratory
Zheleznyakov	1947, 1948	Described flow mechanism and discharge capacity of compound channels in laboratory and field settings
Agasieva and Barekryan	1958-1959	Performed laboratory experiments in compound channels
Sellin	1964	Described and photographically recorded flow structure in compound channels
Udeozo	1967	Measured velocity in compound channels of varying roughness and described flow structure of compound channels

## **Small Scale Laboratory Research**

After the pioneers of the field described the complex flow mechanisms and difficulties associated with modeling flow in two-stage channels, there was an explosion of research to quantify the effects of these mechanisms. Many models of compound channels were constructed in small laboratory flumes (Flume Width < 2 m). These include studies in asymmetric and symmetric flumes (Refer to Table 1.2). These studies mainly focused on collection of velocity and boundary shear stress data in compound channel flumes, but two of them extended their work to include turbulence measurements (Elsawy, McKee, and McKeogh, 1983; Tominaga and Nezu, 1991). Further experimental compound channel flow studies were conducted at small scales with a different fluid medium, air (Refer to Table 1.2). While other studies have also been conducted in small laboratory flumes, this list is presented merely to provide an example of the plethora of compound channel studies conducted at the laboratory scale.

The measurement and experimentation at this scale provided the scientific community with data necessary to begin calibration of numerical models for discharge, velocity, and shear stress prediction. These data also allowed for further refinement of the description of flow processes in compound channels. The computational methods stemming from these studies will be discussed in a later section of this review.

**Table 1.2. Summary of Small Scale (Flume Width < 2m) Laboratory Investigation  
of Straight Compound Channels**

<b>Author</b>	<b>Year</b>	<b>Comment</b>
<u>Small Scale Laboratory Experiments in Asymmetric Compound Channels</u>		
Myers and Elsayy	1975	Interaction of channel and floodplain significantly alters the shear stress distribution
James and Brown	1977	Dimensionless velocity distributions displayed dynamic similarity
Myers	1978	Momentum transfer is critical to flow structure
Rajaratnam and Ahmadi	1981	Dynamic similarity of lateral distribution of depth-averaged velocity
Tominaga and Nezu	1991	LDA turbulence measurements
<u>Small Scale Laboratory Experiments in Symmetric Compound Channels</u>		
James and Brown	1977	Dimensionless velocity distributions displayed dynamic similarity
Rajaratnam and Ahmadi	1979	Dynamic similarity of lateral distribution of depth-averaged velocity
Wormleaton et al.	1982	Apparent shear stress differs across division planes
Elsawy et al.	1983	Quantification of shear layer mixing via hot film anemometry
Knight and Demetriou	1983	Existence of a depth dependent "apparent shear force" between the main channel and floodplain
Knight and Hamed	1983	Introduction of four dimensionless ratios relevant to discharge prediction - $B/b_{ch}$ , $D_r$ , $n_{fp}/n_{ch}$ , $b_{ch}/h_{ch}$
Asano et al.	1985	Dimensionless parameters such as channel width to depth ratio have a "great influence" over the channel-floodplain interaction
Myers	1990	Scale model of River Main
Seckin	2004	Examination of fixed and mobile beds and smooth and rough floodplains
<u>Compound Channel Experiments in Wind Tunnels</u>		
Wright and Carstens	1970	Apparent shear stress on division plane is the same order of magnitude as the boundary shear
Rhodes and Knight	1994, 1995	Secondary flows present on floodplain even in low relative depth conditions

## **Large Scale Laboratory Studies**

As evident, the quantity of data for compound channels was growing rapidly by the late 1980s, but all of the data had been collected in small laboratory flumes and questions about the importance of scale were beginning to be raised. A collaboration of researchers in the United Kingdom recognized the potential differences between the laboratory and field scales and with the funding of the Science and Engineering Research Council (SERC), now the Engineering and Physical Sciences Research Council (EPSRC), constructed a large scale compound channel research facility at the University of Birmingham. This facility, the Flood Channel Facility (FCF), is large enough to reduce scale effects as far as possible in the laboratory setting. The flume measures 56m in length, 10m in width, and has a discharge capacity of  $1.08\text{m}^3/\text{s}$  (Knight and Sellin, 1987). The research efforts using this flume have been divided into four major divisions. Phase A was focused on straight, compound channels with rigid beds and varying geometry. Phase B was focused on rigid bed meandering compound channels in straight floodways. Phase C was focused on straight, compound channels with mobile beds. Phase D is focused on meandering channels with mobile beds (Knight and Sellin, 1987).

These experiments all were for steady, uniform flow conditions. In these experiments, detailed velocity and bed shear stress measurements were recorded in both vertical and lateral directions. In select experiments turbulence was measured using Laser Doppler Anemometry. Refer to Table 1.3.

The resulting set of detailed data collected with the cooperation of many researchers provided the scientific community with a robust set of data to which

numerical and analytical observations can be compared, and this study should be commended for its thorough examination of compound channels.

**Table 1.3. Summary of Large Scale (Flume Width = 10m) Laboratory Investigation of Straight Compound Channels**

Author	Year	Comment
Knight and Sellin	1987	Introduction of Flood Channel Facility and research objectives
Wormleaton and Merret	1990	Discharge estimation through various techniques
Elliot and Sellin	1990	FCF skewed floodplain experiments
Knight and Shiono	1990	Turbulence measurements in shear layer indicate that shear layer spreading onto the floodplain decreases with increasing depth
Myers and Brennan	1990	Flow resistance properties of FCF

### **Field Scale Laboratory Studies**

In the 1970s the United States Geological Survey (USGS) Hydrologic Instrumentation Facility (HIF) conducted experiments at the “field scale.” Their Floodplain Simulation Facility, which measures approximately 1371 m long and 91 m wide and has a discharge capacity of  $6.4 \text{ m}^3/\text{s}$ , provided a scale typical of small natural channels. In this facility the USGS-HIF conducted experiments on steady and unsteady flows for varying vegetated roughness conditions (Collins and Flynn, 1978, 1979).

### **River Measurements**

Along with the controlled laboratory conditions, observations of natural environments were necessary to verify that computational methods being developed were applicable regardless of scale. Such field observations of overbank flows are often costly and difficult to collect, resulting in the relatively small amount of field work reported in



the literature. Extensive field measurements are limited to a few rivers in the United Kingdom and the United States.

Wark, Slade and Ramsbottom (1991) report velocity distributions in various rivers throughout the U.K. Included in these measurements are a few of the many field observations that have been made on the River Severn. This river has been a source of much of the available velocity data in natural channels. In recent years Babaeyan-Koopaei et al. (2002) and Carling et al. (2002) have measured turbulence on the River Severn using an Acoustic Doppler Velocimeter.

Another set of detailed field data comes from the River Main in Northern Ireland, which has been altered to create a compound channel with relatively uniform geometry (Martin and Myers, 1991; Johnston and Higginson, 1991).

In the United States few channels have been used in compound channel analyses and calibration of compound channel models. Although many rivers exhibit compound channel geometry, few studies of velocity in these channels have been reported. One channel that has been used in compound channel velocity studies is Salt Creek at Greenvew, Illinois (Bhowmik and Demissie, 1982). The distribution of velocity in this channel has been observed by the USGS for multiple stages and discharges.

**Table 1.4. Summary of Field Measurement of Straight Compound Channels**

Author	Year	Comment
Bhowmik and Demissie	1982	Conducted a field study of the Salt Creek at Greenvew, IL and the channel's compound nature during flood events
Wark et al.	1991	Report velocity distributions in rivers throughout the United Kingdom
Martin and Myers	1991	Conducted field studies of the River Main in a reach altered to have compound channel geometry
Johnston and Higginson	1991	
Babaeyan-Koopaei et al.	2002	Collected velocity and turbulence data for the River Severn
Carling et al.	2002	

## **Summary of Compound Channel Data**

Studies of flow in compound channels have been conducted on multiple scales and provide a large quantity of data to use in analysis of such channels. In laboratory studies the possibility of scale effects related to roughness and turbulence issues continues to arise (Schoemaker, 1991; Ackers, 1991). Also of concern is the complete development of flow in the laboratory setting. Although the uniform flows considered in laboratories were allowed to become fully developed based on boundary layers, this is not the only type of flow development that needed to be considered. Bousmar et al. (2005) suggested that the distribution of discharge in compound channels may require a longer development length than that of the boundary layer.

An issue aside from the scale effects is the applicability of the geometries considered in laboratory studies. Many of the small scale studies have been conducted in rectangular channels with rectangular floodplains. Laboratory studies have also induced limitations on the width of the floodplains due to constraints of flume size. Many natural channels possess floodplains that are many times wider than the main channel (Udeozo, 1967). Morvan (2005) suggests that the extensive use of the FCF data could bias compound channel models towards channels with relatively narrow floodplains, which may not be observed in nature. The FCF was modeled in such a way as to maximize the main channel width to depth ratio and the floodplain width as well. Although the width used was as wide as possible, the widths observed in nature are significantly greater (Morvan, 2005).

Although the applicability of the large base of compound channel data has been questioned by Bousmar et al. (2005) and Morvan (2005), the array of conditions tested

provides researchers with a large quantity of data with which to test hypotheses on compound channel flow mechanisms and develop models for compound channel flow.

### **1.2.5 Overview of Compound Channel Analysis**

Analysis of velocity in straight, compound channels has taken many forms over the last 90 years. The first approximations of compound channels were to treat the channel as a single entity with a single bulk velocity. Following these methods, the channel was divided into main channel and floodplain subsections and each section was treated as a separate homogeneous unit. As computational ability and analytical understanding increased, the methods for analysis became increasingly complex. Following coarse division of the channel, the section has been divided into small vertical sections and the flow properties were considered laterally. The velocity has also been considered in all three-dimensions of the channel. Each of these methods will be explained in the following sections.

#### **Single Channel Method**

As stated above, the analysis of compound channels was first considered by treating the section as a single entity with a homogeneous equivalent roughness. Appropriate values of roughness were, however, difficult to determine. Einstein (1934) and Horton (1933) suggested the weighting of the roughness values from the main channel and floodplain to obtain a total roughness factor. This cross-section weighted resistance was then to be used in a one-dimensional equation (such as Manning's equation). Many methods have been proposed for weighting the resistance and a thorough review of these is provided by Yen (1991, 2002). These Single Channel

Methods (SCMs) were reasonable first estimates of the stage-discharge relations, but upon applying them to compound channels, it was seen that they often underestimate discharge.

Due to the ease of application of the SCM, correction of this method was pursued. Dracos and Hardegger (1987) proposed that the SCM be adjusted by altering the hydraulic radius and wetted perimeter. James and Brown (1977) suggested an alteration of the Manning equation to include overbank effects.

These single channel methods (SCMs) have been shown to provide relations between the stage and discharge that are of the correct order of magnitude for steady, uniform flow conditions. These simplistic methods cannot possibly encapsulate the complex flow mechanisms described in above sections and provide no lateral resolution of the velocity.

### **Divided Channel Method**

The next, and perhaps the most common, method of estimating compound channel flows is the Divided Channel Method (DCM). This method is generally credited to Lotter (1933) who suggested that the channel be divided into relatively homogeneous subsections and the discharge be computed in each section individually. However, Sellin (1964) alludes to the work of Houk, who's work for the Miami Conservancy district in 1918 lead him to suggest, "When the overflow area was wide and comparatively shallow, and the main channel narrow and deep...the overflow area was arbitrarily separated from the river channel and the discharge of each computed independently." Regardless of who proposed the DCM, many methods of computing the stage-discharge curve in compound

channels have been suggested that are fundamentally based on the basic DCM assumption.

The DCM produces total discharge values of reasonable accuracy, but the distribution of discharge in each subsection may be estimated poorly (Knight and Hamed, 1983; Wormleaton and Hadjipanos, 1985). Due to its desirable simplicity, many corrections of the DCM have been proposed to overcome this error in subsection discharge prediction. These corrections can be broadly classified into six groups: (1) alteration of subsection wetted perimeters; (2) introduction of different arbitrary planes of cross-section division; (3) division of the cross-section by planes of zero shear stress; (4) weighting of multiple forms of the DCM; (5) large shear stresses have been measured across the divisional planes (Myers, 1978) and methods have been proposed to estimate this “apparent” shear stress; and (6) the coherence method of Ackers (explained below). Refer to Table 1.5 for a summary of divided channel methods (DCMs).

**Table 1.5. Summary of Divided Channel Methods (DCM)**

<b>Author</b>	<b>Year</b>	<b>Comment</b>
<u>Original DCM</u>		
Lotter	1933	Division of channel for discharge computation
Houk	1918	Division of channel for discharge computation
<u>Alteration of Wetted Perimeter</u>		
Wright and Carstens	1970	Include length of division plane in wetted perimeter calculation
<u>Different Planes of Cross-section Division</u>		
Deuller et al.	1967	Horizontal planes
Posey	1967	Diagonal planes
Wright and Carstens	1970	Vertical planes
Wormleaton et al.	1982	Accuracy of different planes depend upon their ability to model apparent shear stress
Seckin	2004	Comparison of all DCM methods to Coherence method and Exchange Discharge Model
<u>Estimation of Zero Shear Stress</u>		
Yen and Overton	1973	Use the DCM with planes of zero shear stress
Yen and Ho	1983	In some cases the zero shear interface can be approximated by a diagonal division plane
<u>Weighting of Multiple DCM Forms</u>		
Lambert and Myers	1998	Weighting factor for horizontal and vertical division planes
Cassels et al.	2001	Extension of weighting to mobile bed channels
Atabay and Knight	2006	Recalibration of weighting factor for homogenously roughened channels
<u>Computation of Apparent Shear Stress</u>		
Myers	1978	Apparent shear at channel-floodplain interface is large
Ervine and Baird	1982	Formula for calculation of apparent shear stress
Wormleaton and Merret	1990	Formula for calculation of apparent shear stress
Wormleaton et al.	1982	Apparent shear stress differs across division planes
Knight and Demetriou	1983	Formula for calculation of apparent shear stress
Knight and Hamed	1983	Formula for calculation of apparent shear stress
Prinos and Townsend	1984	Formula for calculation of apparent shear stress
Noutsopoulos and Hadjipanios	1985	Apparent shear stress provides a reliable correction to the DCM
<u>Coherence Method</u>		
Ackers	1991, 1992, 1993	Method of computing compound channel discharge by correcting SCM and DCM approaches

The final method of improving the DCM is an empirical approach proposed by Ackers (1991, 1992, 1993), the coherence method. This approach corrects the DCM computed discharges to better reflect the actual distribution of discharge in the channel. It relies on two dimensionless parameters, the coherence ( $COH$ ) and the discharge adjustment factor ( $DISADF$ ). The coherence is a measure of the ability of the channel to be modeled accurately by the SCM and is defined as the ratio of the SCM computed discharge to the DCM computed discharge ( $COH = Q_{SCM}/Q_{DCM}$ ). The Discharge Adjustment Factor corrects the DCM calculated discharge to more accurately reflect the actual discharge ( $DISADF = Q_{Act}/Q_{DCM}$ ).

Using the data from the University of Birmingham Flood Channel Facility, Ackers computed the DISADF for multiple relative depths and identified four distinct regions of flow with increasing and decreasing amounts of interaction (Figure 1.4). He fit empirical functions to each region of the flow based on geometric parameters determined through dimensional analysis and proposed a sequence of calculations to determine the region of flow and therefore the discharge.

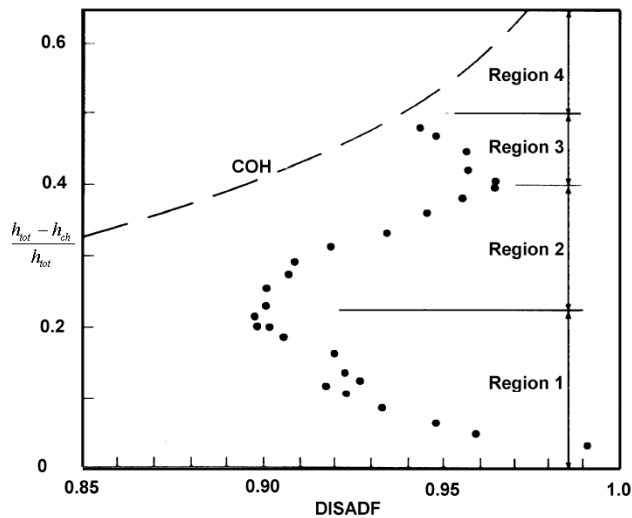


**Figure 1.4. Discharge adjustment factors for Compound Channels (Ackers, 1993)**

Although this method is highly empirical, accurate predictions of discharge by this method have been reported in both laboratory and field settings. Seckin (2004) reports that errors in discharge for fixed boundary laboratory flumes are generally less than 10% and less than 20% for mobile bed flumes. Because of this accuracy and applicability to natural rivers, the United Kingdom National River Authority now recommends the use of this method in discharge computation. The major pitfalls of this method are that it involves tedious calculation and may require some engineering judgment (Bousmar, 2002).

Although all of the DCM methods can provide accurate estimates of discharge, it comes at the cost of the resolution of the distribution of velocity. The assumption of multiple subsections with different velocities in each leads to discontinuities in velocity at the boundaries between the subsections.

### **Lateral Distribution Method (LDM)**

As noted in the previous sections, there exist many forms of stage-discharge computation with varying levels of complexity and accuracy. The SCM approaches provide estimates of discharge, but do not provide information about the distribution of depth-averaged velocity in the channel. The DCM approaches provide coarse estimates of the distribution of velocity, but these methods produce a velocity discontinuity at the channel-floodplain interface. Therefore many methods have been developed for predicting the lateral distribution of velocity in compound channels. These will herein be referred to as Lateral Distribution Methods (LDMs).

To date, most of the LDMs are based on solving the governing equations of open-channel flow through use of a turbulence-closure model (Bousmar and Zech, 2004).



Modeling of open-channel flow through turbulence-based concepts has been pursued at varying levels of complexity. Each of these models begins with simplification of the 3-D Reynolds Averaged Navier-Stokes (RANS) equations (Equation 1.3 and Equation 1.4).

In turbulent flows, the stresses due to turbulence far exceed the stresses due to molecular viscosity. This implies that the momentum equation simplifies to the following:

$$\rho \left( \frac{\partial U_i}{\partial t} + U_j \frac{\partial U_i}{\partial x_j} \right) = - \frac{\partial}{\partial x_j} \overline{\rho u_i' u_j'} + \rho g_i$$

**Equation 1.15**

Boussinesq's eddy viscosity concept assumes that the Reynolds stresses are analogous to molecular viscosity and can be modeled by Equation 1.16.

$$- \overline{\rho u_i' u_j'} = \nu_t \left( \frac{\partial U_i}{\partial x_j} + \frac{\partial U_j}{\partial x_i} \right) - \frac{2}{3} \delta_{ij} k$$

**Equation 1.16**

Where  $\nu_t$  is the eddy viscosity,  $\delta_{ij}$  is the Kronecker matrix ( $\delta_{ij} = 1$  for  $i = j$ ; and  $\delta_{ij} = 0$  for  $i \neq j$ ), and  $k$  is the turbulent kinetic energy (Bousmar, 2002).

Equation 1.5 can be used in conjunction with Equation 1.16 to define the streamwise velocity in three-dimensions. However, if 2-D resolution of the flow is desired, Equation 1.16 can be combined with Equation 1.7 to yield Equation 1.17 for steady, uniform flows:

$$\rho g h_{tot} S_0 + \frac{\partial}{\partial z} h_{tot} \left( \rho \nu_t \frac{\partial U_d}{\partial z} \right) - \tau_b \sqrt{1 + S_{0z}^2} = \frac{\partial}{\partial z} \int_{h_{tot}} \rho U_d W_d dy$$

**Equation 1.17**

Where  $U_d$  and  $W_d$  are the depth-averaged streamwise and lateral velocity, respectively.

$$U_d = \frac{1}{h_{tot}} \int_{h_{tot}} U dy$$

**Equation 1.18**

$$W_d = \frac{1}{h_{tot}} \int_{h_{tot}} W dy$$

**Equation 1.19**

The eddy viscosity is either assumed constant or modeled by a one or two equation model. These models enlist a variety of approaches to modeling the eddy viscosity and can produce the distribution of velocity in two or three dimensions. Some of the models require calibration, while others use constants obtained directly from literature. The eddy viscosity model most commonly applied in compound channels is the Elder Formulation (Table 1.6). This model is often coupled with a model for secondary flows due to the importance of these flows in compound channels. Many other eddy viscosity models have been applied to compound channels (Table 1.7). All of the models provide reasonable estimates of the distribution of velocity in compound channels; however, solutions often require complex analytical and numerical techniques.

**Table 1.6. Summary of Elder Formulations for Eddy Viscosity Models used in the Lateral Distribution Method in Compound Channels**

<b>Author</b>	<b>Year</b>	<b>Secondary Current Model</b>	<b>Comments</b>
Radojkovic and Djordjevic	1985		Numerical Solution of Elder Formulation
Knight et al.	1989		
Shiono and Knight	1988		
Wark et al.	1990		Numerical solution of Elder Formulation in terms of discharge per unit width
Wark et al.	1991		
Lyness et al.	1997		
Wormleaton	1988	Linear Eddy Viscosity Model	Model assumes eddy viscosity can be modeled as the sum of bed generated turbulence and secondary current generated turbulence. Numerical solution.
van Prooijen et al.	2005	Prandtl Mixing Length Eddy Viscosity Model	Modeled eddy viscosity as the sum of the bed generated turbulence (Elder Formulation) and secondary current generated turbulence (Prandtl Mixing Length)
Shiono and Knight	1991	Depth-Averaged secondary currents are assumed to vary linearly across the channel	Analytical Solution for linearly discretized channels (Shiono and Knight Method, SKM)
Knight and Abril	1996		Empirical calibration of SKM
Abril and Knight	2004		Successful field application of the Knight and Abril (1996) calibration
Wormleaton	1996		Used the SKM to described the importance of secondary currents in compound channels
Ervine et al.	2000	Scaled as the depth-averaged velocity	Modified the SKM with a proportionality to describe secondary flows. Model was applied to straight and meandering channels.
Babeyan-Koopaei et al.	2002		Field application of the model of Ervine et al. (2000)
Bousmar and Zech	2002, 2004	Two models: one for dispersion effects and one for other secondary currents	Combined the secondary current models of the SKM and Ervine et al. (2000) to include dispersion and other effects. The model was applied to uniform and nonuniform flows.

**Table 1.7. Summary of other Eddy Viscosity Models applied to Compound Channels**

<b>Eddy Viscosity Model</b>	<b>Author</b>	<b>Year</b>	<b>Comments</b>
Constant Eddy Viscosity	Ogink	1985	$\nu_t = 0.5 \text{ m}^{0.5}/\text{s}$ for the Rhine River
	Wilson et al.	2002	Evaluated constant eddy viscosity model for compound channels in comparison to alternative eddy viscosity models and found it lacking in accuracy.
Linear Eddy Viscosity Model	Alavian and Chu	1985	Eddy viscosity scaled with width of the shear layer and velocity differential between the main channel and floodplain
Prandtl Mixing Length	Lambert and Sellin	1996	Assumed mixing length scales as the product of depth and a constant
k- $\epsilon$ Dissipation model	Krishnappan and Lau	1986	3-D algebraic stress eddy viscosity models
	Larson	1988	
	Kawahara and Tamai	1989	
	Johnston and Higginson	1991	
	Naot et al.	1993	
	Cokljat and Younis	1995	3-D finite volume approach
	Rameshwaran and Naden	2003	
	Pezzinga	1994	3-D Non-linear k- $\epsilon$ models
	Sofialidis and Prinos	1998	
	Sofialidis and Prinos	1999	3-D k- $\omega$ model
	Keller and Rodi	1984, 1988	2-D k- $\epsilon$ models
	Radojkovic and Djordjevic	1985	
Large Eddy Simulation	Wilson et al.	2002	
	Thomas and Williams	1995	
	Bousmar and Zech	2001b, 2001c	

### 1.2.6 Beyond Straight compound channels

As displayed, there have been a large number of studies concerned with accurately modeling and predicting flow in straight, compound channels under steady, uniform flow conditions with rigid beds. While these studies are imperative for the advancement of the field, they are not the only form of experimental, numerical, or analytical research conducted in compound channel environments. Other compound channel studies have focused on skewed channels, meandering channels, vegetated channels, mobile bed channels, unsteady flow in compound channels, obstruction of compound channels by structures, and varying backwater conditions in compound channels (Table 1.8).

**Table 1.8. Summary of alternative Compound Channel studies**

Author	Year	Comment
<u>Skewed Channels</u>		
Ervine and Jasem	1989	Experimental work
Elliot and Sellin	1990	Experimental work in the FCF
Bousmar and Zech	2004, 2005a, 2005b	Narrowing floodplain experimentation and application of the Exchange Discharge Model
Proust et al.	2006	Abrupt floodplain contraction experimentation
<u>Meandering Channels</u>		
Toebe and Sooky	1967	Laboratory experimentation
James and Brown	1977	Laboratory experimentation
Ervine et al.	1993	Conceptual model of meandering channels
Greenhill and Sellin	1993	Stage-discharge prediction
Ervine et al.	2000	LDM Application to meandering channels
Wormleaton and Ewenetu	2006	Numerical model of mobile bed, meandering channels

**Table 1.8. (cont.) Summary of Alternative Compound Channel Studies**

<b>Author</b>	<b>Year</b>	<b>Comment</b>
<u>Vegetated Channels</u>		
Pasche and Rouve	1985	Experimentation and 1-D method for accounting for lateral shear between channel and floodplain
FCF Phase A	1990	FCF experiments using dowel roughened floodplains
Westwater	2001	Dowel roughened floodplain experiments
Helmio	2002	1-D unsteady flow routing through vegetated compound channels
<u>Mobile Bed Channels</u>		
FCF Phase C	2000	Mobile main channel experimentation
Cassels et al.	2001	Application of weighted DCM to mobile bed channel
Knight and Brown	2001	Application of fixed bed models to mobile bed experiments
Karamisheva et al.	2005	Sediment transport in compound channels
Atabay et al.	2005	Sediment transport in compound channels
Tang and Knight	2006	Bedforms of compound channels
<u>Unsteady Flow</u>		
Collins and Flynn	1978, 1979	Unsteady flow experiments in field scale facility with vegetative roughness
Lyness and Myers	1994	Collection of unsteady flow data on the River Main
Helmio	2002	1-D unsteady flow routing
<u>Channel Obstruction</u>		
Sturm	2006	Effects of bridge abutments in compound channels
<u>Backwater</u>		
Lansford and Mitchell	1949	M1 backwater profiles in compound channel
Yen et al.	1985	Backwater computation
Blalock and Sturm	1981	Minimum specific energy
Chaudry and Bhallamudi	1988	Critical depth prediction
Lee et al.	2002	Critical depth prediction
Kolshykin and Ghidaoui	2002	Froude number as a source of shear instability

### ***1.3 Objectives and Scope of Research***

Resolution of the lateral distribution of velocity in compound channels is needed by practitioners for a range purposes spanning from stream restoration design to channel navigation. As evident by this review of the state-of-the-art in compound channel hydraulics, there exists a significant body of work in the research of straight, compound channels. Seckin (2004) states that, “One-dimensional methods still appear to be the primary tool used by engineers for modeling the stage-discharge relationship in compound channels because of their simplicity in application, requiring less effort and fewer data.” Current LDMs use a momentum-based approach to predict velocity in compound channels (Bousmar and Zech, 2004), which is too intricate for simple analyses. Therefore the goal of this research is to develop a practicable, empirical method of predicting the lateral distribution of the streamwise depth-averaged in compound channels by dimensional analysis and verification with experimental data.

A model such as this does, however, require many assumptions to simplify the problem. The following is a list of the major assumptions of the model:

- Natural channels can be effectively represented by simplifying the channel cross-section into trapezoidal main channel and floodplain elements.
- Simple geometry channel geometry:
  - Straight, symmetric, prismatic channel geometry
  - Large width to depth ratios in the main channel and floodplain
- Steady, longitudinally uniform flow
- Homogeneous roughness conditions throughout the cross-section
- Fully turbulent, subcritical flow

Although these assumptions simplify the problem drastically, the model will still be applicable to many situations of concern to engineers. Can an empirical model accurately represent flow as complex as that of a compound channel? Empirical functions such as Acker's Coherence Method have already proven to provide accurate results in compound channels. Empirical models have also been applied to other complex flow systems with great success (e.g., Gamma distribution hydrographs, "top hat" function for density currents, etc.).

By way of dimensional analysis and the wealth of experimental data, this research aims to develop two functions for the lateral distribution of velocity in compound channels: one that is calibratable with observed velocity data and another that has prescribed coefficients generalized for many geometric conditions.



## 2 MODEL DEVELOPMENT

As presented in the previous section, many detailed experiments on the distribution of flow in compound channels have been conducted, and these experiments have provided the data necessary to calibrate a simple empirical model for the distribution of depth-averaged velocity. Trends in the distribution of velocity in compound channels provide the basis for such a model. Figure 2.1 presents “typical” depth-averaged velocity distributions obtained from multiple channel geometries for varying depths. As evident, the velocity is consistently slower on the floodplain and faster in the main channel for all depths. Similarity in the velocity distribution exists across this range of conditions, implying that an appropriate empirical model may be constructed to reproduce these trends in depth-averaged velocity.

From Figure 2.1, one could deduce that there are zones of velocity in compound channels. The first of these zones is on the floodplain, where depth-averaged velocity increases from the water’s edge and then reaches a relatively constant magnitude on the floodplain. The second zone is the shear layer, where flow velocities increase from low floodplain velocities to higher main channel velocities. The final velocity zone is in the main channel, where depth-averaged velocity reaches a relatively constant magnitude throughout the lateral domain. Figure 2.2 presents this concept of “zonal velocity.”

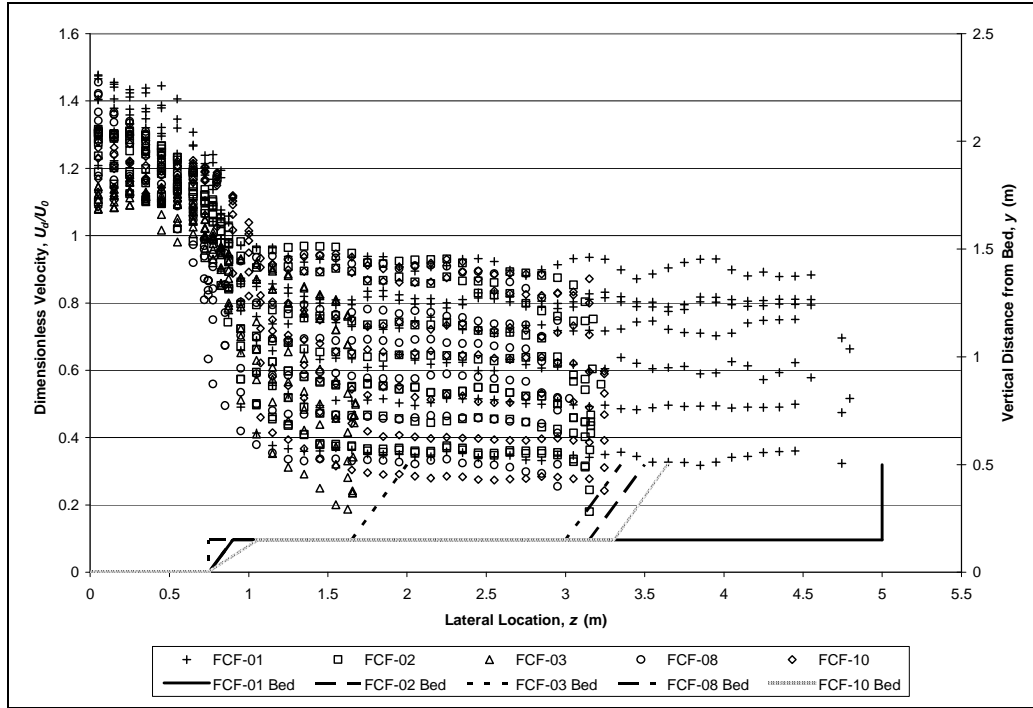


Figure 2.1. “Typical” depth-averaged velocity distributions in Compound Channels

(Figure titles and labels refer to series and test labels explained in Chapter 3)

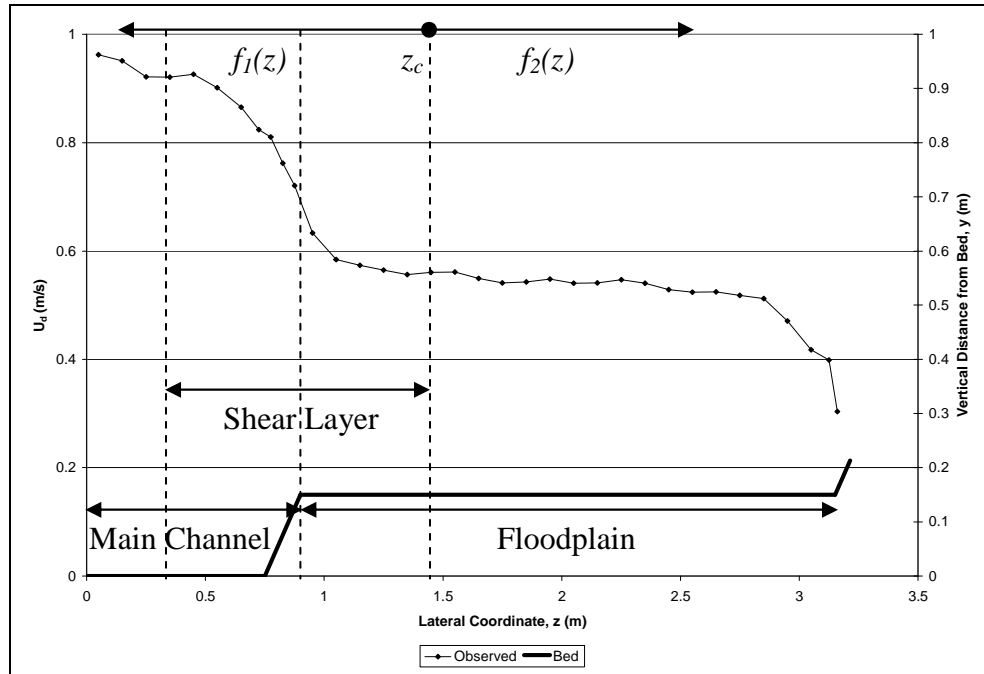


Figure 2.2. Zonal approach to modeling depth-averaged velocity in Compound Channels

This study will model the lateral distribution of depth-averaged velocity by computing the velocity in individual velocity zones. The velocity distribution in the floodplain will be computed by one function,  $f_2(z)$ , and the velocity in the shear layer and main channel will be model as a separate function,  $f_1(z)$ . The shear layer and main channel will be modeled together due to the approximately constant magnitude of depth-averaged velocity in the main channel. This modeling approach, presented in Figure 2.2, allows the distribution of velocity to be divided into two separate problems, that of the trapezoidal floodplain and that of the shear layer and main channel. Dimensional analysis will be used to determine the relevant parameters for predicting the depth-averaged velocity distribution in the main channel and shear layer. For predicting the velocity distribution on the floodplain, a modified form of the Wilkerson and McGahan (2005) function will be utilized. Methods for assessing the critical location between the functions,  $z_c$ , will also be developed.

## ***2.1 Dimensional Analysis***

“Through dimensional considerations the complexities of analysis can be greatly reduced – though by no means eliminated” (Rouse, 1959). Dimensional analysis is based on three main components: parameter selection, combination of parameters into meaningful dimensionless ratios, and the simplification of the system by means of elimination of some of these dimensionless ratios.

### **2.1.1 Parameter Selection**

According to Yen (1991), the selection of parameters influencing flow in open channels can be divided into four main categories: flow, fluid, geometry, and sediment

properties. This study focuses on rigid bed channels; thus, sediment properties are eliminated from consideration as relevant parameters.

The flow properties of the system must be defined in order to assess the depth-averaged velocity at a given lateral location,  $U_d(z)$ . The parameters necessary to adequately define the flow were found to be the volumetric rate of flow ( $Q$ ), the cross-sectional averaged velocity ( $U_0$ ), the depth of flow in the main channel ( $h_{tot}$ ), and the water surface slope, ( $S_w$ ).

**Table 2.1. Flow properties**

[L], length; [T], time; [1], dimensionless		
Symbol	Description	Dimensions
$U_d(z)$	Depth-averaged velocity	$[LT^{-1}]$
$Q$	Discharge	$[L^3T^{-1}]$
$U_0$	Cross-section averaged velocity	$[LT^{-1}]$
$h_{tot}$	Depth of flow	$[L]$
$S_w$	Water surface slope	$[1]$

The set of fluid properties considered are those necessary to adequately describe a homogenous fluid: specific weight ( $\gamma$ ) expresses the effects of gravity on the fluid, density ( $\rho$ ) describes the mass of the fluid, dynamic viscosity ( $\mu$ ) serves as a measure of the fluid resistance, and surface tension ( $Y$ ) accounts for molecular attraction of molecules in shallow flows (such as those potentially observed on the floodplain).

**Table 2.2. Fluid properties**

[L], length; [T], time; [M], mass		
Symbol	Description	Dimensions
$\gamma$	Specific weight of the fluid	$[ML^{-2}T^{-2}]$
$\rho$	Density of the Fluid	$[ML^{-3}]$
$\mu$	Dynamic viscosity of the fluid	$[ML^{-1}T^{-1}]$
$Y$	Surface Tension	$[MT^{-2}]$

Many geometric parameters are necessary to adequately define the complex geometry of a compound channel in three dimensions. However, approximation of a compound channel as a trapezoidal main channel and trapezoidal floodplain allows for definition of the vertical and lateral channel geometry with a minimum of variables. Figure 2.3 presents a schematic of a trapezoidal compound channel and the associated geometric parameters. As displayed, the origin chosen for this analysis is the intersection of the channel centerline and channel bed due to symmetry.

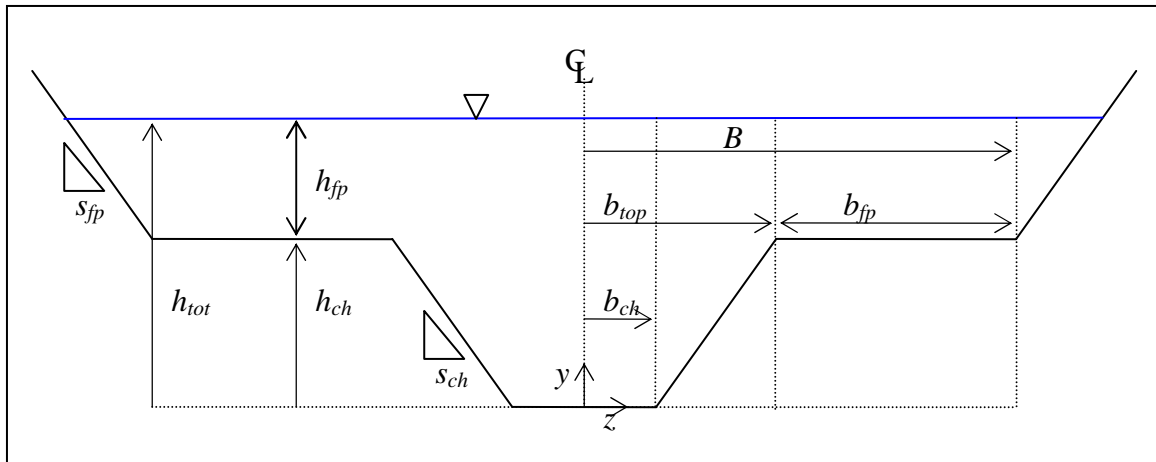


**Figure 2.3. Schematic of Compound Channel geometry**

The variables necessary to adequately define the cross-section of a compound channel are the main channel depth and half-bottom-width ( $h_{ch}$  and  $b_{ch}$ , respectively), the side slopes of the main channel and floodplain ( $s_{ch}$  and  $s_{fp}$ , respectively), and width of the floodplain ( $b_{fp}$ ). Many other useful geometry parameters may be calculated from combinations of these parameters and the known depth of flow in the main channel ( $h_{tot}$ ). Some of these parameters include the top width of the main channel ( $b_{top}$ ), the half-width to the toe of the floodplain ( $B$ ), the floodplain depth ( $h_{fp}$ ), the cross-sectional area ( $A$ ), the wetted perimeter ( $P$ ), and the hydraulic radius ( $R = A/P$ ).

The geometry parameters defined above characterize the channel from a macroscopic point of view, but one important parameter to consider exists at a much smaller scale. The roughness of the channel boundaries will be expressed as a characteristic roughness height,  $k_s$ .

Longitudinal geometry of a compound channel can be adequately defined by two parameters: the slope of the channel bed ( $S_0$ ) and a shape factor for planform changes in channel geometry ( $\Omega$ ).

**Table 2.3. Channel geometry and channel properties**

[L], length; [1], dimensionless		
Symbol	Description	Dimensions
$z$	Lateral coordinate (measured from channel centerline)	[L]
$h_{ch}$	Top of main channel (Overbank depth)	[L]
$b_{ch}$	Half width of the main channel	[L]
$B$	Half width of the floodplain	[L]
$b_{top}$	Half top width of the main channel	[L]
$b_{fp}$	Width of the floodplain	[L]
$s_{ch}$	Main channel side slope (h:v)	[1]
$s_{fp}$	Floodplain side slope (h:v)	[1]
$A$	Cross-section area for given depth	[L <sup>2</sup> ]
$P$	Wetted perimeter	[L]
$R$	Hydraulic Radius	[L]
$k_s$	Channel roughness height	[L]
$S_0$	Bed Slope	[1]
$\Omega$	Dimensionless Planform Shape Factor	[1]

Relevant variables have been identified; however, some of these variables can be eliminated to avoid redundancy in the analysis. For example, of the three variables needed to define the relation between bulk flow and the cross-section ( $Q$ ,  $U_0$ ,  $A$ ), only two are needed to adequately define the system. If variable redundancy is removed, the

parameters necessary to predict the distribution of depth-averaged velocity can be summarized as follows:

$$U_d(z) = f(Q, h_{tot}, S_w, \gamma, \rho, \mu, Y, z, h_{ch}, b_{ch}, b_{fp}, s_{ch}, s_{fp}, S_0, \Omega, k_s, A)$$

**Equation 2.1**

### 2.1.2 Analysis of Flow in a Compound Channel

The relevant parameters are nondimensionalized through scaling, and a more general solution to the problem is obtained. The relevant variables are scaled with density, kinematic viscosity,  $\nu$ , (the ratio of the dynamic viscosity to the fluid density,  $\nu = \mu/\rho$ ), and depth of flow in the main channel to remove basic dimensions of mass, time, and length, respectively.

$$\frac{U_d(z)h_{tot}}{\nu} = f\left(\frac{Q}{\nu h_{tot}}, S_w, \frac{gh_{tot}^3}{\nu}, \frac{Yh_{tot}}{\rho\nu^2}, \frac{z}{h_{tot}}, \frac{h_{ch}}{h_{tot}}, \frac{b_{ch}}{h_{tot}}, \frac{b_{fp}}{h_{tot}}, s_{ch}, s_{fp}, S_0, \Omega, \frac{k_s}{h_{tot}}, \frac{A}{h_{tot}^2}\right)$$

**Equation 2.2**

Combination and rearrangement of some of these dimensionless ratios leads to the expression of the depth-averaged velocity distribution as a function of 13 relevant dimensionless ratios of compound channel flow.

$$\frac{U_d(z)}{U_0} = f\left(R_e, F_r, W_e, \frac{S_w}{S_0}, D_r, \frac{z}{b_{ch}}, \frac{b_{fp}}{h_{fp}}, \frac{b_{ch}}{h_{ch}}, s_{ch}, s_{fp}, \Omega, \frac{k_s}{h_{tot}}\right)$$

**Equation 2.3**

Where  $R_e$  is the Reynolds number,  $F_r$  is the Froude number,  $W_e$  is the Weber number,  $D_r$  is the so-called relative depth ( $D_r = (h_{tot} - h_{ch})/h_{tot}$ ), and  $b_{fp}/h_{fp}$  is the width to depth ratio of the floodplain.

### 2.1.3 Simplification of the Compound Channel Flow Problem

The purpose of the proposed model is to predict the distribution of depth-averaged velocity in rivers; thus some of the terms are negligible because flow in rivers is generally turbulent, subcritical, and deep enough that the effects of surface tension are negligible ( $Re \gg 10^5$ ,  $Fr < 1$ ,  $We \gg 1$ , respectively) (White, 2003). For this analysis a straight channel is assumed to be under uniform flow conditions with uniform relative roughness throughout the cross-section  $\left( \Omega \approx 1, \frac{S_w}{S_0} \approx 1, \frac{k_s}{h_{tot}} \approx \frac{k_s}{h_{tot} - h_{ch}} \right)$ . These final two conditions are not commonly found in nature, but these assumptions have been made in order to simplify an extremely complex problem. With these simplifications and assumptions, the problem is reduced to a set of dimensionless ratios that are both physically meaningful and relevant to the problem considered.

$$\frac{U_d(z)}{U_0} = f\left(D_r, \frac{z}{b_{ch}}, \frac{b_{fp}}{h_{fp}}, \frac{b_{ch}}{h_{ch}}, s_{ch}, s_{fp}, \right)$$

**Equation 2.4**

This analysis assumes that the distribution of depth-averaged velocity in compound channels can be predicted by modeling the distribution of velocity in two separate regions: the main channel/shear layer region and floodplain. The assumption of a region of laterally uniform flow in the main channel occurs in channels that are wide enough for the effects of the side slopes to be significantly reduced; that is,  $b_{ch}/h_{ch}$  must be greater than 3-5, (Yalin, 1979; Chow, 1959). The flow must also be able to obtain lateral uniformity in the floodplain in order for the assumption of velocity zones to hold true. Although coarse, this assumption of wide main channels and floodplains holds true



of most natural systems (Morvan, 2005) and allows for the division of the problem into main channel/shear layer and floodplain components.

If only flow in the main channel and shear layer are considered, the floodplain width and side slope become negligibly important. The absolute position in the channel is not as important as the relative position in the channel; thus, the lateral coordinate is given a reference of the top of the floodplain,  $b_{top}$ , and the depth-averaged velocity distribution can be simplified into the following terms:

$$\frac{U_d(z)}{U_0} = f_1 \left( D_r, \frac{z - b_{top}}{b_{top}}, s_{ch} \right)$$

**Equation 2.5**

## **2.2 Mathematical Model**

From the preceding dimensional analysis, functional forms of the depth-averaged velocity distribution have been obtained for the main channel/shear layer region. This functional form is useful for qualitative assessment of compound channels, but mathematical forms of this relation must be obtained in order to gain a quantitative tool for assessment of the depth-averaged velocity distribution in compound channels.

A form of the logistic function (Equation 2.6) has been chosen to model the depth-averaged velocity distribution in the main channel/shear layer region. This function provides a nonlinear, asymptotic solution to defining the distribution of depth-averaged velocity in the main channel and shear layer.

$$f_1(z) = \frac{U_d(z)}{U_0} = \frac{a_1}{1 + a_2 e^{\frac{a_3(z - b_{top})}{b_{top}}}} + a_4$$

**Equation 2.6**

Where  $a_1$ ,  $a_2$ ,  $a_3$ , and  $a_4$  are model coefficients.

Recalling from section 1.2.2, Wilkerson and McGahan (2005) developed an empirical model for predicting depth-averaged velocity distributions in trapezoidal channels. Equation 1.13 has been adapted to model flow on the trapezoidal floodplain (Equation 2.7) by altering the reference location ( $B$ ) and the relevant parameters ( $h_{fp}$ ,  $s_{fp}$ ).

$$\frac{U_d(z)}{U_{ref}} = 1 - \frac{0.125s_{fp}}{1 + 0.104s_{fp}} \exp\left(2.24s_{fp}^{-0.582} \frac{z - B}{h_{fp}s_{fp}}\right)$$

**Equation 2.7**

As a reference velocity, Wilkerson and McGahan (2005) use the cross-section averaged velocity in the trapezoidal channel. For compound channels, the asymptotic floodplain velocity is used as the reference velocity because the influence of the side slopes on the cross-section averaged velocity in a “wide” floodplain is relatively small. This asymptotic velocity is determined from Equation 2.6 as the depth-averaged velocity at the outer edge of the shear layer,  $U_d(z_c)$ , as defined in Figure 2.2 (Criteria for defining  $z_c$  will be identified in the paragraphs that follow.). The advantage of this approach is that it requires continuity of depth-averaged velocity between the functions. Substitution of this reference velocity into Equation 2.7 leads to a model for the lateral distribution of depth-averaged velocity in trapezoidal floodplains (Equation 2.8).

$$\frac{U_d(z)}{U_d(z_c)} = 1 - \frac{0.125s_{fp}}{1 + 0.104s_{fp}} \exp\left(2.24s_{fp}^{-0.582} \frac{z - B}{h_{fp}s_{fp}}\right)$$

**Equation 2.8**

The Wilkerson and McGahan (2005) model is applicable only for  $1 \leq s_{fp} \leq 3$ .

Therefore, for channels with vertical or nearly vertical side walls ( $s_{fp} \leq 1$ ), another

estimate of depth-averaged velocity must be formulated. The depth-averaged velocity outside the shear layer is approximated as  $U_d(z_c)$ . This is expected to function well except very in the floodplain side slope (Wilkerson, 2007).

Either the adapted Wilkerson and McGahan (2005) model (Equation 2.8) or the assumption of constant floodplain velocity can be coupled with the logistic model (Equation 2.6) to predict the depth-averaged velocity distribution in a compound channel as shown in Figure 2.2. The complete model for depth-averaged velocity in compound channels can thus be expressed as Equation 2.9. This model requires measured velocity data for calibration of the model coefficients.

$$U_d(z) = \begin{cases} U_0 \left( \frac{a_1}{1 + a_2 e^{\frac{a_3(z-b_{top})}{b_{top}}}} + a_4 \right) & ; z \leq z_c \\ U_d(z_c) \left( 1 - 0.125 s_{fp} e^{\frac{2.24 s_{fp}^{-0.582} (z-B)}{s_{fp} h_{fp}}} \right) & ; z > z_c, \quad 1 \leq s_{fp} \leq 3 \\ U_d(z_c) & ; z > z_c, \quad s_{fp} < 1 \end{cases}$$

**Equation 2.9**

In order for the model to be utilized, a method must be specified to identify the critical point between the two functions,  $z_c$ . This critical point has been defined as the lateral location where  $f_1(z)$  is approximately equal to its asymptotic solution ( $f_1(z = \infty) = a_4$ ). Due to the asymptotic nature of the logistic function, a criterion must be set when the function is approximately equal to this asymptotic value. The criterion is defined as the point where the depth-averaged velocity is 0.1% greater than the

asymptotic value,  $a_4 \left( \frac{U_d(z_c)}{U_0} = 1.001a_4 \right)$ . The logistic model (Equation 2.6) may then be

rearranged to obtain a simple relation for the critical point between the two functions,  $z_c$ .

$$z_c = b_{top} + \frac{b_{top}}{a_3} \ln \left( \frac{\frac{a_1}{0.001a_4} - 1}{a_2} \right)$$

### Equation 2.10

In order for the system to be within the scope of this work, the floodplain must be sufficiently wide to develop a region of laterally uniform depth-averaged velocity on the floodplain. To assess whether the floodplain is sufficiently wide, the approximate asymptotic solution to both functions must be obtained. Using a criterion similar to that used in developing  $z_c$ , the asymptotic solution of the adapted Wilkerson and McGahan (2005) model is  $\frac{U_d(z_{a,WM})}{U_d(z_c)} = 0.999$ , where  $z_{a,WM}$  is the location of the approximate asymptotic solution to the WM model. The floodplain is deemed sufficiently wide for this analysis as long as  $z_{a,WM} > z_c$ .

### 3 DATA USED IN MODEL DEVELOPMENT

The model presented in Equation 2.9 can be calibrated for any symmetric compound channel with uniform roughness given sufficient depth-averaged velocity data ( $U_d(z)$ ), channel geometry parameters ( $b_{ch}$ ,  $b_{fp}$ ,  $s_{ch}$ ,  $s_{fp}$ ,  $h_{ch}$ ), and hydraulic characteristics of the system ( $U_0$ ,  $h_{tot}$ ). As presented in section 1.2.4, many studies of compound channels have been conducted at various scales. Data from four such studies (at three scales) have been obtained for calibration and verification of Equation 2.9 (Table 3.1). In this document data are referred to either by “series” or by “series-testnumber”.

**Table 3.1. Laboratory Data Used in this Study**

Scale	Facility	Authors	Year	Series	Number of Tests
Small Scale Laboratory	Waterways Experiment Station	James and Brown	1977	JB-01	8
				JB-02	6
				JB-03	9
				JB-12	2
Large Scale Laboratory	University of Birmingham	Seckin	2004	S-03	10
	Flood Channel Facility (FCF) at the University of Birmingham	Knight and Sellin	1987	FCF-01	8
				FCF-02	9
				FCF-03	10
				FCF-08	7
				FCF-10	8
Field Scale Laboratory	Hydrologic Instrumentation Facility (HIF) Floodplain Simulation Facility	Collins and Flynn	1978	CF	19

As indicated in section 1.2.4, small scale laboratory (Flume Width < 2 m) studies have been conducted by many researchers. Data from two such studies have been used in

this analysis, James and Brown (1977) and Seckin (2004). James and Brown (1977) conducted experiments in a tilting flume 26.8m long, 1.52m wide, and 0.45m deep with channel boundaries of molded from concrete. Both symmetric and asymmetric compound channels were examined, but for the purposes of this study, only data from symmetric channels will be utilized. Velocities were recorded at multiple lateral locations for a given depth via a 3.175 mm pitot tube connected to a pressure transducer. Seckin (2004) conducted similar experiments in a flume 18m long, 1.213m wide, and 0.4m deep. This flume was configured as a rectangular compound channel with PVC channel boundaries. Depth-averaged velocity was measured by a 13mm Novar Nixon miniature propeller current meter at 0.4 depth. Velocity was measured at each lateral location five times on 10s intervals and these five measurements were averaged to obtain an estimate of the depth-averaged velocity. The geometric properties of these two small scale laboratory studies can be seen in Table 3.2.

Detailed data have also been obtained from the large scale Flood Channel Facility at the University of Birmingham. As previously explained this facility is 56m long, 10m wide, and 0.25m deep. This flume has been used to test multiple compound channel geometries, channel boundaries, and planform conditions. The test conditions used in this analysis are those of straight channels with uniform concrete channel boundaries. The depth-averaged velocity was obtained by measuring point velocities throughout the cross-section with 10mm diameter miniature propeller meters and depth-averaging. The geometric properties of these data sets can also be seen in Table 3.2.

Data from the United States Geological Survey's (USGS) Hydrologic Instrumentation Facility (HIF) Floodplain Simulation Facility has also been obtained.

This outdoor facility was extremely large with the test facility measuring 820m long, 91.4m wide, and 0.91m deep. The channel boundaries of this facility were comprised of grass roughness tested at multiple lengths to examine the effects of variable roughness (Note: “Series” label has been modified to express grass length in mm in some references in this document). Due to the test facility size, velocity and depth data were recorded at multiple cross-sections via standard wading procedures. For this analysis, only data from one cross-section will be used. The geometric properties of these experiments are also presented in Table 3.2.

**Table 3.2. Geometric properties of tests used in this study**

Series	Number of Tests	Slope (*10 <sup>3</sup> )	Main Channel Half-Width	Floodplain Half-Width	Main Channel Depth	Main Channel Side Slope	Floodplain Side Slope
		$S_0$	$b_{ch}$ (m)	$B$ (m)	$h_{ch}$ (m)	$s_{ch}$	$s_{fp}$
JB-01	8	1, 2, 3	0.09	0.71	0.05	1	1
JB-02	6	1, 2, 3	0.09	0.51	0.05	1	1
JB-03	9	1, 2, 3	0.09	0.33	0.05	1	1
JB-12	2	1	0.12	0.69	0.07	1	1
S-03	10	2.024	0.20	0.61	0.05	0	0
FCF-01	8	1.027	0.75	5.00	0.15	1	0
FCF-02	9	1.027	0.75	3.15	0.15	1	1
FCF-03	10	1.027	0.75	1.65	0.15	1	1
FCF-08	7	1.027	0.75	3.00	0.15	0	1
FCF-10	8	1.027	0.75	3.30	0.15	2	1
CF	19	0.4	1.53	45.70	0.3	2	2
Range	96	0.4-3	0.09-1.53	0.33-45.70	0.05-0.3	0-2	0-2

Although a range of geometric conditions is important in any empirical study, the range of dimensionless properties is perhaps more important to ensure that the model is applicable over many scales. The dimensionless properties of the test cases used in this study are displayed in Table 3.3.

**Table 3.3. Dimensionless properties of tests used in this study**

Series	Number of Tests	Main Channel Side Slope	Floodplain Side Slope	Range of Relative Depth	Range of Floodplain Aspect Ratios	Channel Aspect Ratio
		$s_{ch}$	$s_{fp}$	$D_r$	$b_{fp}/h_{fp}$	$b_{ch}/h_{ch}$
JB-01	8	1	1	0.002 - 0.278	29.1 - 152.0	1.75
JB-02	6	1	1	0.123 - 0.285	18.2 - 51.8	1.75
JB-03	9	1	1	0.084 - 0.336	7.4 - 40.8	1.75
JB-12	2	1	1	0.068 - 0.213	26.8 - 99.8	1.75
S-03	10	0	0	0.162 - 0.460	9.6 - 22.8	3.98
FCF-01	8	1	0	0.050 - 0.500	41.0 - 269.9	5.00
FCF-02	9	1	1	0.050 - 0.500	16.3 - 113.1	5.00
FCF-03	10	1	1	0.050 - 0.500	5.0 - 46.1	5.00
FCF-08	7	0	1	0.050 - 0.500	22.5 - 132.4	5.00
FCF-10	8	2	1	0.050 - 0.500	24.9 - 149.1	5.00
CF	19	2	2	0.430 - 0.641	81.3 - 192.8	5.08
Range	96	0 - 2	0 - 2	0.002 - 0.641	5.0 - 269.9	1.75 - 5.08

As displayed these data provide a large range of experimental conditions to which the model can be applied; however, the scope of this project eliminates some of the data for use in calibration of the model. The main channel of the James and Brown (1977) data is not hydraulically wide according to the defined criteria, and the different character of the roughness in the Collins and Flynn (1978) data set precludes its use in calibration of the model being developed. Although the exclusion of these data limits the range of variables tested, the quantity and quality of data from the Seckin (2004) and Flood Channel Facility (1987) data sets still provides confidence in the range of data available for calibration of the empirical model (Table 3.4). The exclusion of the James and Brown (1977) and Collins and Flynn (1978) data sets also allows the limitations of the model to be examined.



**Table 3.4 Dimensionless properties of data available for model calibration**

Series	Number of Tests	Main Channel Side Slope	Floodplain Side Slope	Range of Relative Depth	Range of Floodplain Aspect Ratios	Channel Aspect Ratio
		$s_{ch}$	$s_{fp}$	$D_r$	$b_{fp}/h_{fp}$	$b_{ch}/h_{ch}$
S-03	10	0	0	0.162 - 0.460	9.6 - 22.8	3.98
FCF-01	8	1	0	0.050 - 0.500	41.0 - 269.9	5
FCF-02	9	1	1	0.050 - 0.500	16.3 - 113.1	5
FCF-03	10	1	1	0.050 - 0.500	5.0 - 46.1	5
FCF-08	7	0	1	0.050 - 0.500	22.5 - 132.4	5
FCF-10	8	2	1	0.050 - 0.500	24.9 - 149.1	5
Range	52	0-2	0-1	0.050 - 0.500	5.0 - 269.9	3.98-5

The limited range of channel aspect ratios in the calibration data sets (Table 3.4) is a cause of concern to the robustness of the resulting model. The use of channel top width,  $b_{top}$ , as a scaling parameter for the lateral coordinate (Equation 2.6 and Equation 2.9) may also induce uncertainty in the application of this limited range of channel aspect ratios due to the parameter's dependence upon both the channel aspect ratio and the channel side slope. For this reason, it is hypothesized that channel bottom width ( $b_{ch}$ ) or channel side slope width ( $s_{ch}h_{ch}$ ) may be more appropriate scaling parameters. These complications limit the results of this analysis to the channels similar to those listed in Table 3.4.

## 4 DATA ANALYSES AND RESULTS

The following chapter will discuss the application of the model developed in Chapter 2 (Equation 2.9) for the prediction of the lateral distribution of depth-averaged velocity in the compound channels described in Chapter 3.

### 4.1 General, Calibratable Model

Values of the coefficients ( $a_i$ ) of Equation 2.9 can be determined for any compound channel using the method of least squares given the geometric character of the system ( $b_{ch}$ ,  $b_{fp}$ ,  $h_{ch}$ ,  $s_{ch}$ ,  $s_{fp}$ ), hydraulic characteristics of the channel ( $U_0$ ,  $h_{tot}$ ), and sufficient depth-averaged velocity data ( $z$ ,  $U_d(z)$ ).

The reader will recall that in order for the system to be within the scope of this work, the floodplain must be sufficiently wide to develop a region of laterally uniform depth-averaged velocity on the floodplain. For this analysis as long as  $z_{a,WM} - z_c > 0$ , the floodplain is sufficiently wide for use of the model. In order to make this dependent on system properties instead of model solutions, the relationship between these calculated values and the floodplain width to depth ratio ( $b_{fp}/h_{fp}$ ) is considered. Figure 4.1 shows that when  $b_{fp}/h_{fp} < 15-25$ ,  $z_{a,WM} - z_c$  is often negative, implying that the two portions of the model (logistic function and adapted Wilkerson and McGahan function) have not both reached the asymptotic solutions required for use of the proposed model (Equation 2.9). For this analysis, a floodplain is considered wide when  $b_{fp}/h_{fp}$  is greater than 15. This value was chosen as a compromise between physical realism and data needs for calibration of an empirical model.

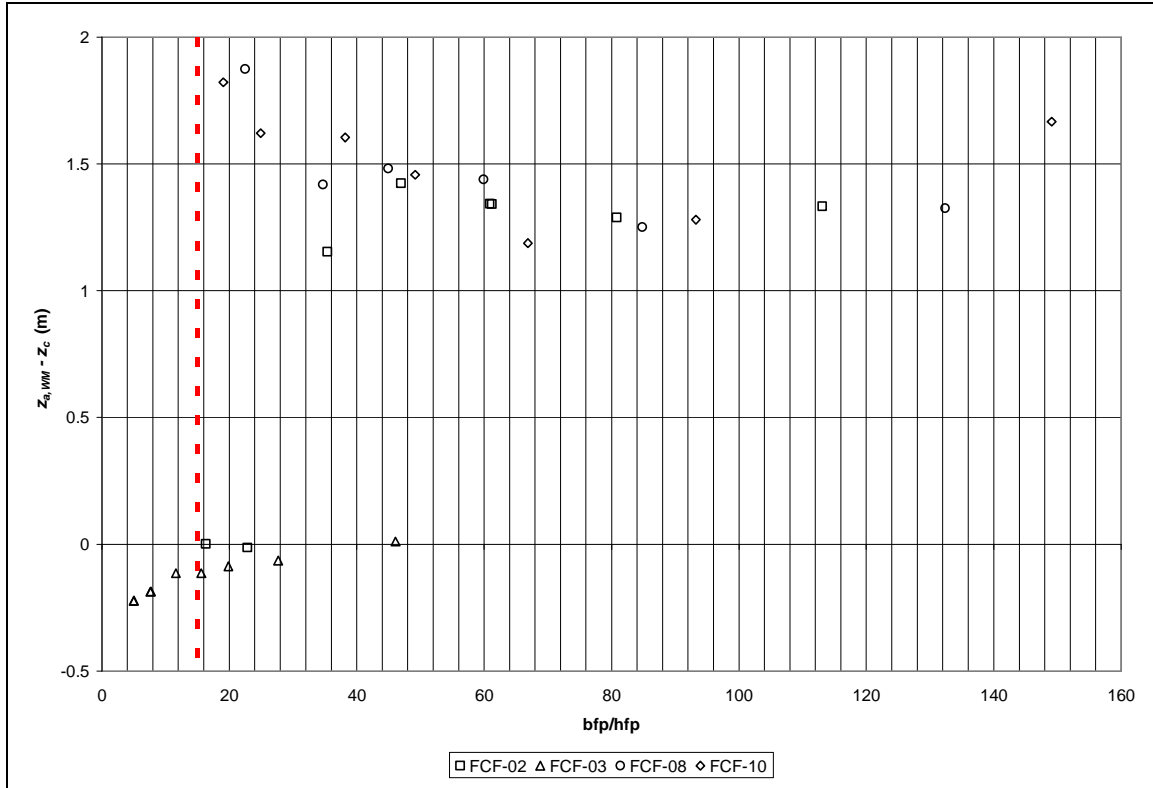


**Figure 4.1. Development of compound channel wide floodplain criteria**

The model has been applied to the data sets of Table 3.4 to examine whether the form of Equation 2.9 is appropriate. Seven of these data sets were eliminated for use due to a lack of sufficient depth-averaged velocity data in the floodplain. Nine other data sets were eliminated based on the wide floodplain criterion. Two data sets (FCF-010602 and FCF-020402) were reserved for model validation. Therefore, of the 52 data sets in the FCF and Seckin experiments, only 34 were available for model validation (Table 4.1). The predicted and observed distributions of depth-averaged velocity for each of the 34 data sets may be viewed in Figure A.1-Figure A.34 in Appendix A. The optimized coefficients and fit statistics for each of the data sets may be viewed in Table A.1.

**Table 4.1. Data sets used in validation of Equation 2.9**

Series	Number of Tests	Main Channel Side Slope	Floodplain Side Slope	Range of Relative Depth	Range of Floodplain Aspect Ratios	Channel Aspect Ratio
		$s_{ch}$	$s_{fp}$	$D_r$	$b_{fp}/h_{fp}$	$b_{ch}/h_{ch}$
S-03	4	0	0	0.263 - 0.343	15.6 - 22.8	3.98
FCF-01	6	1	0	0.092 - 0.400	41.0 - 269.9	5
FCF-02	7	1	1	0.117 - 0.479	16.3 - 113.1	5
FCF-03	4	1	1	0.098 - 0.243	15.6 - 46.1	5
FCF-08	6	0	1	0.102 - 0.400	22.5 - 132.4	5
FCF-10	7	2	1	0.100 - 0.464	19.1 - 149.1	5
Total	34	0-2	0-1	0.050 - 0.500	5.0 - 269.9	3.98-5

Figure 4.2 displays a typical velocity profile derived by Equation 2.9. The model was optimized by least squares analysis. This figure shows that the model closely predicts the distribution of depth-averaged velocity in a compound channel.

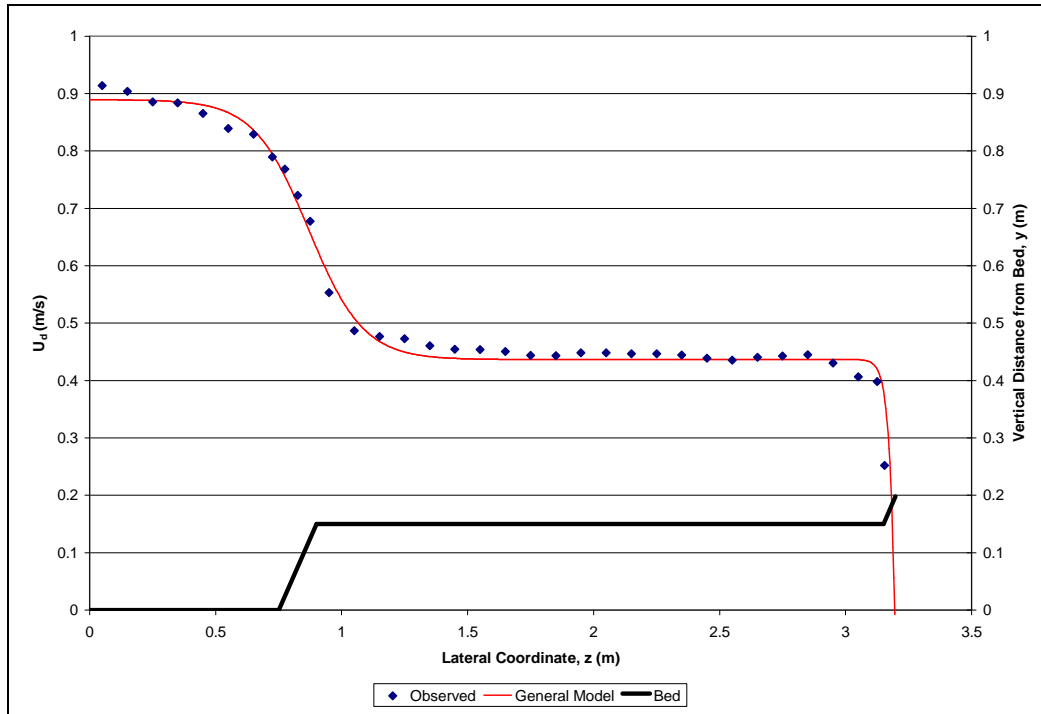


**Figure 4.2. Depth-averaged velocity distribution predicted by Equation 2.9 for test case FCF-020501**

For the 34 data sets considered, the model produces coefficients of determination ( $R^2$ ) of 0.826 to 0.995 with an average of 0.971 and a median of 0.985. The estimated standard error ( $s$ ) of the function had a range of 0.009 to 0.032 m/s, an average of 0.018 m/s, and a median of 0.016 m/s.

In order to assess accuracy of the results obtained by the model, each measured depth-averaged velocity data point was considered in comparison to its value as predicted by the model (Figure 4.3). A line of perfect agreement is shown on the plot as a solid line, and lines of 10% and 20% error are displayed as dashed lines. 95% of predicted depth-averaged velocities lie within 10% of the observed value and 98% of predicted depth-averaged velocities lie within 20% of their observed value.

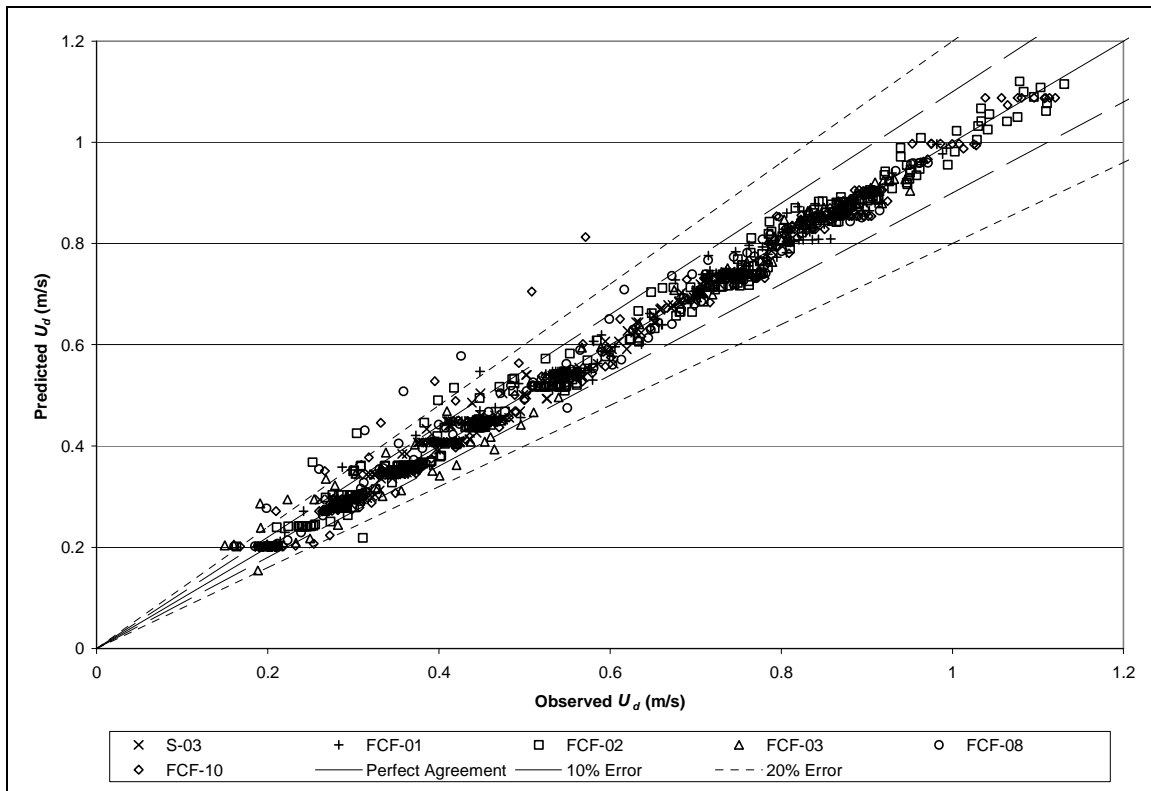


**Figure 4.3. Results of Equation 2.9 as displayed observed and predicted velocities**

The high coefficients of determination, low standard error, and predicted values close to unity lead to the conclusion that the form of the function (Equation 2.9) is reasonable for the range of geometries considered.

## ***4.2 Continuously-Varying Parameter Model***

Application of the general, calibratable model (Equation 2.9) indicates that the proposed function can be calibrated to provide a reasonable description of the depth-averaged velocity distribution. However, this model requires detailed measurement of depth-averaged velocity in order to calibrate the model, which is often impractical or impossible to obtain in the field setting. Therefore, a more generic form of the model is sought that will not require depth-averaged velocity data for calibration. A generic predictive model for depth-averaged velocity in compound channels was derived by optimizing the coefficients of Equation 2.9 for the above data sets and regressing these coefficients with the significant dimensionless ratios presented in Equation 2.5. This produced a continuously varying parameter model (CV model) whose coefficients are a function of the channel and floodplain geometry. This model will rely on prescribed coefficients determined by calibration and regression of model coefficients.

The CV model was calibrated with the Seckin (2004) and Flood Channel Facility data sets used in the previous section. The regression of all coefficients  $a_i$  with the dimensionless ratios of Equation 2.5 ( $D_r$  and  $s_{ch}$ ) allowed for general relations to be determined using least squares analysis. Residuals of the predictions were examined, and if the residual exceeded  $\pm 2$  standard deviations beyond the mean residual, the point was identified as an outlier and removed to prevent skewing to outlying data (Hill and Lewicki, 2006). After outliers were removed, 26 data sets remained (Table 4.2).

**Table 4.2. Data sets used in calibration of the continuously varying model**

Series	Number of Tests	Main Channel Side Slope	Floodplain Side Slope	Range of Relative Depth	Range of Floodplain Aspect Ratios	Channel Aspect Ratio
		$s_{ch}$	$s_{fp}$	$D_r$	$b_{fp}/h_{fp}$	$b_{ch}/h_{ch}$
S-03	3	0.0	0.0	0.297 - 0.343	15.6 - 19.3	3.98
FCF-01	4	1.0	0.0	0.092 - 0.246	84.0 - 269.9	5.00
FCF-02	7	1.0	1.0	0.117 - 0.479	16.3 - 120.1	5.00
FCF-03	1	1.0	1.0	0.153	27.65	5.00
FCF-08	5	0.0	1.0	0.102 - 0.302	34.7 - 132.4	5.00
FCF-10	6	2.0	1.0	0.100 - 0.398	19.1 - 149.1	5.00
Range	26	0-2	0-1	0.092 - 0.479	15.6 - 269.9	3.98 - 5.0

Coefficient  $a_1$  was found to be highly correlated with the relative depth (ratio of the depth of flow in the floodplain to that in the main channel). As the relative depth becomes large, the difference between the depth-averaged velocity in the main channel and on the floodplain would become small; as it does the coefficient  $a_1$  approaches zero. The following exponential model was found to provide a good fit of the data (Equation 4.1 and Figure 4.4) and the appropriate physical limits. The exponential model also provided randomly distributed residuals (Figure 4.5).

$$a_1 = 1.333e^{-2.872D_r}$$

$$R^2 = 0.915$$

**Equation 4.1**

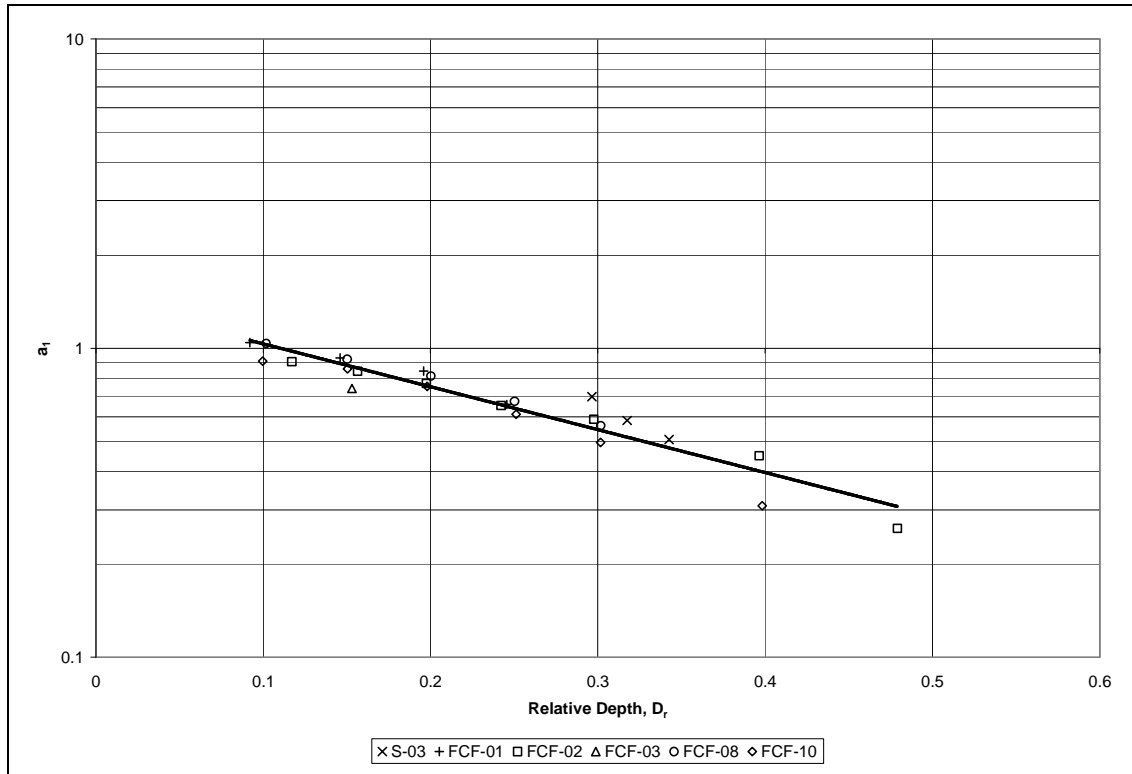


**Figure 4.4. Exponential model of coefficient  $a_1$  with relative depth,  $D_r$**

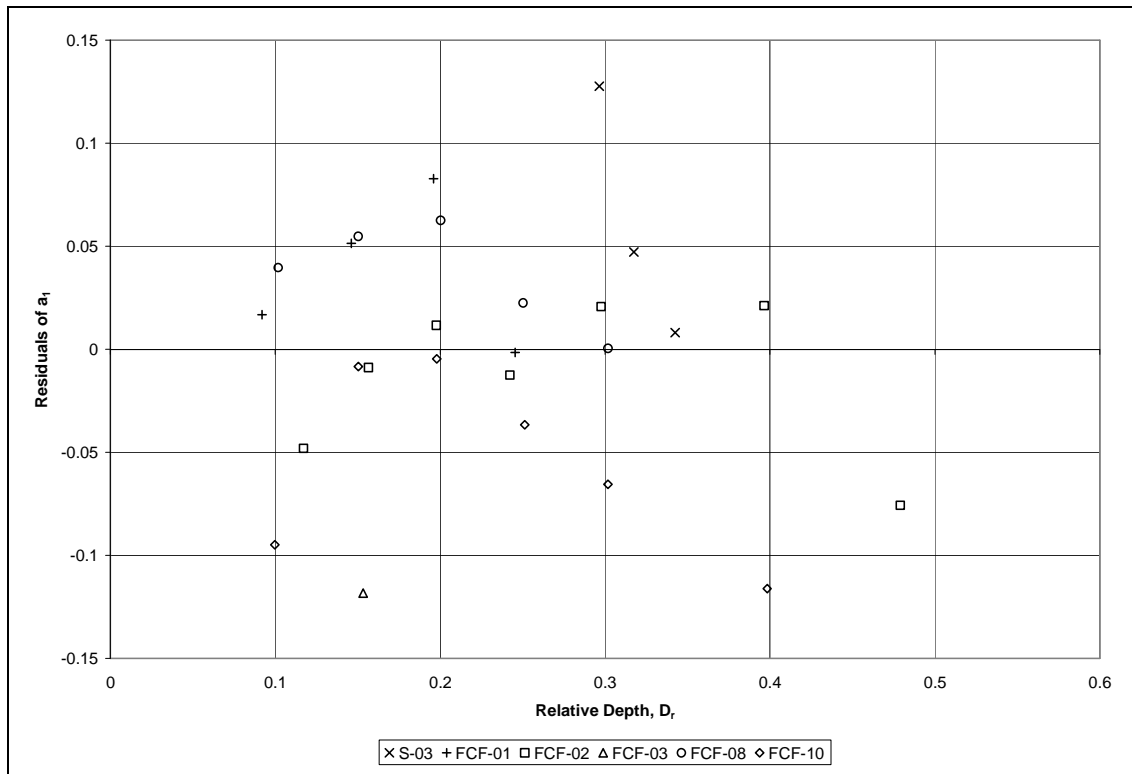


**Figure 4.5. Residuals resulting from Equation 4.1**



Coefficients  $a_2$  and  $a_3$  did not correlate with any of the relevant dimensionless variables. These coefficients were expected to vary with the width of the channel side slope,  $s_{ch}h_{ch}$ . It is hypothesized that the use of  $b_{top}$  as a scaling parameter over a small range of channel aspect ratios may have induced this unexpected result in the analysis. As stated,  $a_2$  and  $a_3$  showed little variability over the calibration range; therefore, these parameters were approximated as constant over the range of conditions examined. The mean values of the two parameters were  $a_2 = 1.583$  and  $a_3 = 7.989$ . Figure 4.6 presents a summary of the calibrated coefficients,  $a_2$  and  $a_3$ , in the form of boxplots. Definitions of boxplots varies among references; therefore, for use in this document, boxplots will be defined in the form of Schmidt (2002), where the “box” is defined as the upper and lower quartiles with the median value represented between them and the “whiskers” are defined as the largest or smallest value within one step (the upper quartile minus the lower quartile times 1.5) of the upper or lower quartile, respectively. Outliers are plotted as points beyond the “whiskers”.

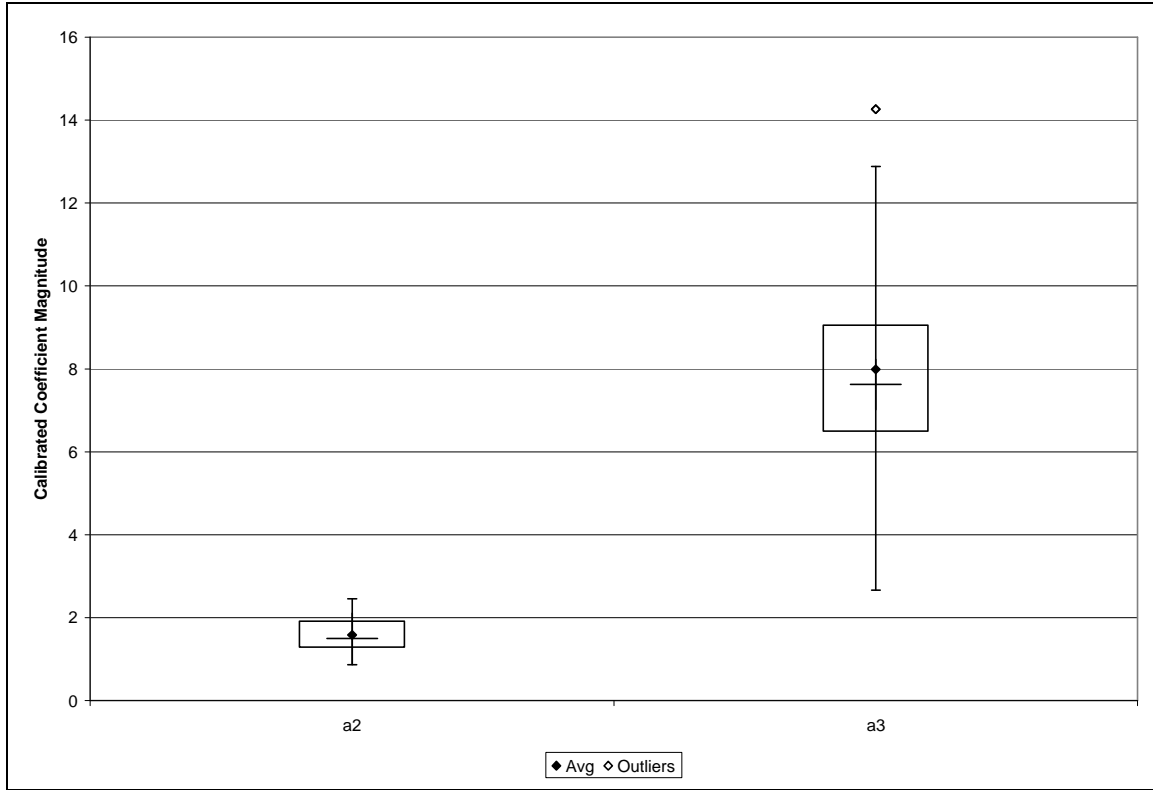


**Figure 4.6. Boxplot of coefficients  $a_2$  and  $a_3$**

Coefficient  $a_4$  was also found to be highly correlated to relative depth. A power function provided the best fit of the data along with appropriate limits for the coefficient. As the relative depth approaches zero (in-bank flow), coefficient  $a_4$  approaches zero because there would be no velocity on the floodplain. Hypothetically speaking if the relative depth approaches infinity, coefficient  $a_4$  also approaches infinity. The model (Equation 4.2 and Figure 4.7) and the resulting residuals (Figure 4.8) are displayed.

$$a_4 = 1.527D_r^{0.642}$$

$$R^2 = 0.939$$

**Equation 4.2**

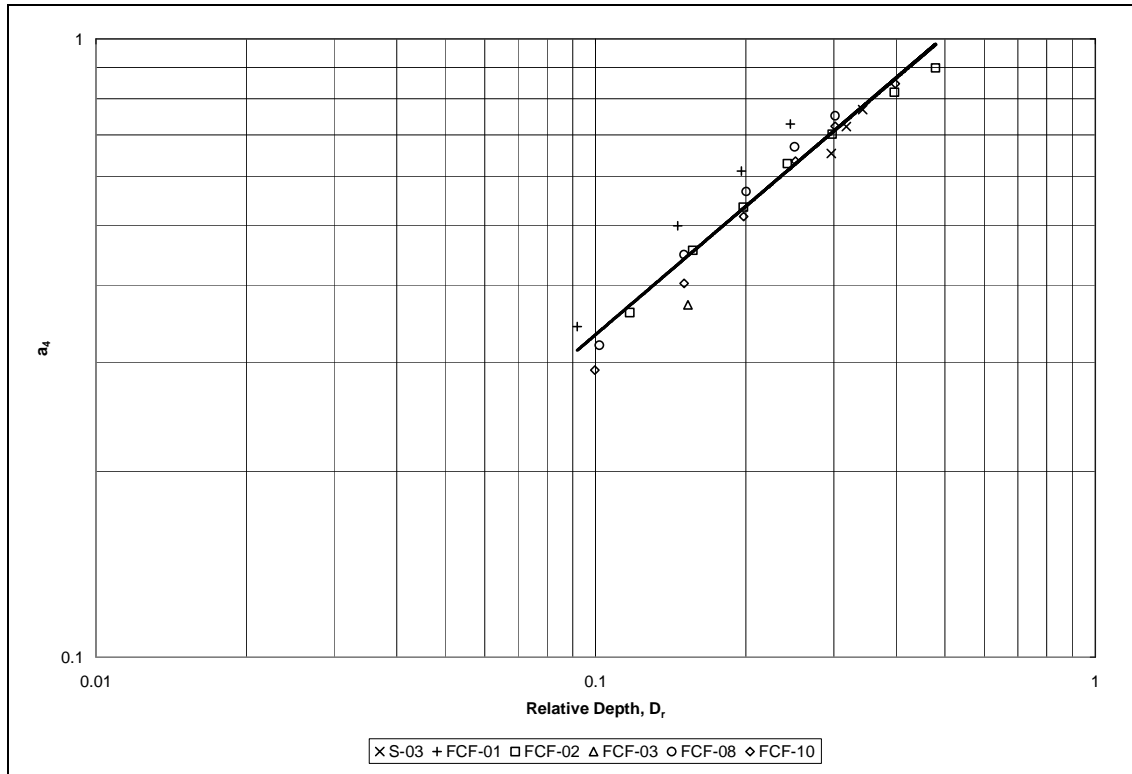


**Figure 4.7. Model of coefficient  $a_4$  with relative depth,  $D_r$**

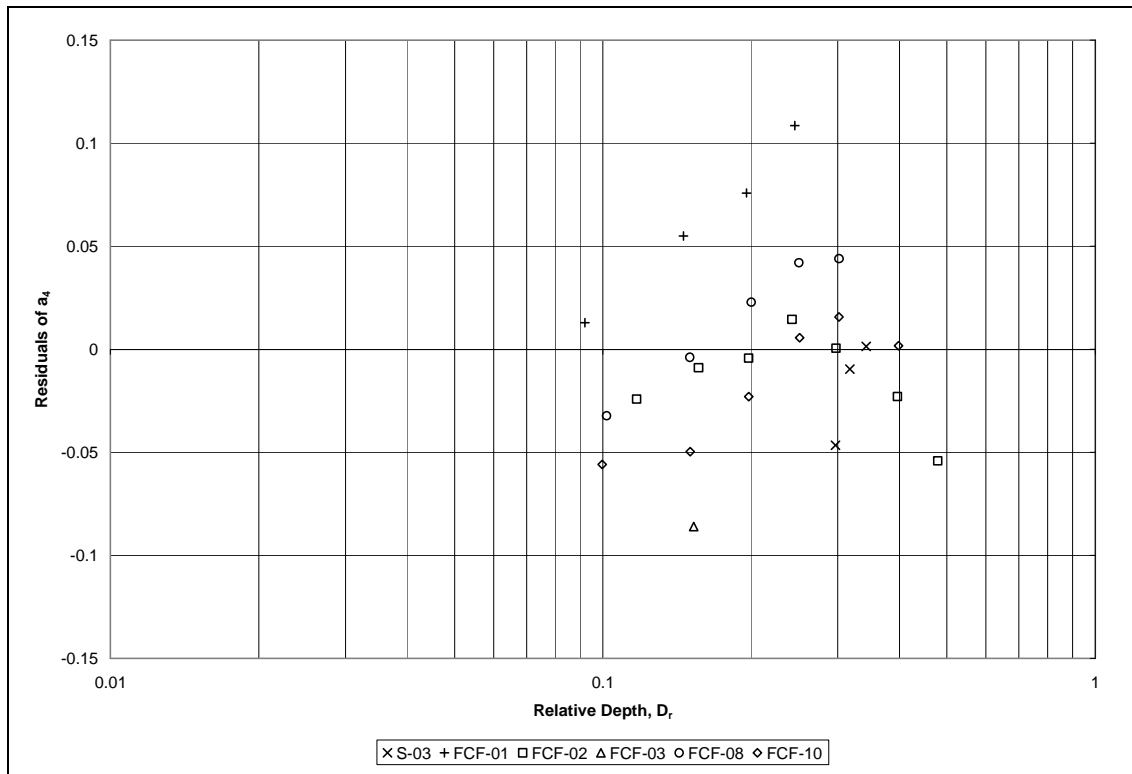


**Figure 4.8. Residuals resulting from Equation 4.2**

Combining each of these expressions with Equation 2.9 leads to a continuously varying parameter model for predicting the distribution of depth-averaged velocity in trapezoidal compound channels.

$$U_d(z) = \begin{cases} U_0 \left( \frac{1.333e^{-2.872D_r}}{1 + 1.583e^{\frac{7.989(z-b_{top})}{b_{top}}}} + 1.527D_r^{0.642} \right) & ; z \leq z_c \\ U_d(z_c) \left( 1 - 0.125s_{fp} e^{\frac{2.24s_{fp}^{-0.582}(z-B)}{s_{fp}h_{fp}}} \right) & ; z > z_c, \quad 1 \leq s_{fp} \leq 3 \\ U_d(z_c) & ; z > z_c, \quad s_{fp} < 1 \end{cases}$$

**Equation 4.3**

#### **4.2.1 Application of Continuously Varying Model to Calibration Data**

In order to assess whether the coefficient relations in the continuously varying parameter model (Equation 4.3) are appropriate, the model was applied to the data for which it was calibrated. The observed and predicted lateral distributions of depth-averaged velocity for each test may be seen in Appendix A. The statistical properties of each distribution are presented in Table A.1 in Appendix A. The observed variance in the CV model was evaluated by plotting observed and predicted values of the depth-averaged velocity (Figure 4.9). Among the 987 data points, 78% are within the 10% of the observed values and 96% are within 20% of the observed values.

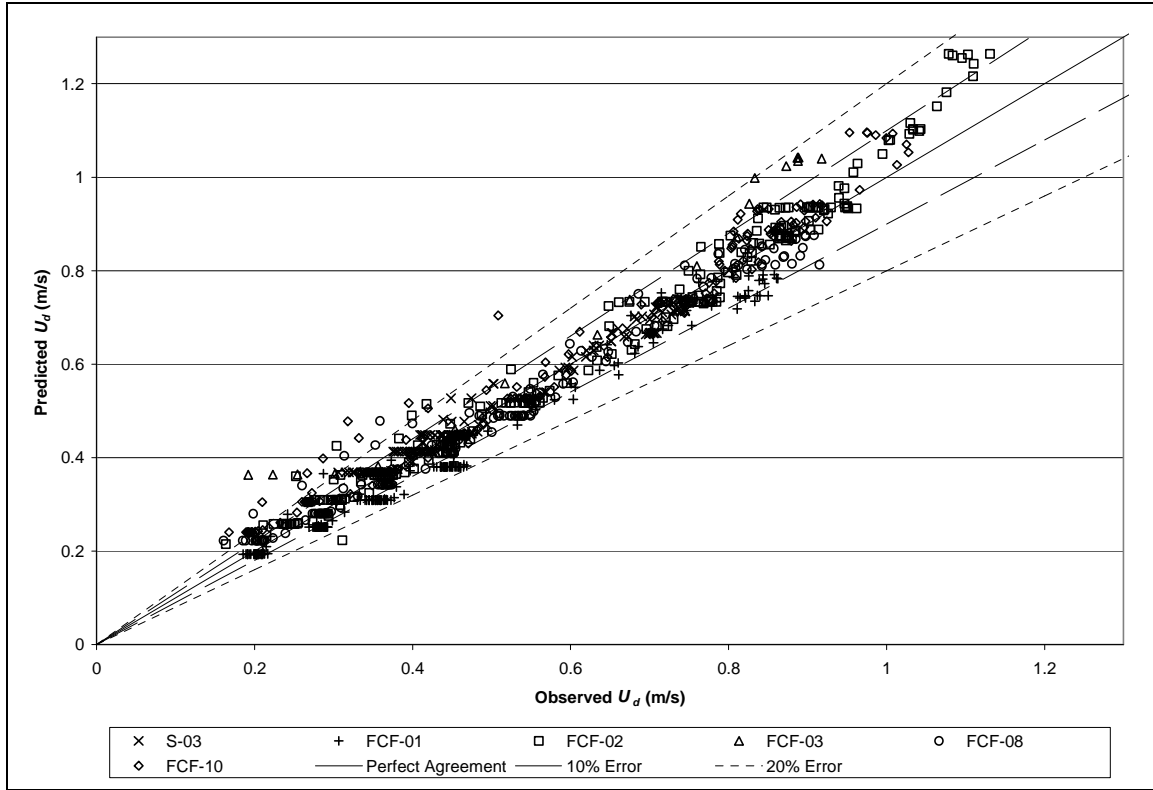


**Figure 4.9. Continuously varying model results for data used in calibration**

The model predictions were also assessed by standard statistical metrics. The model produced coefficients of determination ( $R^2$ ) from 0.503 to 0.990 with a mean of 0.918 and a median of 0.964. The standard error of the model varied from 0.015 m/s to 0.105 m/s with a mean of 0.038 m/s and a median of 0.027 m/s. Although  $R^2$  values are low in some cases, the trends of the velocity distribution are appropriately represented. Figure A.13, Figure A.32, and Figure A.17 present plots of the data sets with the highest, median, and lowest  $R^2$  values ( $R^2 = 0.990$ , 0.964, and 0.503, respectively) for the continuously varying parameter model as it has been applied to the data with which it was calibrated.

## 4.2.2 Validation of Continuously Varying Model

In order to evaluate the generality of Equation 4.3, two data sets representative of typical channels with and without floodplain side slopes were withheld for validation purposes (FCF-010602 and FCF-020402). Figure A.35 and Figure A.36 present the predicted depth-averaged velocity distributions for these data sets. The results from the application of the CV model to these data are plotted in Figure 4.10. Among the plotted points, 54% are within the 10% of the observed values and 100% are within 20% of the observed values.

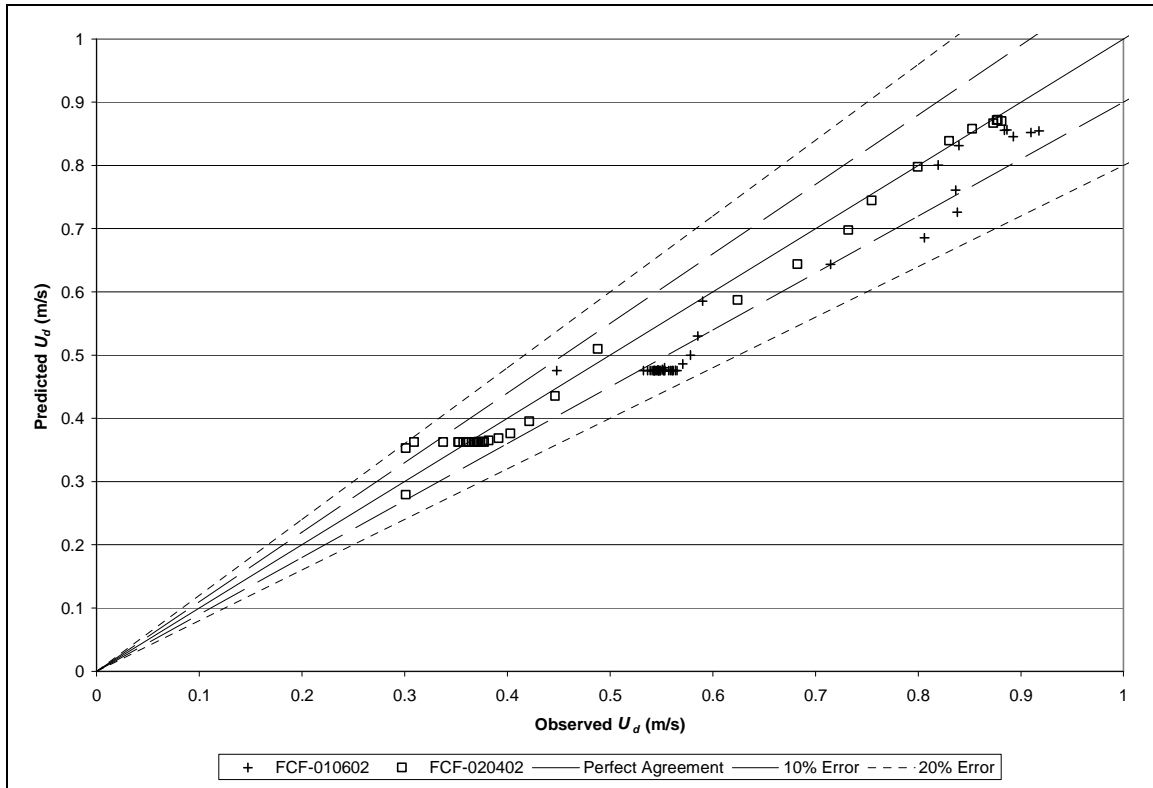


**Figure 4.10. Continuously varying parameter model results for validation data**

### **4.2.3 Extension Beyond Model Calibration Range**

Although the model should only be applied to the geometric conditions for which it has been developed, examination of the model's utility beyond the tested range provides the user with knowledge of the response of the model to use beyond its limitations. The model has been applied to three data sets beyond the calibrated range and outside the scope of this research to examine the effects of narrow main channels, narrow floodplains, and varying roughness conditions.

#### **Prediction of Depth-Averaged Velocity**

Application of the CV model to the small scale laboratory data of James and Brown (1977) allowed for examination of the effects a narrow main channel ( $b_{ch}/h_{ch}=1.75$ ) has on compound channel flow. The CV model did not closely predict the depth-averaged velocity profile for all tests considered (Figure 4.11). The scatter of this prediction is believed to be caused by the effects of the narrow main channel on the distribution of flow in the channel. A typical velocity distribution for this data set has been provided for reference to the magnitude and lateral location of errors in the predicted velocity distribution for both the CV and general models (Figure 4.12).

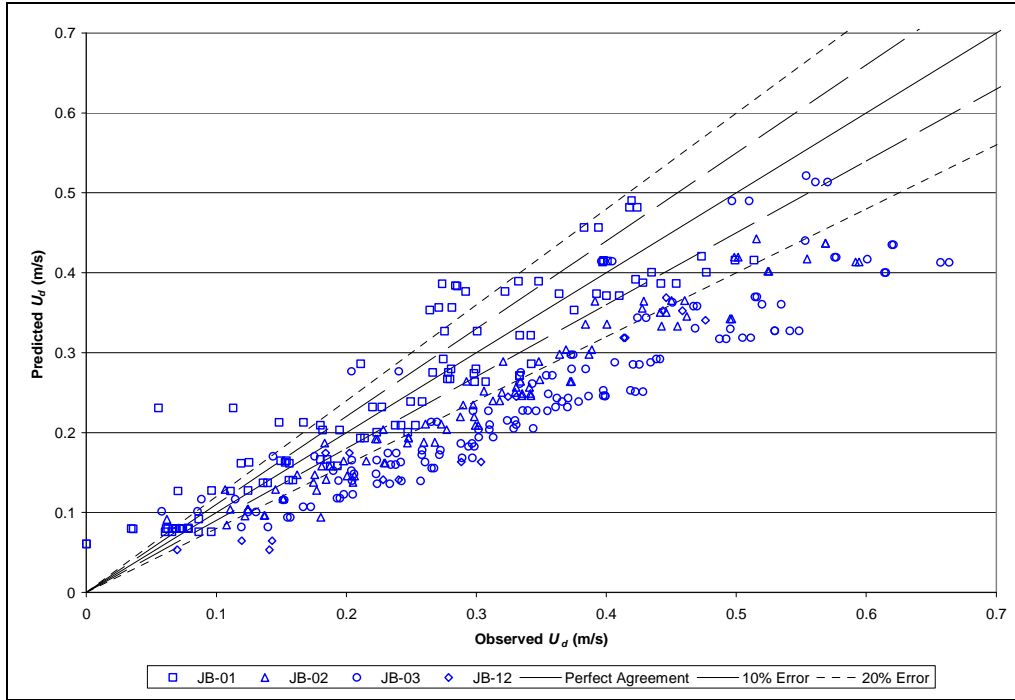


**Figure 4.11. Results of the continuously-varying parameter model as applied to channels of low main channel aspect ratio**

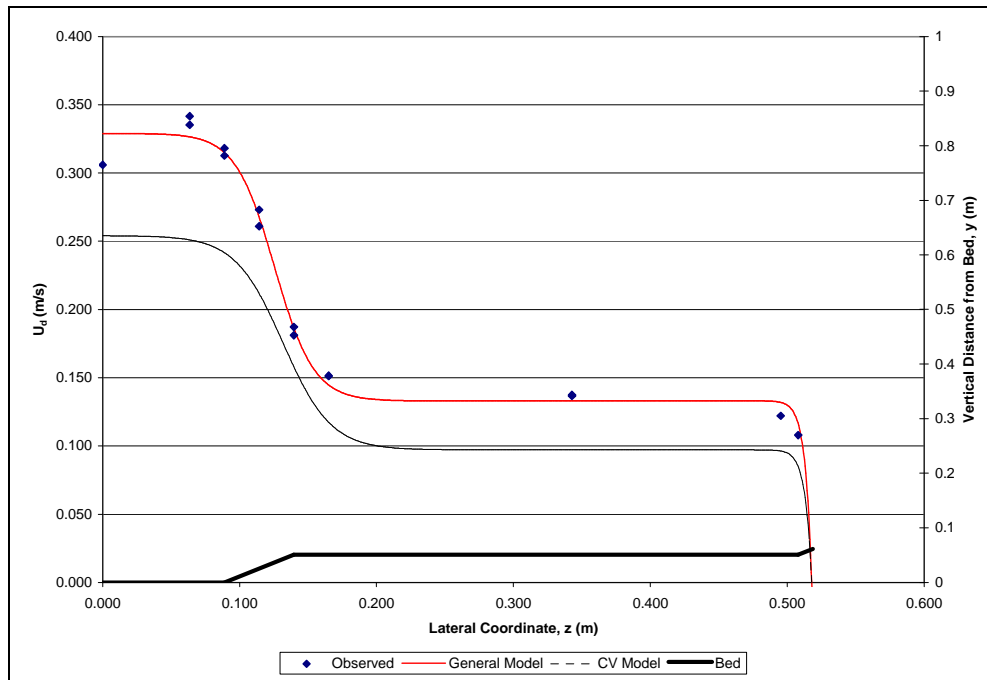


**Figure 4.12. Depth-averaged velocity distribution as predicted by the CV and general models for JB-02-A-02 ( $R^2 = 0.574$  and  $0.988$ , respectively)**



Tests with narrow floodplains were removed from the calibration data sets. The tests of Seckin (2004) that contained narrow floodplains ( $b_{fp}/h_{fp} < 15$ ) will now be used to examine how the model responds to floodplains that are not wide enough for velocity to become laterally uniform. The CV model predicts 98% of depth-averaged velocities within 20% of the observed values (Figure 4.13). Although the model predicts values close to the observed values, there is a systematic over prediction of velocity throughout the channel. The close fit could be an artifact of using this channel geometry in model calibration. General use of the model is not recommended in narrow floodplains. A typical velocity distribution for this data set has been provided for reference to the magnitude of the overprediction of the velocity distribution (Figure 4.14).

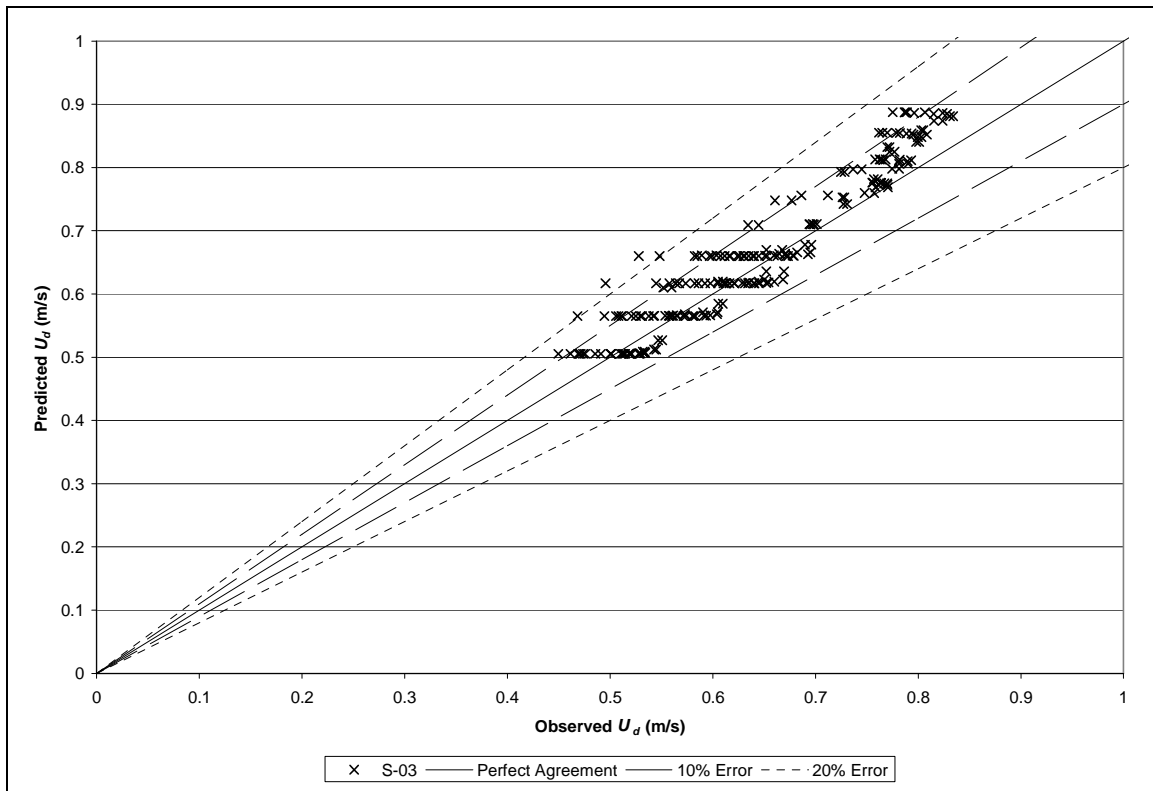


**Figure 4.13. Results of the continuously varying parameter model as applied to channels with narrow floodplains**

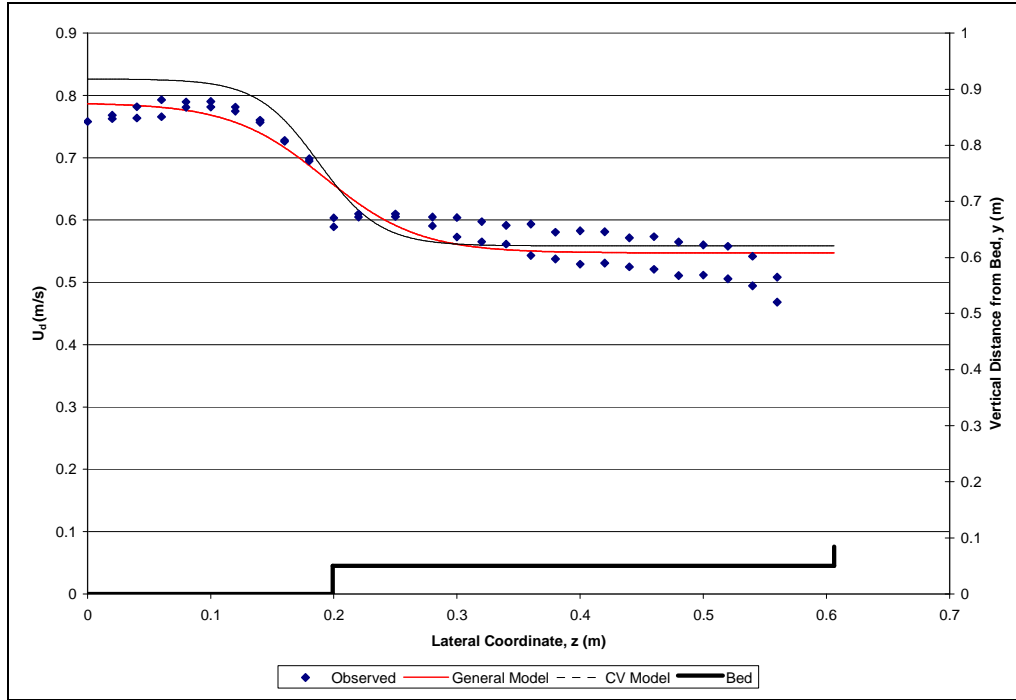


**Figure 4.14. Depth-averaged velocity distribution as predicted by the CV and general models for S-03-240 ( $R^2 = 0.876$  and  $0.999$ , respectively)**

In order to test the ability of the model to respond to varying roughness scales, the model was applied to a set of field scale laboratory tests by Collins and Flynn (1978). This extremely large, vegetated flume was used to examine the effects of relative roughness on the flow in compound channels. The CV model was applied to the 19 test cases, but only 45% of the predicted depth-averaged velocity values were within 20% of the observed values (Figure 4.15). The floodplain velocities were predicted closely by the model, but the main channel/shear layer velocities were poorly predicted. Figure 4.15 shows how the model drastically underpredicts velocity in the main channel. A typical depth-averaged velocity distribution has been displayed in order to illustrate the underprediction of main channel velocity (Figure 4.16).

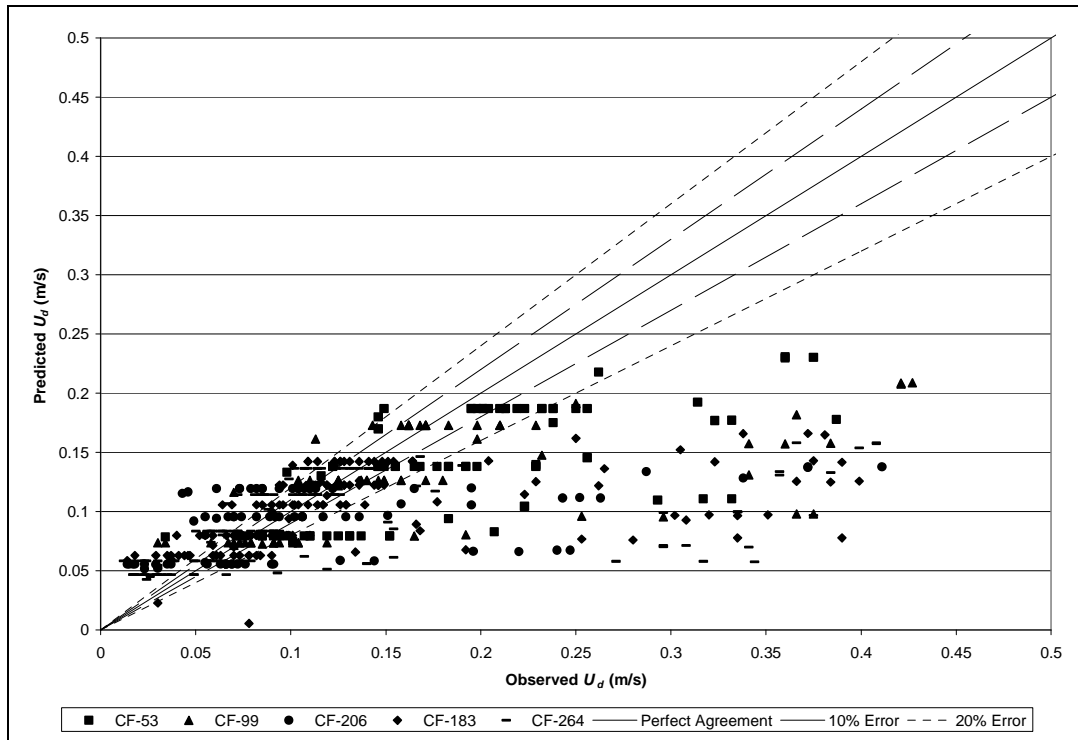


**Figure 4.15. Results of the CV model as applied to large, vegetated channels**

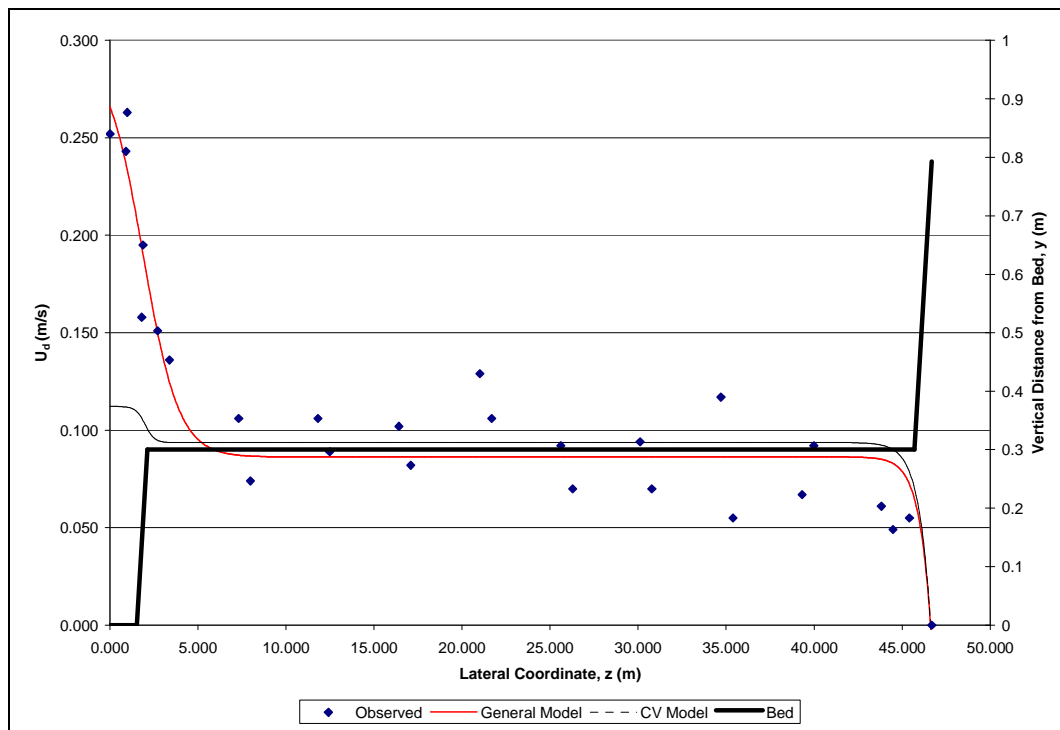


**Figure 4.16. Depth-averaged velocity distribution as predicted by the CV and general models for CF-206-10, ( $R^2 = 0.203$  and  $0.896$ , respectively)**

## Coefficient Errors

The errors associated with application of the CV model beyond the calibration range highlights the need for model calibration for conditions beyond the calibration range. This section examines the magnitude of the errors of each of the prescribed coefficient relations and presents guidance for calibration of these coefficients. The general, calibratable model (Equation 2.9) has been applied to each of the extension data sets and produced depth-averaged velocity distributions with high correlation to observed velocity distributions ( $R^2 = 0.76$  to  $0.99$ ). The prescribed coefficient relations will be examined relative to these optimized coefficients.

The underestimation of main channel velocity in the James and Brown (1977) and Collins and Flynn (1978) data sets implies a miscalculation of the  $a_1$  coefficient. Figure 4.17 displays the optimized coefficients for these tests as compared to the optimized coefficients for the calibration data sets along with best fit lines for the calibration and extension data sets. In the Collins and Flynn (1978) data, mean grass length is indicated by the series name, for example test CF-53 has a mean grass length of 53 mm and CF-99 has a mean grass length of 99 mm. As grass length increases and protrudes further into the flow, the coefficient  $a_1$  becomes larger for the same relative depth. This implies that with increasing uniform roughness, the velocity differential between the floodplain and main channel becomes larger. This large range of values for  $a_1$  implies that the CV model (Equation 4.3) is highly dependent upon channel roughness, and caution should be exercised when extending the CV model to channels with large roughness elements (e.g. vegetation).

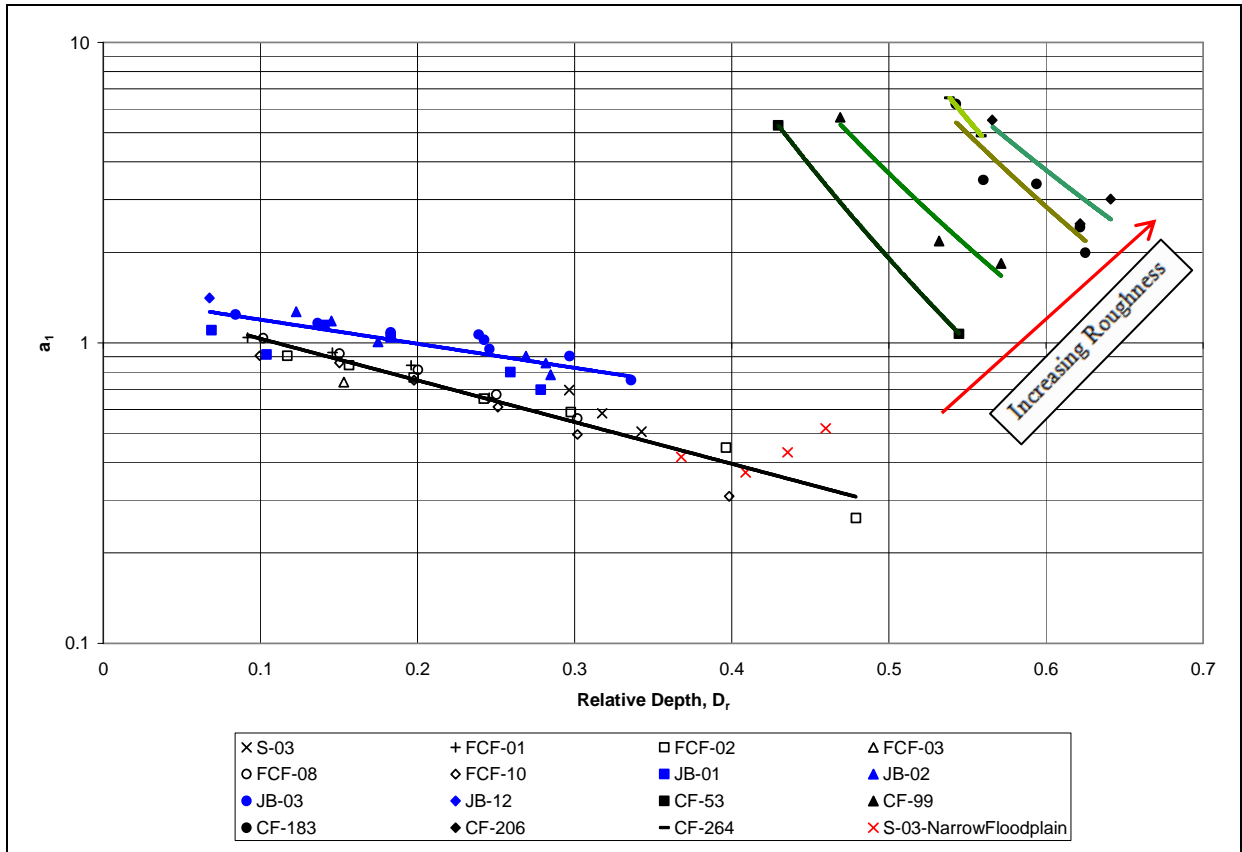


**Figure 4.17. Comparison of prescribed model coefficient  $a_1$  to data beyond the project scope**

Coefficients  $a_2$  and  $a_3$  do not display large discrepancies from calibrated values even for flow conditions that are vastly different from those used in model calibration. Figure 4.18 and Figure 4.19 display the residuals of the coefficients from the mean values calibrated in section 4.2. Coefficient  $a_2$  shows little variability even as applied to conditions well beyond those to which it was calibrated. Coefficient  $a_3$  shows some dependency upon channel geometry and roughness, but the calibrated mean derived in section 4.2 appears to offer a reasonable estimate of this value.

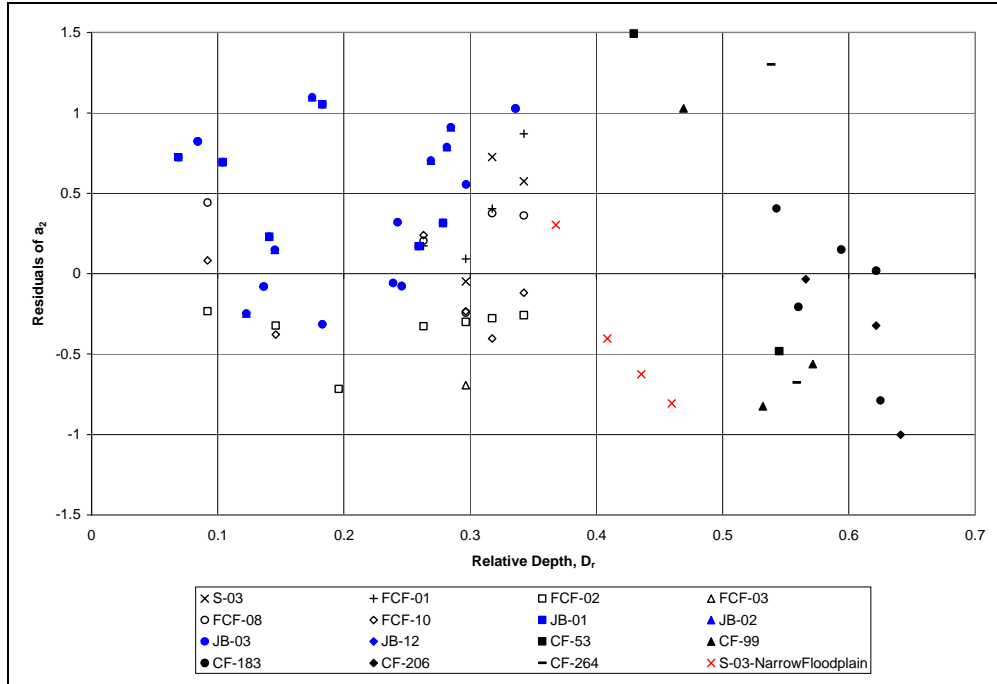


**Figure 4.18. Comparison of prescribed model coefficient  $a_2$  to data beyond the project scope**

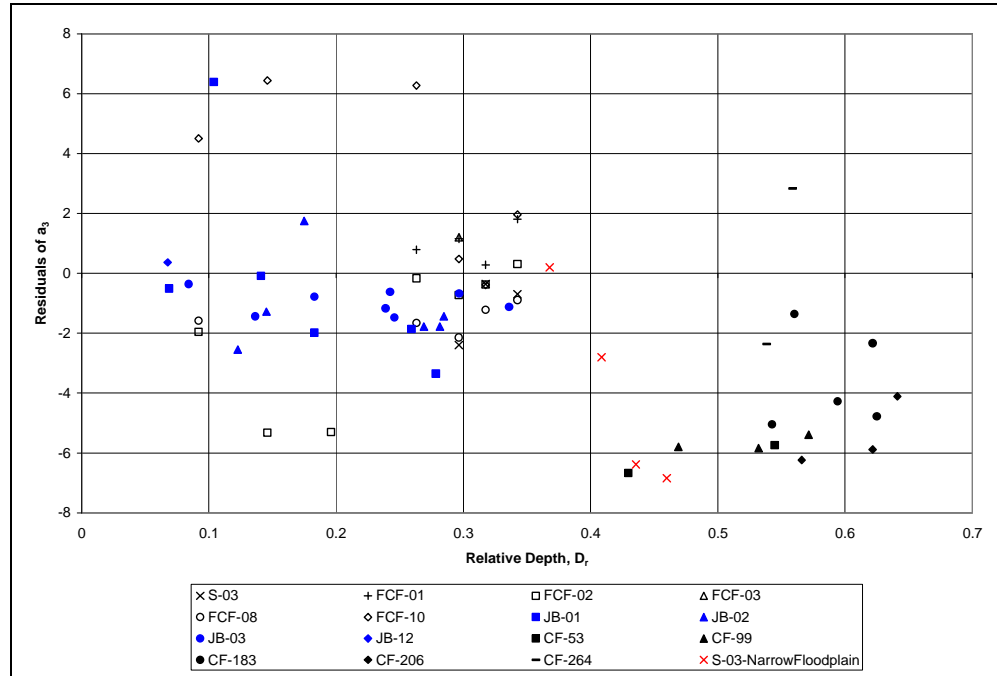


**Figure 4.19. Comparison of prescribed model coefficient  $a_3$  to data beyond the project scope**

The predicted floodplain velocity is in large part represented by the coefficient  $a_4$ . Therefore, correct estimation this coefficient is critical for accurate prediction of the depth-averaged velocity on the floodplain. Figure 4.20 presents the optimized values of  $a_4$  for the data sets used in calibration and those beyond the scope of this project. The optimized values of this coefficient indicate that the prescribed relation for  $a_4$  appears to be reasonable for the vegetated floodplains of the Collins and Flynn (1978) data sets, but inappropriate for the narrow main channels of the James and Brown (1977) data set. This indicates that the main channel has the greatest influence on the floodplain when the asymptotic velocity is not reached, as in the case of a narrow main channel.

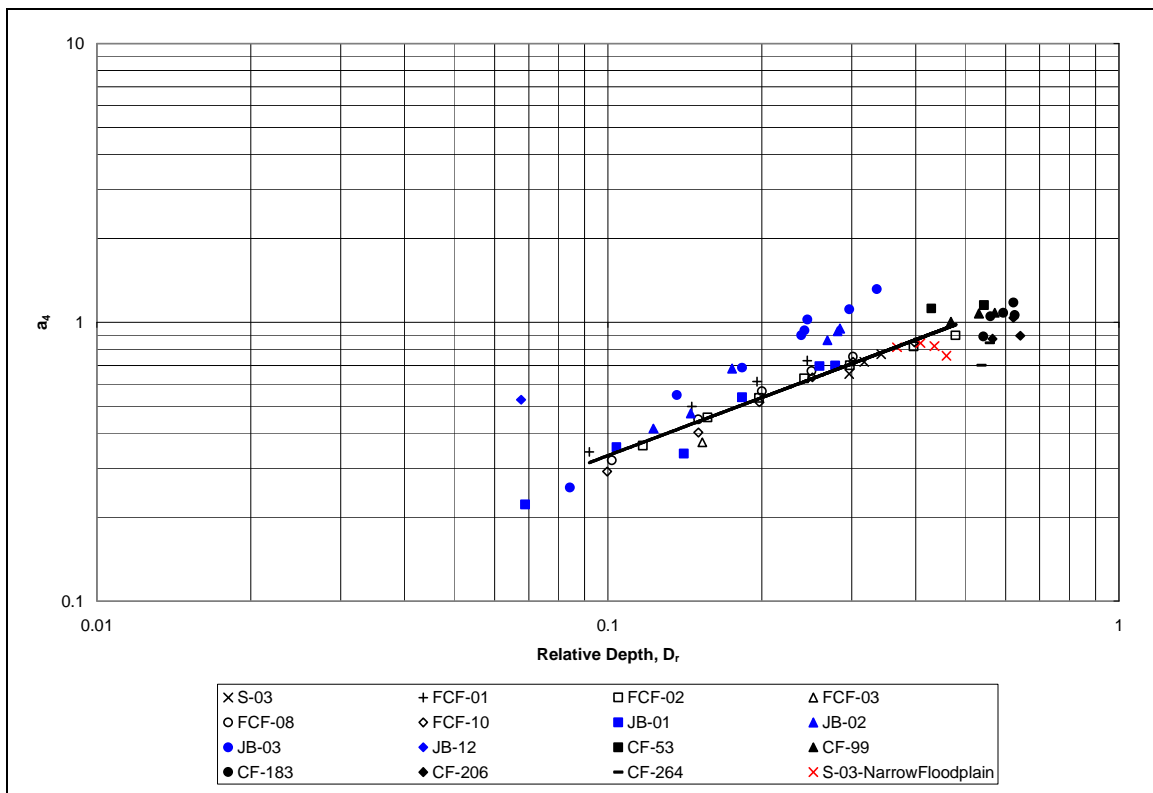


**Figure 4.20. Comparison of the prescribed model coefficient  $a_4$  to data beyond the project scope**

From the response of each of the prescribed coefficients to extension beyond the range of calibration, a basic calibration approach can be recommended. The model appears to be the most dependent upon accurate estimates of the coefficients  $a_1$  and  $a_4$  because these coefficients model the asymptotic velocity in the main channel and on the floodplain, respectively. Therefore, calibration of these coefficients is deemed the most critical with greater priority given to  $a_1$  due to the large variability of observed values. Coefficients  $a_2$  and  $a_3$  showed little variability over a broad range of conditions with coefficient  $a_3$  varying more than coefficient  $a_2$ . From these basic observations it is therefore recommended that if calibration of the CV model is desired the coefficients should be calibrated in the following order as data are obtained:  $a_1$ ,  $a_4$ ,  $a_3$ , and  $a_2$ .

### ***4.3 Model Comparison***

In order to assess the usefulness of the developed models, their accuracy must be compared to that of other models used for the prediction of depth-averaged velocity in compound channels. Two commonly used models are: the Divided Channel Method (DCM) with vertical boundaries not included in wetted perimeter calculations and the Shiono and Knight Method (SKM) (Shiono and Knight, 1991). The former is more commonly applied to prediction of discharge, but does offer a small amount of resolution in the velocity profile. The SKM is an analytical method based on the momentum equations and an eddy viscosity model. Each of these methods has been described in greater detail in section 1.2.5. Figure 4.21 displays the depth-averaged velocity profile predicted by each of these models, the general model developed in this work, and the CV model of this work for the validation data set FCF-020402. The ability of the model to accurately model observed depth-averaged velocity points is displayed in Figure 4.22.



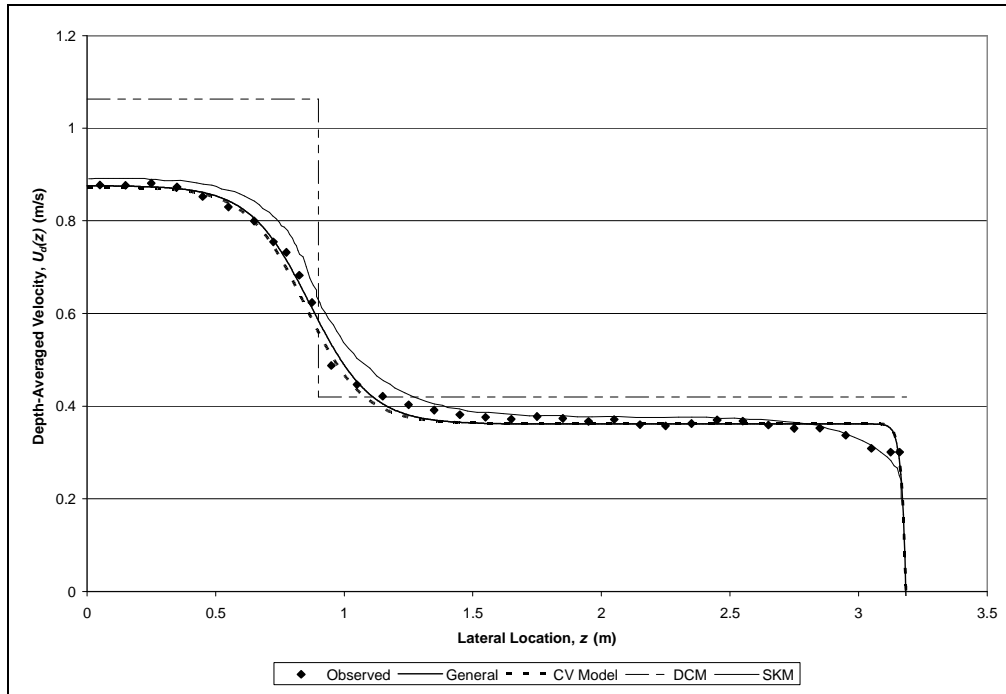


**Figure 4.21. Depth-averaged velocity distribution of FCF-020402 as computed by different methods**

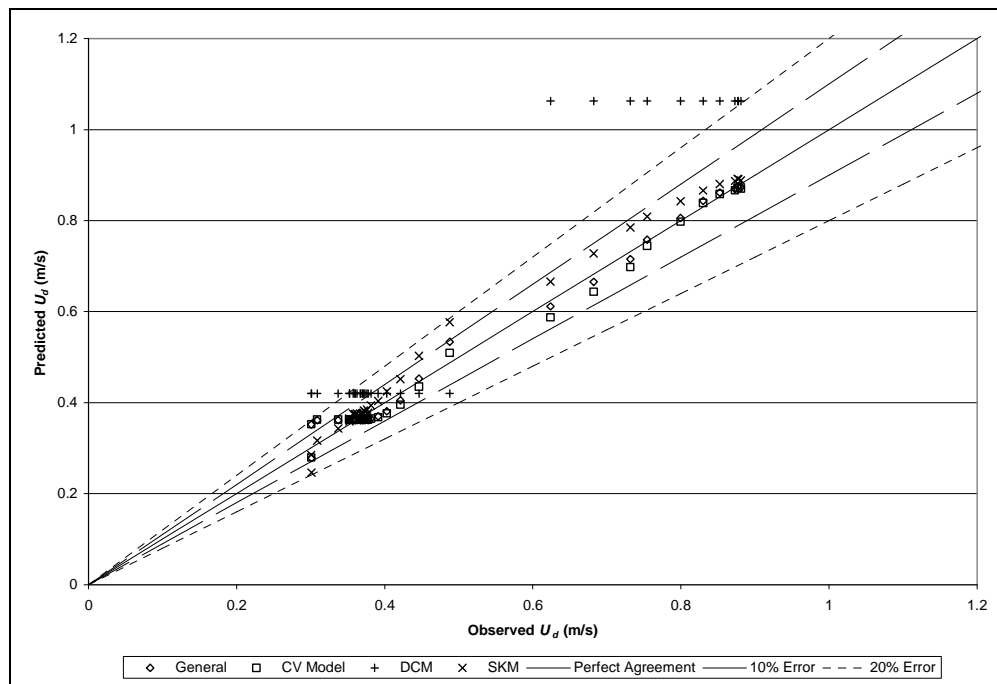


**Figure 4.22. Results of various models for predicting depth-averaged velocity distributions (test case FCF-020402)**

The models developed herein appear to produce results of an equivalent caliber to the analytical model of Shiono and Knight (1991). The analytical SKM is obviously preferred to the empirical methods developed here, but the ease of application of the models developed herein encourages their use. The general, calibratable model does not rely on prescribed coefficients and can be applied to any channel within the scope of this research provided there is enough depth-averaged velocity data for calibration.

#### ***4.4 Discussion***

Two models have been presented for the prediction of the depth-averaged velocity distribution in compound channels: a general, calibratable model and a continuously varying parameter model. The models produce reasonable predictions of the depth-averaged velocity distribution for the range of calibration. Extension of the CV model beyond the calibration range does, however, induce significant errors in the prediction. The calibratable model has been shown to be applicable beyond the range tested. Each of these models was compared to two standard methods: the Divided Channel Method (DCM) and the Shiono and Knight Method (SKM). The models predicted the velocity distribution better than the DCM and with comparable accuracy to the predictions of the SKM for the range of calibration.

Although there are limitations to the models developed, it has been shown that accurate predictions of the depth-averaged velocity distribution can be made with proper calibration of the model. The general model is recommended when sufficient depth-averaged velocity data are available. Although the CV model produced erroneous results when applied beyond the calibration range, the form of the function was still reasonable.

Recalibration of the CV model would be appropriate for extension of the model beyond the calibration range, and a calibration approach has been identified.

The advantage of the models developed is the ease of application of a single function for the prediction of depth-averaged velocity in compound channels. To demonstrate the utility of a simple model, two applications of the model will now be presented: discharge prediction through velocity indexing and estimation of shear layer location and width.

## 5 APPLICATION I – DISCHARGE PREDICTION

Prediction of discharge in compound channels is an issue that has been approached from many angles. Some of the approaches summarized in section 1.2.5 include: Single Channel Method (SCM), Divided Channel Method (DCM), Ackers Method, and various Lateral Distribution Methods (LDMs). Another common method of discharge prediction in compound channels is by using an index-velocity rating. In this method an “index” velocity is measured at the same location for various flow measurements. This index velocity is then related to the observed mean velocity through a variety of models. A continuous stage record provides a relation between stage and cross-sectional area for the same flow measurements. From these relations the area can be determined for any stage, and the mean velocity can be found for any measured index velocity. The discharge is the product of the area and mean velocity (Rantz, 1982b).

Index-velocity relations take many forms, but two more commonly applied forms are presented in Equation 5.1 and Equation 5.2 (Sloat and Gain, 1995; Hittle et al., 2001; Morlock et al., 2002; Ruhl and Simpson, 2005). These equations provide two empirical approaches of estimating cross-sectional mean velocity from a measured index velocity. Equation 5.1 presents a simple linear model relating the two velocities while Equation 5.2 assumes the mean velocity is a function of the index velocity and stage. Both models rely on discharge measurements to calibrate the coefficients,  $c_i$ . In compound channels, index velocity ratings are often formulated separately for inbank and overbank measurements. The use of a separate index-velocity rating for overbank flows requires numerous overbank discharge measurements with which to accurately calibrate the

models. Overbank discharges are rare and measurement of these discharges is often time consuming, costly, and dangerous.

$$U_0 = c_1 U_{index} + c_2$$

**Equation 5.1**

$$U_0 = c_3 U_{index} + c_4 U_{index} h_{tot} + c_5$$

**Equation 5.2**

### ***5.1 Use of the Continuously Varying Model for Predicting Discharge***

Both the general model (Equation 2.9) and the continuously varying parameter model (Equation 4.3) are tools for the lateral prediction of depth-averaged velocity in compound channels, but they can also be used as index velocity ratings to predict discharge in compound channels. The models each take the form of Equation 5.3.

$$\frac{U_d(z)}{U_0} = f(z, Geometry, a_i)$$

**Equation 5.3**

If a measurement of depth-averaged velocity is used as an index velocity ( $U_{index}(z) = U_d(z)$ ), then the model can be rearranged as an index velocity relation (Equation 5.4).

$$U_0 = \frac{U_{index}(z)}{f(z, Geometry, a_i)}$$

**Equation 5.4**

Regardless of whether the general or continuously varying version of the model is used, Equation 5.4 represents a physically based index velocity rating that uses a depth-averaged velocity distribution to predict discharge as opposed to the empirical models

presented in Equation 5.1 and Equation 5.2. If the continuously varying parameter model is used, no overbank discharge measurements are necessary for calibration. Due to the ability of the model to predict discharge without calibration, the continuously varying model will now be assessed as a velocity rating tool.

### 5.1.1 Model Application to Calibration Range

The success of the CV model to provide an accurate index velocity rating and discharge prediction will now be assessed by applying the model to the compound channel data for which it was calibrated (Table 3.4).

For simplicity, the index velocity used in the following application is the observation of depth-averaged velocity nearest the channel centerline. The location of the index velocity near the center of the channel ensures that the velocity is being predicted by the logistic function. Therefore the index-velocity rating takes the form of Equation 5.5. Knowledge of channel geometry, stage, and index velocity are the only necessary variables to estimate the cross-sectional mean velocity.

$$U_0 = \frac{U_{index}(z)}{\frac{1.333e^{-2.872D_r}}{1 + 1.583e^{\frac{7.989(z-b_{top})}{b_{top}}}} + 1.527D_r^{0.642}}$$

**Equation 5.5**

The utility of the CV model as an index-velocity rating is that it does not require the overbank discharge measurements required of standard velocity indexing ratings (Equation 5.1 and Equation 5.2). Often when no overbank measurements are available for calibration, inbank velocity ratings are extended to overbank conditions. Therefore, in order to compare the accuracy of discharge estimates without available overbank

discharge data, the CV model is compared to inbank calibrations of common index velocity relations (Equation 5.1 and Equation 5.2).

Inbank velocity data exist for 3 of the Flood Channel Facility data series (FCF-01, FCF-02, FCF-03). These inbank measurements were used to calibrate the two empirical index velocity relations (Equation 5.1 and Equation 5.2). The CV model has been applied to the same three data sets. Figure 5.1 presents the results of each of the models for prediction of the cross-sectional mean velocity. Figure 5.2 presents the range of the absolute errors associated with each index velocity rating in the form of a boxplot.

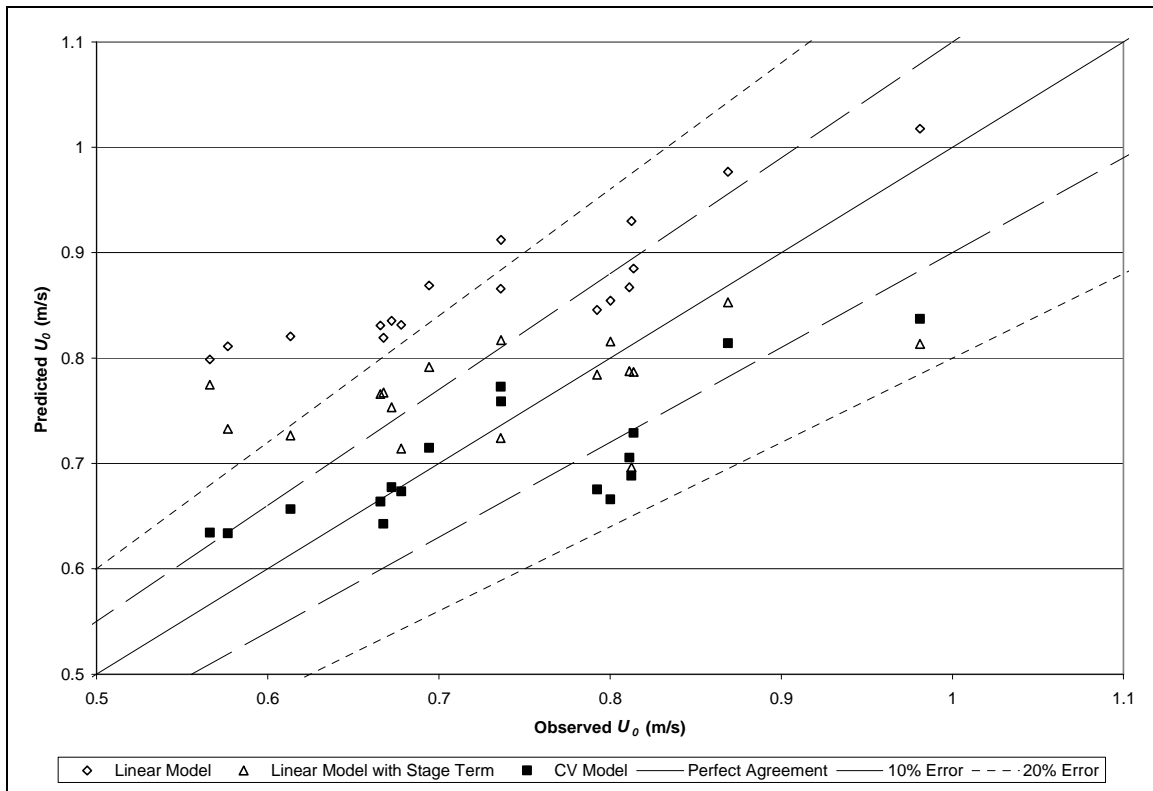


**Figure 5.1. Results of prediction of cross-sectional mean velocity by multiple velocity rating models**

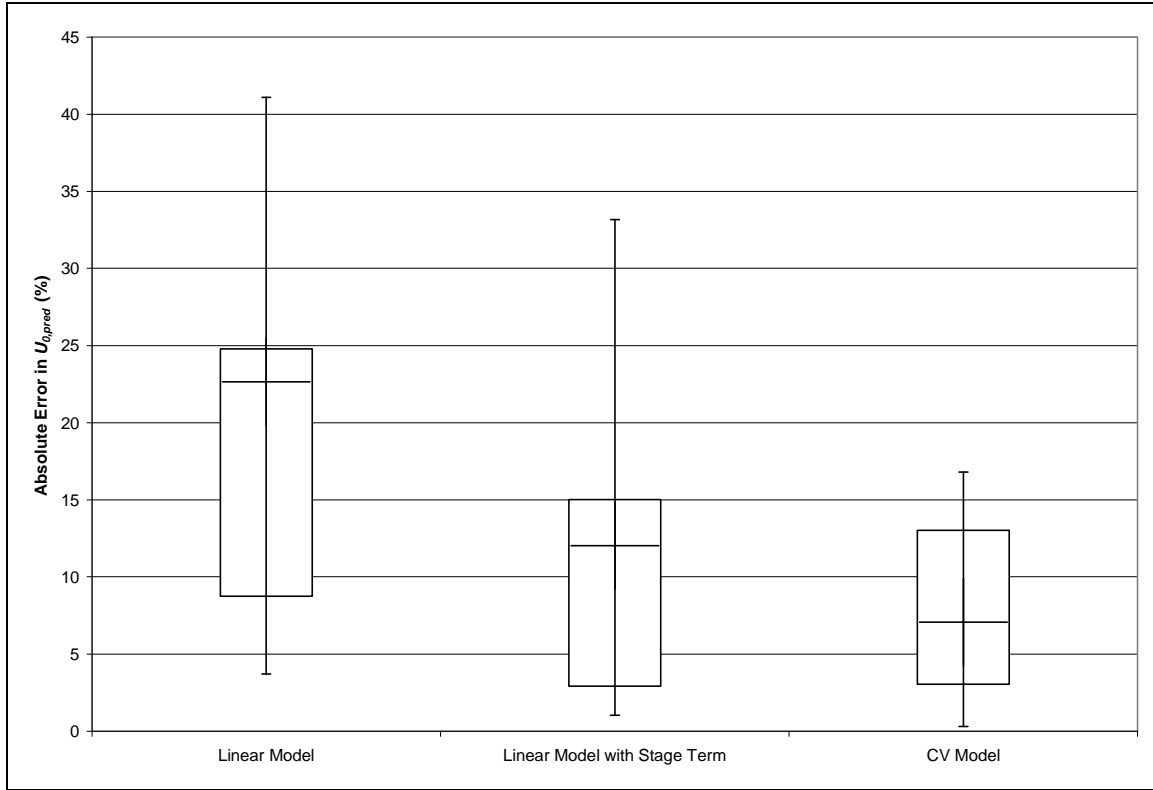


**Figure 5.2. Absolute error of multiple index velocity relations**

The CV model was also applied to the validation data sets (FCF-010602 and FCF-020402) to remove bias of results due to calibration. Inbank calibrations of Equation 5.1 and Equation 5.2 were also applied. Table 5.1 presents the absolute errors associated with use of each of these models to predict cross-sectional mean velocity.



**Table 5.1. Error in prediction of cross-sectional mean velocity for multiple velocity indexing models**

Test	Absolute Error (%)		
	Linear Model	Linear Model with Stage Term	CV Model
FCF-010602	25.0	5.2	3.5
FCF-020402	24.1	11.9	0.6

### 5.1.2 Extension beyond Model Calibration Range

The CV model's ability to extend beyond the range of calibration will now be assessed by the capacity of the model to predict mean velocity in the James and Brown (1977) and Collins and Flynn (1978) data sets. Figure 5.3 presents the predictions of cross-sectional mean velocity relative to the observed values. The model predicts the mean velocity rather poorly for both data sets. In order for the CV model to be used as an accurate velocity rating tool, accurate prediction of depth-averaged velocity in the main channel is critical. The poor prediction of the depth-averaged velocity in the main channel explained in section 4.2.3 has been shown to influence the errors associated with the mean velocity prediction. As shown in section 4.2.3, the asymptotic velocity of the floodplain shows less variability over geometric and roughness conditions. It is therefore hypothesized that if an index velocity on the floodplain was chosen, the prediction of mean velocity would be improved.

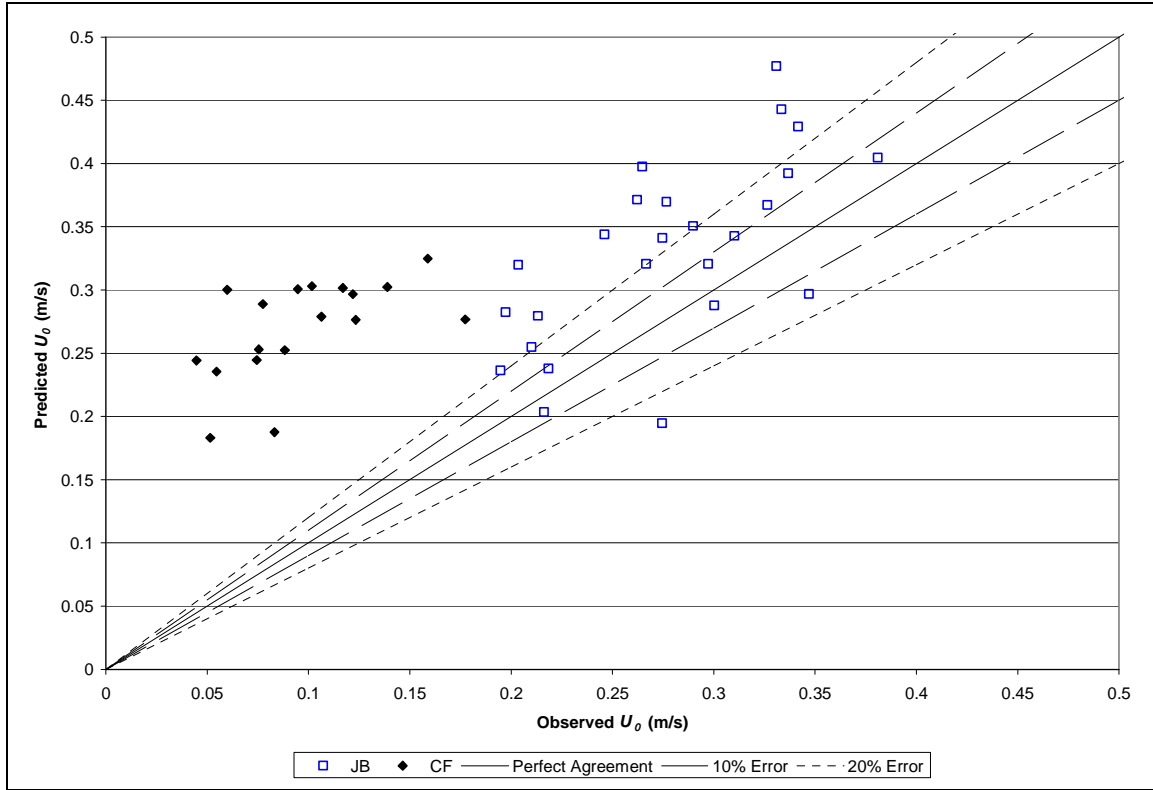


**Figure 5.3. Results of the CV model as applied to data beyond the project scope**

## 5.2 Discussion of Discharge Prediction

This chapter has shown that the models developed for prediction of the lateral distribution of depth-averaged velocity in compound channels can be applied to the prediction of discharge in compound channels in the form of index velocity ratings. These models provide a physical basis for overbank index velocity ratings.

The continuously varying parameter model (CV model) was applied to multiple compound channel experiments and was found to predict mean velocity within  $\pm 17\%$  of the observed values for calibration data sets. The model predicted less than 5% error in mean velocity for the validation data sets. This model requires no calibration to predict mean velocity; therefore, it is quite practicable as a tool for discharge prediction until reliable calibration data can be collected.

The model was also used to predict mean velocity in channels outside the scope of work. The results showed that the accuracy of the mean velocity prediction is highly dependent upon the accuracy of the depth-averaged velocity prediction of the index velocity. Therefore it is recommended that the depth-averaged velocity most accurately and reliably predicted be used as the index velocity if the CV model is to be applied as a velocity rating tool.

## 6 APPLICATION II – PREDICTION OF SHEAR LAYER LOCATION AND WIDTH IN COMPOUND CHANNELS

From the pioneering compound channel studies identifying large vortices along the main channel/floodplain interface (Sellin, 1964; Udeozo, 1967) to recent studies quantifying momentum transfer in these channels (van Prooijen, et al., 2005; Rameshwaran and Shiono, 2007), considerable effort has been made to investigate the turbulent structure of compound channels. This study has focused on prediction of the lateral distribution of depth-averaged velocity, but the models developed herein could be used to make some basic observations on the structure of the flow in compound channels. This chapter will highlight one potential use of the models developed, namely to predict the location ( $z_{ib}$  and  $z_{ob}$ ) and width ( $\delta$ ) of the shear layer (Figure 6.1).

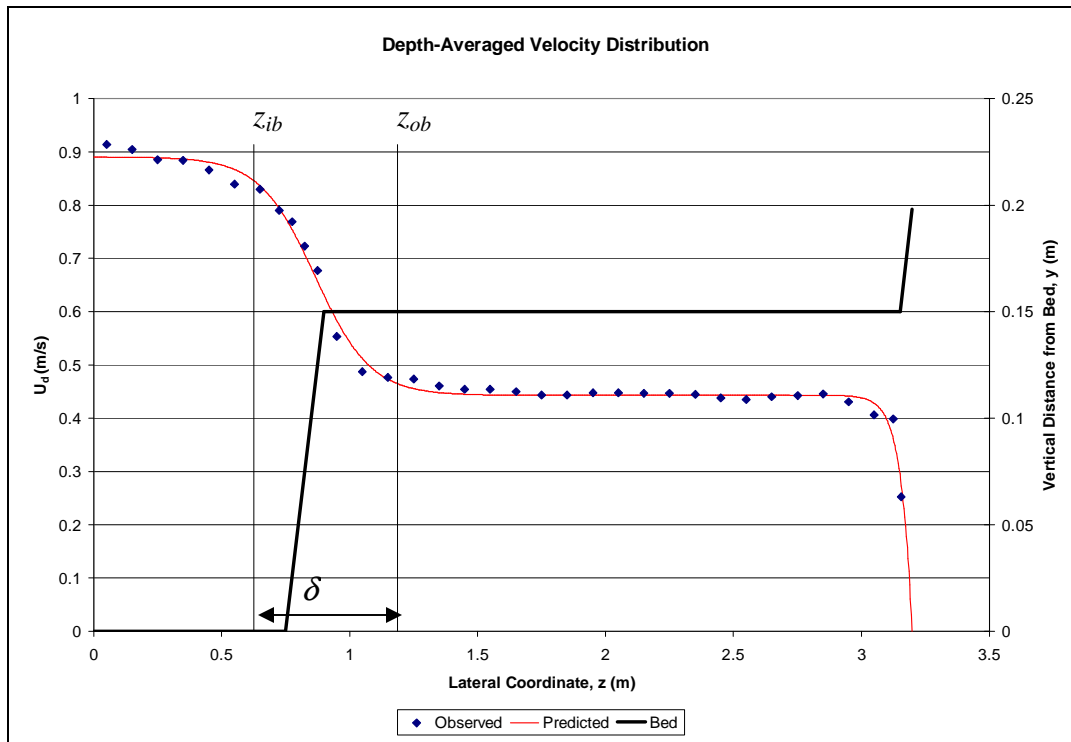


Figure 6.1. Compound channel shear layer schematic

Knowledge of the location and width of the shear layer is important for many applications. For example, flow measurement instrumentation should be positioned to minimize the errors in discharge prediction, and the placement of an instrument within the secondary current influenced flow of the shear layer would maximize this error. The width of the shear layer is also important for complex numerical simulation of compound channels. Many numerical models have been developed for prediction of the three-dimensional velocity profile in compound channels (Pezzinga, 1994; Sofialidis and Prinos, 1999). Knowledge of the most highly variant flow zone would allow for refinement of the numerical grid in the shear layer, and therefore better prediction of the velocity. The shear layer width is also used in the lateral distribution models of Alavian and Chu (1985) and van Prooijen et al. (2005). Rameshwaran and Shiono (2007) recently identified the model of Alavian and Chu (1985) as preferable to other LDMs in prediction of depth-averaged velocity and shear stress distributions. This multitude of applications encourages the development of a simple method for predicting the width and location of the shear layer in compound channels.

### ***6.1 Derivation of a Model for Shear Layer Width and Location***

Alavian and Chu (1985), Rhodes and Knight (1995), and van Prooijen et al. (2005) have all identified criteria for defining the width of the shear layer. All of these methods rely on some velocity or boundary shear stress criteria. For example, Rhodes and Knight (1995) define the boundaries of the shear layer as the lateral location when the depth-averaged velocity reaches a value within 5% of its laterally uniform value on the floodplain and in the main channel. These Authors propose 5% as a “compromise

between the conflicting requirements of a sufficiently large shear-layer width and a reasonably accurate estimate of it” (Rhodes and Knight, 1995).

Due to their asymptotic nature, both the general and continuously varying parameter models (Equation 2.9 and Equation 4.3, respectively) lend themselves to analysis of the width and location of the shear layer. In order to use the models, equations for the inner and outer bounds of the shear layer,  $z_{ib}$  and  $z_{ob}$ , respectively, must be developed. In the main channel and on the floodplain, the flow becomes laterally uniform, and the logistic model approaches its asymptotic limits (Equation 6.1 and Equation 6.2).

$$\lim_{z \rightarrow -\infty} \frac{U_d(z)}{U_0} = a_1 + a_4$$

**Equation 6.1**

$$\lim_{z \rightarrow \infty} \frac{U_d(z)}{U_0} = a_4$$

**Equation 6.2**

The location of the inner and outer boundaries of the shear layer can then be determined by specifying the points where there is a  $\varepsilon\%$  defect in the velocity profile from the asymptotic values (Rhodes and Knight, 1995) for both the main channel and the floodplain (Equation 6.3 and Equation 6.4, respectively).

$$\frac{U_d(z_{ib})}{U_0} = (1 - \varepsilon)(a_1 + a_4)$$

**Equation 6.3**

$$\frac{U_d(z_{ob})}{U_0} = (1 + \varepsilon)a_4$$

**Equation 6.4**

If these expressions are used in conjunction with the general model, equations for the location and width of the shear layer can be derived. Scaling of the shear layer quantities with the main channel top width,  $b_{top}$ , provides a more generic tool for assessment of the relative location of these boundaries (Equation 6.5 and Equation 6.6) and the shear layer width (Equation 6.7).

$$\frac{z_{ib}}{b_{top}} = 1 + \frac{1}{a_3} \ln \left[ \frac{1}{a_2} \left( \frac{a_1}{(1 - \varepsilon)a_1 - \varepsilon a_4} - 1 \right) \right]$$

**Equation 6.5**

$$\frac{z_{ob}}{b_{top}} = 1 + \frac{1}{a_3} \ln \left[ \frac{1}{a_2} \left( \frac{a_1}{\varepsilon a_4} - 1 \right) \right]$$

**Equation 6.6**

$$\frac{\delta}{b_{top}} = \frac{z_{ob}}{b_{top}} - \frac{z_{ib}}{b_{top}} = \frac{1}{a_3} \ln \left( \frac{\left( \frac{1 - \varepsilon}{\varepsilon^2} \right) a_1^2 - \left( \frac{2 - \varepsilon}{\varepsilon} \right) a_1 a_4 + a_4^2}{a_1 a_4 + a_4^2} \right)$$

**Equation 6.7**

Following Rhodes and Knight (1995), the criteria for the boundaries of the shear layer are set as the lateral locations where the depth-averaged velocity is within 5% of its asymptotic value ( $\varepsilon=0.05$ ). With this approximation, the equation for the width of the shear layer can be simplified to the following form:

$$\frac{\delta}{b_{top}} = \frac{1}{a_3} \ln \left( \frac{380a_1^2 - 39a_1a_4 + a_4^2}{a_1a_4 + a_4^2} \right)$$

**Equation 6.8**

## **6.2 Estimation of Shear Layer Width and Location**

This simple method of predicting the location and width of the shear layer allows the model user to examine the general flow structure in compound channels. For instance, if the prescribed relations of the CV model are utilized, the shear layer location and width are a function of relative depth alone and observations can be made regarding the general structure of compound channel shear layers over varying relative depth.

The CV model has been implemented to estimate the size and position of the shear layer for the calibration data sets. Since the general model provided estimates of the depth-averaged velocity distribution that showed little discrepancy from observed values, the model was also assumed to produce accurate estimates of the shear layer width and location. Figure 6.2 presents the CV model predictions of the shear layer location and width and the shear layer dimensions of the calibration data sets as calculated by the general model. As evident, the CV model provided reasonable agreement with the general model when estimating the location of the shear layer with 74% and 91% of the data points lying within 20% of the general model calculated values for the inner and outer boundaries, respectively. However, the errors in these estimates were compounded when estimating the shear layer width with only 50% of predicted values lying within 20% of the general model predicted values.



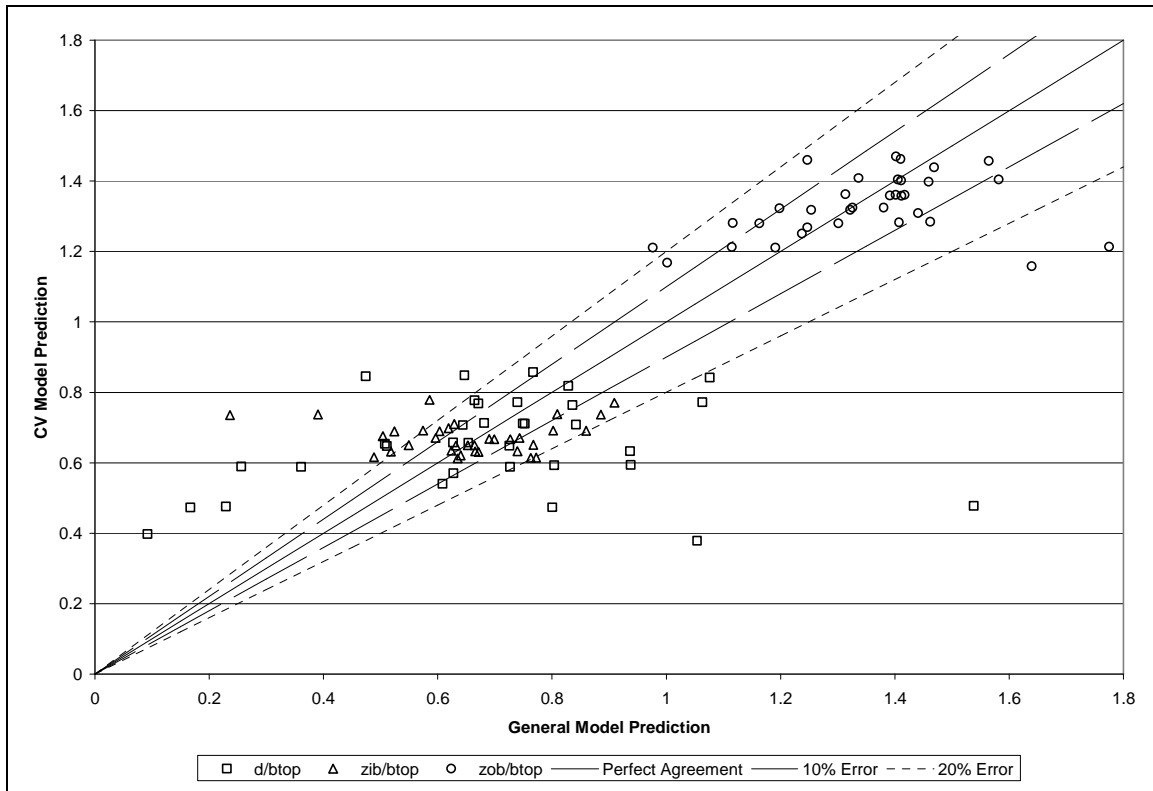


**Figure 6.2. Results of application of the CV Model to estimation of shear layer location and width**

Although the CV model does not provide accurate estimates of the shear layer width, practicable observations can still be made from these predictions. Figure 6.3 and Figure 6.4 display the CV model predictions for shear layer location and width. As previously mentioned, knowledge of the shear layer location allows for minimization of potential flow measurement errors due to instrument placement. Figure 6.3 shows that, in general, the inner boundary of the shear layer rarely intrudes into the main channel more than one quarter of the channel top width. This implies that flow measurement instrumentation (e.g. an “uplooking” ADCP) should be placed at a very minimum one quarter of the channel top width from the banks. This inner boundary also shows little variability with large changes in relative depth, so interference by the shear layer in

extreme events is of minimal concern. The outer boundary of the shear layer displays significant changes in location depending on flow depth. This boundary is on the floodplain for all events except large floods ( $D_r > 0.7$ ). For more frequent floods ( $D_r < 0.1$ ), the shear layer is shown to extend onto the floodplain more than one quarter of the channel top width. Therefore, instrumentation placed on floodplains should be located a significant distance from the channel banks to minimize measurement errors.

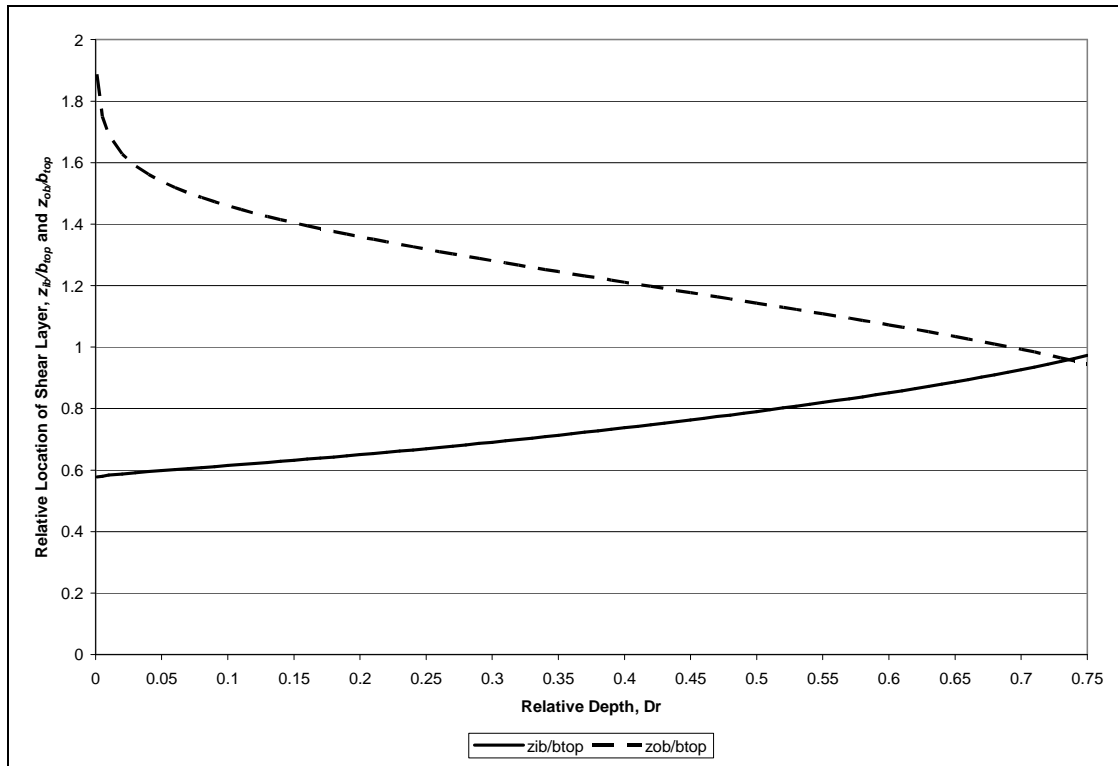


**Figure 6.3. Relative location of shear layer**

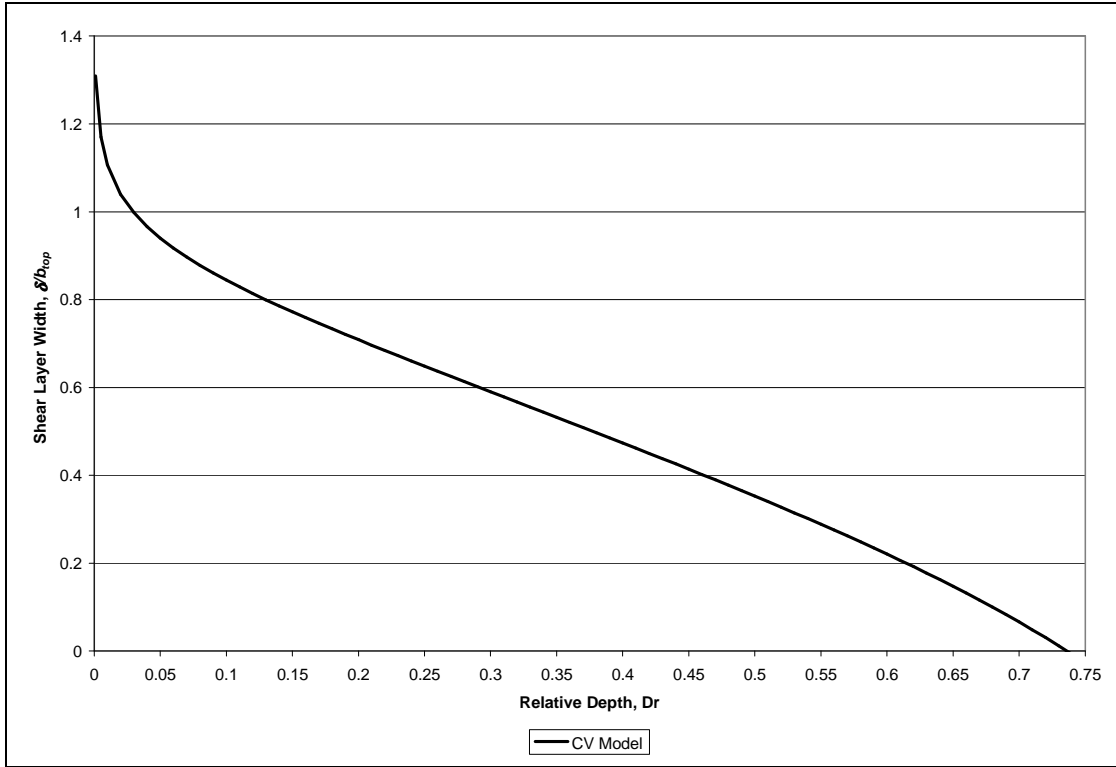


**Figure 6.4. Dimensionless shear layer width,  $\delta b_{top}$**

The CV model predictions of the shear layer width have shown significant variability, but the model can still provide useful, qualitative trends of shear layer width. The shear layer width has been shown to be approximately zero at relative depths of greater than 0.73 implying that for channels conveying extremely large floods, the shearing of the flow due to velocity gradient becomes relatively unimportant at large relative depths. This is consistent with the observation of Ackers (1992) who found for high relative depths a compound channel behaves as a single channel.

The models developed herein have been applied to estimation of shear layer width and location to prove their utility in producing basic observations of compound channel flow structure. The quantitative estimates of the CV model showed significant discrepancy from observed values; however, the qualitative observations agreed with those of previous researchers.

## 7 SUMMARY AND RECOMMENDATIONS

### 7.1 *Summary*

The lateral distribution of depth-averaged velocity has been shown to be of importance for many applications in compound channels. Compound channels have been examined by many researchers both experimentally and analytically. Many theoretically based models exist to model the lateral distribution of depth-averaged velocity; however, there exist no simple empirical approaches to this complex problem. This research therefore aimed to obtain a simple model by way of dimensional analysis, and calibrate and verify this model with the wealth of experimental data obtained. The research was limited to the simplest compound channel environment: wide, symmetric, straight compound channels of homogenous roughness under uniform flow conditions.

The lateral distribution of depth-averaged velocity in compound channels was assessed as three regions of velocity: the laterally uniform region of the main channel, the trapezoidal floodplain, and the region of rapid change in between the two, the shear layer. Two functions were used to model the lateral velocity distribution across these three regions. The model of Wilkerson and McGahan (2005), which was developed for use in trapezoidal channels, was adapted for use in trapezoidal floodplains. A logistic function was used to model the lateral distribution of velocity in the shear layer and main channel. These functions were assumed to meet at a critical location on the floodplain where the depth-averaged velocity is laterally uniform.

The combination of these functions led to a general, calibratable model for the lateral distribution of depth-averaged velocity in compound channels. This model

requires geometric and hydraulic data along with depth-averaged velocity data in order to calibrate the model coefficients. This model provided accurate predictions of the velocity distribution with 95% of predicted depth-averaged velocities lying within 10% of their observed values.

The coefficients of this general model were output for 34 data sets. These coefficients were then analyzed to ascertain correlations with geometric and hydraulic characteristics of the channels. These relations were used to develop a continuously-varying parameter model that requires only basic geometric and hydraulic character of a system in order to predict the distribution of depth-averaged velocity. For the data for which the model was calibrated, 78% of predicted depth-averaged velocities were within 10% of their observed values, and for the validation data within the calibration range, 54% of predicted depth-averaged velocities were within 10% of their observed values and 100% of predicted values were within 20% of the observed values. The model was tested beyond its calibration range using data that was out of the scope of the research, and the model provided poor estimates of the lateral distribution of depth-averaged velocity. For this reason, the general model is recommended whenever depth-averaged velocity data are available, and the continuously varying parameter model should only be applied within the range of geometric and hydraulic conditions used for calibration.

Application of the model to the prediction of discharge in compound channels was examined. The forms of the models developed lend themselves well to use in index velocity relations. The continuously varying parameter model was used to predict the discharge in compound channels, and provided accurate results: less than 20% error for the calibration data and less than 5% error for the validation data. Commonly used index

velocity ratings produced less accurate results when extended to overbank conditions (23 and 12% average errors, respectively).

The continuously varying model was applied to the analysis of the complex flow structure of compound channels. The model provided a useful tool for qualitative assessment of the location and width of the shear layer.

Two models have been presented for lateral prediction of depth-averaged velocity. These models provide practicable tools for the prediction of the lateral distribution of depth-averaged velocity in compound channels. The models should be applied only to the range of geometric and hydraulic characteristics for which they were developed. The models have been shown to have applications in the prediction of discharge and analysis of flow structure in compound channels.

## **7.2 *Recommendations***

The research presented in this thesis demonstrated the potential of using a simple empirical function to model the lateral distribution of depth-averaged velocity in compound channels. The following section highlights potential improvements and applications of such a model.

### **7.2.1 Model Improvement**

The continuously varying model has been shown to accurately model the velocity distribution for those channels for which it was calibrated, however the model does not accurately predict the velocity distribution for all channels, and further research is warranted for the improvement of the model. It is hypothesized that errors may have been introduced to the analysis by the use of channel top width,  $b_{top}$ , as a scaling

parameter. These errors would be further magnified by the narrow range of calibration for the channel aspect ratio. It is thought that the width of the channel side slope,  $s_{ch}h_{ch}$ , would perhaps serve as a better scaling parameter.

The critical point between the two functions,  $z_c$ , was defined as the point where the depth-averaged velocity is within 0.1% of the asymptotic velocity. This criterion was chosen to ensure that the depth-averaged velocity reached its asymptotic value on the floodplain. It is hypothesized that the criterion could be eased to better coincide with the criterion used in analysis of the shear layer width (5%).

The model has been shown to be easily applied to many situations, but further research is needed to identify a robust approach to calibrating the many coefficients of the model. The prescribed relations of the continuously varying parameter model proved to work well for the calibration range, but beyond the calibration range the accuracy declined. Replacement of the prescribed relations with relations calibrated to each channel is recommended. Thus, an order of calibration is required for calibrating the model as data are obtained.

Although the model works well for the channels examined, most natural compound channels are far from straight, symmetric channels with homogeneous roughness under uniform flow conditions. Further research is therefore needed to extend the scope of the model to include: heterogeneous roughness in the cross-section (e.g. forested floodplains), asymmetry of the channel geometry, meandering, narrow floodplains, and variable backwater conditions.

Further research is also needed to refine the calibration of the model. More data increase the robustness of any empirical model. Therefore, it is suggested that the

continuously varying parameter model be recalibrated as data become available.

Particular emphasis should be placed on the calibration of the model with data from natural rivers.

### **7.2.2 Applications of Model**

Two applications of the model have been presented as proof of the utility of a tool for the prediction of the lateral distribution of depth-averaged velocity in compound channels. These applications are not the only potential applications of this type of model.

First and foremost, the model could be applied to its design purpose, prediction of the lateral distribution of velocity in compound channels. Knowledge of the velocity distribution has implications for modeling edge effects during flow measurement, improvement of stream restoration design, and improvement of navigation analyses.

The model has been shown as a tool for index velocity ratings. Further research is needed to examine the robustness of the model to the application of flow measurement.

As was shown in Chapter 6, the model has potential to aid researchers in identifying the structure of flow in compound channels. These observations could then be used as qualitative tools to refine flow measurement instrumentation or numerical modeling of compound channels.

Further research is needed to examine the potential of coupling the model with a resistance relation to predict shear stress. Prediction of the lateral distribution of shear stress in compound channels could be used for riprap design, sediment transport analyses, and flow measurement instrumentation (placement of gaging to prevent sediment deposition on sensors).



## BIBLIOGRAPHY

- Abril, J. B. and D. W. Knight. (2004). "Stage-Discharge Prediction for Rivers in Flood Applying a Depth-Averaged Model." *Journal of Hydraulic Research*. IAHR, 42 (6), 616-629.
- Ackers, P. (1991). "Discussion on 4 papers of the Journal of Hydraulic Research, 28 (2), 1990. *Journal of Hydraulic Research*. IAHR, 29 (2), 263-271.
- Ackers, P. (1992). "Hydraulic Design of Two-Stage Channels." *Proceedings of the Institute of Civil Engineers, Water, Maritime & Energy*, London, 96, 247-257.
- Ackers, P. (1993). "Flow Formulae for Straight Two-Stage Channels." *Journal of Hydraulic Research*. IAHR, 31 (4), 509-531.
- Alavian, V. and V.H. Chu. (1985). "Turbulent Exchange Flow in Shallow Compound Channel." *Proceedings of the 21<sup>st</sup> IAHR Congress*, IAHR, Melbourne, Australia, Vol. 3, 446-451.
- American Society of Civil Engineers. (2000). Hydraulic Modeling: Concepts and Practice. ASCE Manuals and Reports on Engineering Practice No. 97. ASCE, Reston, Virginia.
- Arnold, U., J. Hottges, and G. Rouve. (1989). "Turbulence and Mixing Mechanisms in Compound Open Channel Flow." *Proceedings of the 23<sup>rd</sup> IAHR Congress*. IAHR, Ottawa, Canada, A133-140.
- Asano, T., H. Hashimoto, and K. Fujita. (1985). "Characteristics of variation of Manning's Roughness Coefficient in Compound Cross-section." *Proceeding of the 21<sup>st</sup> IAHR Congress*, IAHR, Melbourne, Australia, Vol. 6.
- Atabay, S. and D.W. Knight. (2006). "1-D Modelling of Conveyance, Boundary Shear, and Sediment Transport in Overbank Flow." *Journal of Hydraulic Research*. IAHR, 44 (6), 739-754.
- Atabay, S., D. W. Knight, and G. Seckin. (2005). "Effects of Overbank Flow on Fluvial Sediment Transport Rates." *Proceedings of the Institute of Civil Engineers, Water Management*, London, 158, 25-34.
- Babaeyan-Koopaei, K., D.A. Ervine, and R.H.J. Sellin. (2001). "Development of a UK Database for Predicting Flood Levels for Overbank Flows." *Journal of the Institution of Water and Environmental Management*. Vol. 15 (4), 244-251.
- Babaeyan-Koopaei, K., D.A. Ervine, P.A. Carling, and Z. Cao. (2002). "Velocity and Turbulence Measurements for Two Overbank Flow Events in River Severn." *Journal of Hydraulic Engineering*. ASCE, 128 (10), 891-900.

- Barishnikov, N.B. and G.V. Ivanov. (1971). "Role of flood discharge of a river channel." *Proceedings of the 14<sup>th</sup> IAHR congress*, Paris, 1971, 141-144.
- Berz, G. (2000). "Flood Disasters: Lessons from the Past – Worries for the Future." *Proceedings of the 28<sup>th</sup> Congress of IAHR*. IAHR, Graz, Australia, 9-16.
- Bhowmik, N.G. and M. Demissie. (1982). "Carrying Capacity of Floodplains." *Journal of the Hydraulics Division*. ASCE, Vol. 108 (3), 443-452.
- Blalock, M.E. and T. Sturm. (1981). "Minimum Specific Energy in Compound Open Channels." *Journal of the Hydraulics Division*. ASCE, Vol. 107 (6), 299-717.
- Blanckaert, K. and U. Lemmin. (2006). "Means of Noise Reduction in Acoustic Turbulence Measurements." *Journal of Hydraulic Research*. IAHR, 44 (1), 3-17.
- Booij, R. and J. Tukker. (2001). "Integral Model of Shallow Mixing Layers." *Journal of Hydraulic Research*. IAHR, 39 (2), 169-179.
- Bousmar, D. (2002). "Flow modeling in compound channels: Momentum transfer between main channel and prismatic or non-prismatic floodplains." PhD Thesis, Universite catholique de Louvain, Louvain, France.
- Bousmar, D. N. Riviere, S. Proust, A. Paquier, R. Morel, and Y. Zech. (2005). "Upstream Discharge Distribution in Compound-Channel Flumes." *Journal of Hydraulic Engineering*. ASCE, 131 (5), 408-412.
- Bousmar, D., N. Wilkin, J. H. Jacquemart, and Y. Zech. (2004). "Overbank Flow in Symmetrically Narrowing Floodplains." *Journal of Hydraulic Engineering*. ASCE, 130 (4), 305-312.
- Bousmar, D. and Y. Zech. (1999). "Momentum Transfer for Practical Flow Computation in Compound Channels." *Journal of Hydraulic Engineering*. ASCE, 125 (7), 696-706.
- Bousmar, D. and Y. Zech. (2001a). "Secondary-Current Significance in Momentum Transfer for Compound Channels Flow Modelling." *Proceedings of the 29<sup>th</sup> IAHR Congress*. IAHR, Beijing, China, 185-195.
- Bousmar, D. and Y. Zech. (2001b). "Periodic Turbulent Structures Modelling in a Symmetric Compound Channel." *Proceedings of the 29<sup>th</sup> IAHR Congress*. IAHR, Beijing, China, 244-249.

Bousmar, D. and Y. Zech. (2001c). "Discussion of Two-Dimensional Solution for Straight and Meandering Overbank Flows, by D.A. Ervine, K. Babaeyan-Koopaei, and R.H.J. Sellin, 2000, 126 (9)." *Journal of Hydraulic Engineering*. ASCE, 128 (5), 5501-551.

Bousmar, D. and Y. Zech. (2004). "Velocity Distribution in Non-Prismatic Channels." *Proceedings of the Institute of Civil Engineers Water, Maritime and Energy*. Vol. 157, June, 99-108.

Bridge, J.S. (2003). Rivers and Floodplains: Forms, Processes, and Sedimentary Records. Blackwell Publishing, Malden, Massachusetts.

Cao, Z., J. Meng, G. Pender, and S. Wallis. (2006). "Flow resistance and momentum flux in compound open channels." *Journal of Hydraulic Engineering*. ASCE, 132 (12), 1272-1282.

Carling, P.A., Z. Cao, M.J. Holland, D.A. Ervine, and K. Babaeyan-Koopaei. (2002). "Turbulent Flow Across a Natural Compound Channel." *Water Resources Research*. AGU, 38 (12), 6.1-6.12.

Cassels, Lambert, and Myers. (2001). "Discharge Prediction in Straight Mobile Bed Compound Channels." *Proceedings of the Institute of Civil Engineers Water, Maritime and Energy*. Vol. 148 (3), 177-188.

Chaudry, M.H. (1993). Open Channel Flow. Prentice Hall, Englewood Cliffs, New Jersey.

Chaudry, M.H. and S.M. Bhallamudi. (1988). "Computation of Critical Depth in Symmetrical Compound Channels." *Journal of Hydraulic Research*. IAHR, Vol. 26 (4), 377-396.

Chiu, C. L. and C. A. Abidin Said. (1995). "Maximum and Mean Velocities and Entropy in Open-Channel Flow." *Journal of Hydraulic Engineering*. ASCE, 121 (1), 26-35.

Chiu, C. L. and J. D. Chiou. (1986). "Structure of 3-D Flow in Rectangular Open Channels." *Journal of Hydraulic Engineering*. ASCE, 112 (11), 1050-1068.

Chiu, C. L. and G. F. Lin. (1983). "Computation of 3-D Flow and Shear in Open Channels." *Journal of Hydraulic Engineering*. ASCE, 109 (11), 1424-1440.

Chiu, C.L. and N.C. Tung. (2002). "Maximum Velocity and Regularities in Open Channel Flow." *Journal of Hydraulic Engineering*. ASCE, 128 (4), 390-398.

Chiu, C. L., W. Jin and Y. C. Chen. (2000). "Mathematical Models of Distribution of Sediment Concentration." *Journal of Hydraulic Engineering*. ASCE, 126 (1), 16-23.

- Chow, V.T. (1959). Open-Channel Hydraulics. McGraw-Hill, London, England.
- Collins, D.L. and K.M. Flynn. (1978). "A Summary of Measured Hydraulic Data for the Series of Steady and Unsteady Flow Experiments over Uniform Grass Roughness." Open-File Basic Data Report 78-808, U.S. Geological Survey.
- Deuller, J.W., G.H. Toebes, and B.C. Udeozo. "Uniform Flow in Idealized Channel-Floodplain Geometries." *Proceedings of the 12<sup>th</sup> IAHR Congress*. IAHR, Vol. A, 218-225.
- Dey, S. and M.F. Lambert. (2006). "Discharge prediction in compound channels by end depth method." *Journal of Hydraulic Research*. IAHR, Vol. 44 (6), 767-776.
- Dracos, T. and P. Hardegger. (1987). "Steady uniform flow in prismatic channels with flood plains." *Journal of Hydraulic Research*. IAHR, Vol. 25 (2), 169-185.
- Elliot, S.C.A. and R. H. Sellin. (1990). "SERC Flood Channel Facility: Skewed Flow Experiments." *Journal of Hydraulic Research*. IAHR, 28 (2), 197-214.
- Ervine, D.A. and J.I. Baird. (1982). "Rating Curves for Rivers with Overbank Flows." *Proceedings of Institution of Civil Engineers, Part II*, Vol. 73, 465-472.
- Ervine, D.A., K. Babaeyan-Koopaei, and R.H.J. Sellin. (2000). "Two-Dimensional Solution for Straight and Meandering Overbank Flows." *Journal of Hydraulic Engineering*. ASCE, 126 (9), 653-669.
- Ervine, D.A. and H.K. Jasem. (1989). "Flood Mechanisms in Meandering Channels with Floodplains." *Proceedings of the 23<sup>rd</sup> IAHR Congress*. IAHR, Ottawa, Canada, B449-456.
- Fischer, H.B., E.J. List, R.C.Y. Koh, J. Imberger, and N.A. Brooks. (1979). Mixing in Inland and Coastal Waters. Academic Press Inc., New York.
- Fukuhara, T. and A. Murota. (1990). "Discharge Assessment in Compound Channel with Floodplain Roughness." *Proceedings of the International Conference on River Flood Hydraulics*, John Wiley & Sons, Chichester, England, 153-162.
- Greenhill, R.K., and R.H.J. Sellin. (1993). "Development of a simple method to predict discharge in compound meandering channels." *Proceedings of the Institute of Civil Engineers, Water, Maritime & Energy*, London, 101, 37-44.
- Helsel, D. R. and R. M. Hirsch. (2002). "Chapter A3: Statistical Methods in Water Resources." *Techniques of Water Resources Investigations, Book 4, Chapter A3*, United States Geological Survey.

- Helmio, T. (2002). "Unsteady 1D Flow Model of Compound Channel with Vegetated Floodplain." *Journal of Hydrology*. Elsevier Science, 269, 89-99.
- Helmio, T. (2004). "Flow Resistance due to Lateral Momentum Transfer in Partially Vegetated Rivers." *Water Resources Research*. AGU, Vol. 40 (5).
- Higginson, N.N.J. and H.T. Johnston. (1990). "Effect of Scale Distortion in a Compound River Channel Model Study." *Proceedings of the International Conference on River Flood Hydraulics*, John Wiley & Sons, Chichester, England, 391-401.
- Hill, T. and P. Lewicki. (2006). STATISTICS Methods and Applications. StatSoft Tulsa, Oklahoma.
- Hittle, C., E. Patino, and M. Zucker. (2001). "Freshwater Flow from Estuarine Creeks into Northeastern Florida Bay." Water-Resources Investigations Report 01-4164, U.S. Geological Survey.
- Holden, A.P. and C.S. James. (1989). "Boundary shear distribution on floodplains." *Journal of Hydraulic Research*. IAHR, Vol. 27 (1), 75-89.
- Houk, I.E. (1918). "Calculation of Flow in Open Channels." *Technical Report (Part IV)* for the Miami Conservation District. Miami, Ohio.
- James, M. and B. J. Brown. (1977). "Geometric Parameters that Influence Floodplain Flow" Research Report H-77-1, U.S. Army Corps of Engineers Waterways Experiment Station, Vicksburg, Mississippi.
- Johnston, H. T. and N. N. J. Higginson. (1991). "Physical and Mathematical Modelling of Boundary Resistance in a Two-Stage Channel." In Channel Flow Resistance: A Centennial of Manning's Formula. Water Resources Publications, Littleton, Colorado, 356-369.
- Karamisheva, R. D., J. F. Lyness, W.R.C. Myers, and J.B.C. Cassells. (2005). "Improving Sediment Discharge Prediction for Overbank Flows." *Proceedings of the Institute of Civil Engineers: Water Management*. Vol. 158 (3), 603-613.
- Kawahara, H. and N. Tamai. (1989). "Mechanism of Lateral Momentum Transfer in Compound Open Channel Flow." *Proceedings of the 23<sup>rd</sup> IAHR Congress*. IAHR, Ottawa, Canada, B463-470.
- Keller, R. J. and W. Rodi. (1988). "Prediction of Flow Characteristics in Main Channel/Floodplain Flows." *Journal of Hydraulic Research*. IAHR, 26 (4), 425-441.
- Knight, D. W. (2006a). "Introduction to Flooding and River Basin Modelling." In *River Basin Modelling for Flood Risk Mitigation*. Eds. D. W. Knight and A. Y. Shamseldin. Taylor and Francis: New York, 1-19.

- Knight, D. W. (2006b). "River Flood Hydraulics: Theoretical Issues and Stage-Discharge Relationships." In *River Basin Modelling for Flood Risk Mitigation*. Eds. D. W. Knight and A. Y. Shamseldin. Taylor and Francis: New York, 301-334.
- Knight, D. W. (2006c). "River Flood Hydraulics: Validation Issues in One-Dimensional Flood Routing Methods." In *River Basin Modelling for Flood Risk Mitigation*. Eds. D. W. Knight and A. Y. Shamseldin. Taylor and Francis: New York, 335-385.
- Knight, D. W. and J. B. Abril. (1996). "Refined Calibration of a depth-averaged Model for Turbulent Flow in a Compound Channel." *Proceedings of the Institute of Civil Engineers Water, Maritime and Energy*. Vol. 118, September, 151-159.
- Knight, D. W. and F. A. Brown. (2001). "Resistance Studies of Overbank Flow in Rivers with Sediment using the Flood Channel Facility." *Journal of Hydraulic Research*. IAHR, 39 (3), 283-301.
- Knight, D. W. and J. D. Demetriou. (1983). "Floodplain and Main Channel Flow Interaction." *Journal of Hydraulic Engineering*. ASCE, 109 (8), 1073-1092.
- Knight, D. W. and M. E. Hamed. (1984). "Boundary Shear in Symmetrical Compound Channels." *Journal of Hydraulic Engineering*. ASCE, 110 (10), 1412-1430.
- Knight, D. W. and R. J. Sellin. (1987). "SERC Flood Channel Facility." *Journal of the Institution of Water and Environmental Management*. Vol. 1 (2), 198-204.
- Knight, D. W. and K. Shiono. (1990). "Turbulence Measurements in a Shear Layer Region of a Compound Channel." *Journal of Hydraulic Research*. IAHR, 28 (2), 175-196.
- Knight, D. W. and K. Shiono. (1996). "River Channel and Floodplain Hydraulics." Chapter in *Floodplain Processes*. John Wiley & Sons Ltd, 139-181.
- Knight, D. W., J. D. Demetriou, and M.E. Hamad. (1984). "Stage Discharge Relationships for Compound Channels." *Proceedings of the 1<sup>st</sup> International Conference on Channels and Channel Control Structures* (ed. K. V. H. Smith), Springer, 4.21-4.35.
- Knight, D.W., P.G. Samuels, and K. Shiono. (1990). "River Flow Simulations: Research and Developments." *Journal of the Institution of Water and Environmental Management*. Vol. 4 (2), 163-175.
- Knight, D. W., K. Shiono, and J. Pirt. (1989). "Prediction of Depth Mean Velocity and Discharge in Natural Rivers with Overbank Flow." *Proceedings of the International Conference on Hydraulics and Environmental Modelling of Coastal, Estuarine, and River Waters*, R. A. Falconer, P. Goodwin, and R. G. S. Matthew, eds. Gower Technical, Bradford, U. K., 419-428.

- Kolyshkin, A. A. and M. S. Ghidaoui. (2002). "Gravitational and Shear Instabilities in Compound and Composite Channels." *Journal of Hydraulic Engineering*. ASCE, 128 (12), 1076-1086.
- Krishnappan, B.G. and Y.L. Lau. (1986). "Turbulence Modelling of Floodplain Flows." *Journal of Hydraulic Engineering*. ASCE, Vol. 112 (4), 251-266.
- Lambert, M.F. and W.R.C. Myers. (1998). "Estimating the Discharge Capacity in Straight Compound Channels." *Procedures of the Institute of Civil Engineers: Water, Maritime, and Energy*. Vol. 130, 84-94.
- Lambert, M. F. and R. H. J. Sellin. (1996). "Discharge Prediction in Straight Compound Channels Using the Mixing Length Concept." *Journal of Hydraulic Research*. IAHR, 34 (3), 381-394.
- Lansford, W.M. and W.D. Mitchell. (1949). "An investigation of the backwater profile for steady flow in prismatic channels." University of Illinois Engineering Experiment Station Bulletin Series No. 381.
- Lean, G.H. and T.J. Weare. (1979). "Modeling Two-dimensional Circulating Flow." *Journal of the Hydraulics Division*. ASCE, Vol. 105 (1), 17-26.
- Lee, P. J., M. F. Lambert, and A. R. Simpson. (2002). "Critical Depth Prediction in Straight Compound Channels." *Proceedings of the Institute of Civil Engineers Water, Maritime and Energy*. Vol. 154 (4), 317-332.
- Lyness, J. F. and W. R. C. Myers. (1994). "Comparisons between Measured and Numerically Modelled Unsteady Flows in a Compound Channel Using Different Representations of Friction Slope." *Proceedings of the Second International Conference on River Flood Hydraulics*, John Wiley & Sons, Chichester, England, 391-401.
- Lyness, J.F., W.R.C. Myers, and J.B. Wark. (1997). "The use of different conveyance calculations for modeling flows in a compact compound channel." *Journal of the Institute of Water and Environmental Management*. Vol. 11 (5), 335-340.
- Martin, L.A. and W.R.C. Myers. (1991). "Measurement of overbank flow in a compound river channel." *Proceedings – Institution of Civil Engineers, Research and Theory*. Vol. 91, 645-657.
- Moramarco, T., C. Saltalippi, and V. P. Singh. (2004). "Estimation of Mean Velocity in Natural Channels Based on Chiu's Velocity Distribution Equation." *Journal of Hydraulic Engineering*. ASCE, 130 (1), 42-50.

- Morlock, S.E., H.T. Nguyen, and J.H. Ross. (2002). "Feasibility of Acoustic Doppler Velocity Meters for the Production of Discharge Records from United States Geological Survey Streamflow-Gaging Stations." Water-Resources Investigations Report 01-4157, U.S. Geological Survey.
- Morvan, H. P. (2005). "Channel Shape and Turbulence Issues in Flood Flow Hydraulics." *Journal of Hydraulic Engineering*. ASCE, 131 (10), 862-865.
- Myers, W.R.C.. (1978). "Momentum transfer in a compound channel." *Journal of Hydraulic Research*. IAHR, Vol. 16 (2), 139-150.
- Myers, W.R.C.. (1987). "Velocity and Discharge in Compound Channels." *Journal of Hydraulic Engineering*. ASCE, Vol. 113 (6), 753-766.
- Myers, W. R. C. (1990). "Physical Modeling of a Compound River Channel." *Proceedings of the International Conference on River Flood Hydraulics*, John Wiley & Sons, Chichester, England, 381-390.
- Myers, W.R.C.. (1991). "Influence of Geometry on Discharge Capacity of Open Channels." *Journal of Hydraulic Engineering*. ASCE, 117 (5), 676-680.
- Myers, W. R. C. and E. K. Brennan. (1990). "Flow Resistance in a Compound Channel." *Journal of Hydraulic Research*. IAHR, 28 (2), 141-155.
- Myers, W.R.C. and E.M. Elsayy. (1975). "Boundary Shear in Channel with Floodplain." *Journal of the Hydraulics Division*. ASCE, 101 (7), 933-946.
- Myers, W. R. C. and J. F. Lyness. (1997). "Discharge Ratios in Smooth and Rough Compound Channels." *Journal of Hydraulic Engineering*. ASCE, 123 (3), 182-188.
- Myers, W. R. C., J.F. Lyness, and J. Cassells. (2001). "Influence of Boundary Roughness on Velocity and Discharge in Compound River Channels." *Journal of Hydraulic Research*. IAHR, 39 (3), 311-319.
- Naot and W. Rodi. (1982). "Calculation of Secondary Currents in Channel Flow." *Journal of Hydraulic Engineering*. ASCE, 108 (8), 984-969.
- Naot, D., I. Nezu, and H. Nakagawa. (1993). "Hydrodynamic Behavior of Compound Rectangular Open Channels." *Journal of Hydraulic Engineering*. ASCE, 119 (3), 390-408.
- Nezu, I. (2005). "Open Channel Flow Turbulence and Its Research Prospects in the 21<sup>st</sup> Century." *Journal of Hydraulic Engineering*. ASCE, 130 (4), 229-246.
- Nezu, I. and H. Nakagawa. (1993). "Turbulence in Open-Channel Flows." *IAHR Monograph Series*, A. A. Balkema, Rotterdam, 1-281.



- Nicollet, G. and M. Uan. (1979). "Ecoulements permanents a surface libe et lits compose." *La Houille Blanche*, No. 1, 21-30.
- Noutsopoulos, G.C. and P.A. Hadjipanous. (1983). "Discharge Computations in Compound Channels." *Proceedings of the 20<sup>th</sup> IAHR Congress*, IAHR, Moscow, 173-180.
- Odell, R. (2000). "A Two-Dimensional Velocity Distribution Model for Gradually Varied Open Channel Flow Using Poisson's Equation." PhD Thesis, Utah State University, Logan, Utah.
- Ogink, H.J.M. (1985). "The Effective Viscosity Coefficient in 2-D Depth-Averaged Flow Models." *Proceedings of the 21<sup>st</sup> IAHR Congress*, IAHR, Melbourne, Australia, Vol. 3, 475-479.
- Ozbek, T., M. B. Kocyigit, and O. Kocyigit. (2004). "Comparison of Methods for Predicting Discharge in Straight Compound Channels Using the Apparent Shear Stress Concept." *Turkish Journal of Engineering and Environmental Science*. Vol. 28, 101-109.
- Pappenberger, F., P. Matgen, K. J. Beven, J. B. Henry, L. Pfister, and P. de Fraipont. (2004). "The Influence of Rating Curve Uncertainty on Flood Inundation Predictions." *Flood Risk Assessment*, Bath, September 7-8, 2004, 1-14.
- Pasche, E. and G. Rouve. (1985). "Overbank Flow with Vegetatively Roughened Floodplains." *Journal of Hydraulic Engineering*. ASCE, 111 (9), 1262-1278.
- Pezzinga, G. (1994). "Compound Velocity Distribution in Compound Channel Flows by Numerical Modeling." *Journal of Hydraulic Engineering*. ASCE, 120 (10), 1176-1198.
- Posey, C.J.F. (1967). "Computations of Discharge including Overbank Flow." *Civil Engineering*, ASCE, Vol. 37 (4), 62-63.
- Prinos, P., R. Townsend, and S. Tavoularis. (1985). "Structure of Turbulence in Compound Channel Flows." *Journal of Hydraulic Engineering*. ASCE, 111 (9), 1246-1261.
- Proust, S., N. Riviere, D. Bousmar, A. Paquier, Y. Zech, and R. Morel. (2006). "Flow in Compound Channel with Abrupt Floodplain Contraction." *Journal of Hydraulic Engineering*. ASCE, 132 (9), 958-970.
- Radojkovic, M. and S. Djordjevic. (1985). "Computation of Discharge Distribution in Compound Channels." *Proceedings of the 21<sup>st</sup> IAHR Congress*, IAHR, Melbourne, Australia, Vol. 3.

- Rajaratnam, N. and R.M. Ahmadi. (1979). "Interaction Between Main Channel and Floodplain Flows." *Journal of the Hydraulics Division*. ASCE, Vol. 105 (5), 573-588.
- Rajaratnam, N. and R.M. Ahmadi. (1981). "Hydraulics of Channels with Floodplains." *Journal of Hydraulic Research*. IAHR, Vol. 19 (1), 43-60.
- Rameshwaran, P. and P. S. Naden. (2003). "Three-Dimensional Numerical Simulation of Compound Channel Flows." *Journal of Hydraulic Engineering*. ASCE, 129 (8), 645-652.
- Rameshwaran, P. and K. Shiono. (2007). "Quasi two-dimensional model for straight overbank flows through emergent vegetation on floodplains." *Journal of Hydraulic Research*. IAHR, 45 (3), 302-315.
- Rantz, S.E. et. al. (1982a). "Measurement and Computation of Streamflow: Volume 1. Measurement of Stage and Discharge." Water-Supply Paper 2175, U. S. Geological Survey.
- Rantz, S.E. et. al.. (1982b). "Measurement and Computation of Streamflow: Volume 2. Computation of Discharge." Water-Supply Paper 2175, U. S. Geological Survey.
- Rastogi, A.K. and W. Rodi. (1978). "Prediction of Heat and Mass Transfer in Open Channels." *Journal of the Hydraulics Division*. ASCE, Vol. 104 (HY3), 397-420.
- Rhodes, D.G. and D.W. Knight. (1994). "Velocity and Boundary Shear in a Wide Compound Duct." *Journal of Hydraulic Research*. IAHR, 32 (5), 743-764.
- Rhodes, D.G. and D.W. Knight. (1995). "Lateral Shear in a Wide Compound Duct." *Journal of Hydraulic Engineering*. ASCE, 121 (11), 829-832.
- Rouse, H. (1959). Advanced Mechanics of Fluids. New York: John Wiley and Sons.
- Ruhl, C.A. and M.R. Simpson. (2005). "Computation of Discharge Using the Index-Velocity Method in Tidally Affected Areas." Scientific Investigations Report 2005-5004, U.S. Geological Survey.
- Schmidt, A.R. (2002). "Analysis of Stage-Discharge Relations for Open Channel Flows and their Associated Uncertainties." PhD. Thesis, University of Illinois Urbana-Champaign, Department of Civil and Environmental Engineering.
- Schoemaker, H. J. (1991). "Discussion on 4 papers of Journal of Hydraulic Research, 28 (2), 1990." *Journal of Hydraulic Research*. IAHR, 29 (2), 259-263.
- Seckin, G. (2004). "A Comparison of One-Dimensional Methods for Estimating Discharge Capacity of Straight Compound Channels." *Canadian Journal of Civil Engineering*. Vol. 31, 619-631.

- Seckin, G. (2005). "Maximum and Mean Velocity Relationships in Laboratory Flumes with Different Cross-Sectional Shapes." *Canadian Journal of Civil Engineering*. Vol. 32, 413-419.
- Sellin, R.H.J. (1964). "A laboratory Investigation into the Interaction Between Flow in the Channel of a River and that over its Floodplain." *La Houille Blanche*, 7, 793-801.
- Sellin, R. H. J., D. A. Ervine, and B. B. Willets. (1993). "The Behavior of Meandering Two-Stage Channels." *Proceedings of the Institute of Civil Engineers, Water, Maritime & Energy*, London, 101 (2), 99-111.
- Shiono, K. and D. W. Knight. (1988). "Two-Dimensional Analytical Solution for a Compound Channel." *Proceedings of the 3<sup>rd</sup> International Symposium on Refined Flow Modelling and Turbulence Measurements*, Tokyo, Japan, July, 503-510.
- Shiono, K. and D. W. Knight. (1990). "Mathematical Models of Flow in Two or Multi Stage Straight Channels." *Proceedings of the International Conference on River Flood Hydraulics*, John Wiley & Sons, Chichester, England, 229-238.
- Shiono, K. and D. W. Knight. (1991). "Turbulent Open Channel Flows with Variable Depth Across the Channel." *Journal of Fluid Mechanics*. Cambridge, U.K., 222, 617-646.
- Shiono, K., J. S. Al-Romaih and D. W. Knight. (1999). "Stage-Discharge Assessment in Compound Meandering Channels." *Journal of Hydraulic Engineering*. ASCE, 125 (1), 66-77.
- Sloat, J.V. and W.S. Gain. (1995). "Application of Acoustic Velocity Meters for Gaging Discharge of Three Low-Velocity Tidal Streams in the St. Johns River Basin, Northeast Florida." Water-Resources Investigations Report 95-4230, U.S. Geological Survey.
- Smart, G. M. (1992). "Stage-Discharge Discontinuity in Composite Flood Channels." *Journal of Hydraulic Research*. IAHR, 30 (6), 817-833.
- Sofialidis, D. and P. Prinos. (1998). "Compound Open-Channel Flow Modeling with Nonlinear Low-Reynolds k- $\epsilon$  Models." *Journal of Hydraulic Engineering*. ASCE, 124 (3), 253-262.
- Sofialidis, D. and P. Prinos. (1999). "Numerical Study of Momentum Exchange in Compound Open Channel Flow." *Journal of Hydraulic Engineering*. ASCE, 125 (2), 152-165.
- Streeter, V.L. and E. B. Wylie. (1975). Fluid Mechanics. McGraw-Hill, New York, New York.

- Sturm, T. W. (2004). Enhanced Abutment Scour Studies for Compound Channels, FHWA-RD-99-156, Federal Highway Administration.
- Sturm, T. W. (2006). "Scour Around Bankline and Setback Abutments in Compound Channels." *Journal of Hydraulic Engineering*. ASCE, 132 (1), 21-32.
- Sturm, T. W. and A. Sadiq. (1996). "Water Surface Profiles in Compound Channel with Multiple Critical Depths." *Journal of Hydraulic Engineering*. ASCE, 122 (12), 703-709.
- Tamai, N., T. Aseada, and H. Ikeda. (1986). "Study on generation of periodical large surface eddies in a composite channel flow." *Water Resources Research*. AGU, Vol. 22, (7), 1129-1138.
- Tang, X. and D. W. Knight. (2006). "Sediment Transport in River Models with Overbank Flows." *Journal of Hydraulic Engineering*. ASCE, 132 (1), 77-86.
- Thomas, T.G. and J.J.R. Williams. (1995). "Large Eddy Simulation of Turbulent Flow in an Asymmetric Compound Channel." *Journal of Hydraulic Research*. IAHR, Vol. 33 (11), 825-842.
- Tingsanchali, T. and Ackerman, N. L. (1976). "Effects of Overbank Flow in Flood Computations." *Journal of the Hydraulics Division*. ASCE, Vol. 12 (7), 1013-1025.
- Toebes, G.H. and A.A. Sooky. (1967). "Hydraulics of Meandering Rivers with Floodplains." *Journal of the Waterways and Harbors Division*, ASCE. Vol. 93 (WW2), 213-226.
- Tominaga, A. and I. Nezu. (1991). "Turbulent Structure in Compound Open-Channel Flows." *Journal of Hydraulic Engineering*. ASCE, 117 (1), 21-41.
- Udeozo, B.N.C. (1967). "Uniform Flow in Idealized Channel-Floodplain Geometries." M.S. Thesis, Purdue University, Department of Civil Engineering.
- Uijttewaal, W.S.J. and R. Booij. (2000). "Effects of Shallowness on the Development of Free-Surface Mixing Layers." *Physics of Fluids*. American Institute of Physics, 12 (2), 392-420.
- Van Prooijen, B. C. and W. S. J. Uijttewaal. (2002). "A Linear Approach for the Evolution of Coherent Structures in Shallow Mixing Layers." *Physics of Fluids*. American Institute of Physics, 14 (12), 4105-4114.
- Van Prooijen, B. C., J. A. Battjes, and W. S. J. Uijttewaal. (2005). "Momentum Exchange in Straight Uniform Compound Channel Flow." *Journal of Hydraulic Engineering*. ASCE, 131 (3), 175-183.

Wark, J.B., P.G. Samuels, and D.A. Ervine. (1990). "A Practical Method of Estimating Velocity and Discharge in Compound Channels." *Proceedings of the International Conference on River Flood Hydraulics*, John Wiley & Sons, Chichester, England, 163-172.

Wark, J. B., J. E. Slade and D. M. Ramsbottom. (1991). "Flood Discharge Assessment by the Lateral Distribution Method." *Rep. SR 277*, HR Wallingford, Ltd., Wallingford, England.

Weber, J. F. and A. N. Menendez. (2004). "Performance of Later Velocity Distribution Models for Compound Channel Sections." *River Flow 2004, Proceedings of the Second International Conference on Fluvial Hydraulics, 23-25 June 2004, Napoli, Italy*.

Westwater, D. (2001). "Modelling Hydrodynamic and Shallow Water Processes over Vegetated Floodplains." PhD Thesis, Cardiff University.

White, F. M. (2003). Fluid Mechanics: Fifth Edition. McGraw-Hill, New York, NY.

Wilkerson, G.V. (2007). "Flow Through Trapezoidal and Rectangular Channels with Rigid Cylinders." *Journal of Hydraulic Engineering*. ASCE, 133 (5), 521-533.

Wilkerson, G. V. and J. L. McGahan. (2005). "Depth-Averaged Velocity Distribution in Straight Trapezoidal Channels." *Journal of Hydraulic Engineering*. ASCE, 131 (6), 509-512.

Williams, D. T. and P. Julien. (1991). "Examination of Stage-Discharge Relationships of Compound Composite Channels." In Channel Flow Resistance: A Centennial of Manning's Formula. Water Resources Publications, Littleton, Colorado, 341-355.

Wilson, C. A. M. E., P. D. Bates, and J. M. Hervouet. (2002). "Comparison of Turbulence Models for Stage-Discharge Rating Curve Prediction in Reach-Scale Compound Channel Flows Using Two-Dimensional Finite Element Methods." *Journal of Hydrology*. Vol. 257 (1-4), 42-58.

Wormleaton, P.R. (1988). "Determination of Discharge in Compound Channels Using the Dynamic Equation for Lateral Velocity Distribution." *International Conference on Fluvial Hydraulics*, Budapest, Hungary, 98-103.

Wormleaton, P. R. (1996). "Floodplain Secondary Circulation as a Mechanism for Flow and Shear Stress Redistribution in Straight Compound." *Coherent Flow Structures in Open Channels*. P. J. Ashworth, S. J. Bennet, J. L. Best, and S. J. McLelland, eds. Wiley, Chichester, England, 581-608.

- Wormleaton, P.R. and M. Ewunetu. (2006). "Three-dimensional k- $\epsilon$  numerical modeling of overbank flow in a mobile bed meandering channel with floodplains of different depth, roughness, and planform." *Journal of Hydraulic Research*. IAHR, Vol. 44 (1), 18-32.
- Wormleaton, P. R. and P. Hadjipanous. (1985). "Flow Distribution in Compound Channels." *Journal of Hydraulic Engineering*. ASCE, 111 (2), 357-361.
- Wormleaton, P. R. and D. J. Merrett. (1990). "An Improved Method of Calculation for Steady Uniform Flow in Prismatic Main Channel/Floodplain Sections." *Journal of Hydraulic Research*. IAHR, 28 (2), 157-174.
- Wormleaton, P. R., J. Allen, and P. Hadjipanous. (1982). "Discharge Assessment in Compound Channel Flow." *Journal of Hydraulic Engineering*. ASCE, 108 (9), 975-994.
- Wormleaton, P. R., J. Allen, and P. Hadjipanous. (1983). "Discussion of Discharge Assessment in Compound Channel Flow." *Journal of Hydraulic Engineering*. ASCE, 108 (9). Discussions by R. W. Buchanan, C.L. Yen and S.Y. Ho, and C.J. Posey, 1564-1567.
- Wright, RR. and H.R. Carstens. (1973). "Linear Mometum Flux to Overbank Sections." *Journal of the Hydraulics Division*. ASCE, Vol. 96 (HY9), 1781-1793.
- Yalin, M.S. (1971). Theory of Hydraulic Models. The Macmillan Press Ltd., New York, New York.
- Yang, S. Q., J. X. Yu, and Y. Z. Wang. (2004). "Estimation of Diffusion Coefficients, Lateral Shear Stress, and Velocity in Open Channels with Complex Geometries." *Water Resources Reach*. AGU, Vol. 40 (5), 1-8.
- Yen, B. C. (1991). "Hydraulic Resistance in Open Channels." In Channel Flow Resistance: A Centennial of Manning's Formula. Water Resources Publications, Littleton, Colorado, 1-135.
- Yen, B.C. and S.Y. Ho. (1985). "Discussion of 'Flow Distribution in Compound Channels' by Wormleaton and Hadjipanous." *Journal of Hydraulic Engineering*. ASCE, 108 (9), 1561-1563.
- Yen and Overton. (1973). "Shape Effects on Resistance in Floodplain Channels." *Journal of the Hydraulics Division*. ASCE, Vol. 99 (HY01), 219-238.
- Yen, Camacho, Kohane, and Westrich. (1985). "Significance of Floodplains in Backwater Computation." *Proceedings of the 21<sup>st</sup> IAHR Congress*, IAHR, Melbourne, Australia, Vol. 3.

Zheleznyakov, G.V. (1965). "Relative Deficit of Mean Velocity of Instable River Flow; Kinematic Effect in River Bends with Floodplains." *Proceedings of the 11<sup>th</sup> International Conference of the IAHR*, Leningrad, USSR, 1-16.

Zheleznyakov, G. V. (1971). "Interaction of Channel and Floodplain Streams." *Proceedings of the 14<sup>th</sup> International Association of Hydraulic Research*, Paris, 144-148.

Zheleznyakov, G. V. (1985). "Problem of the Interaction of the Main Channel and the Floodplain Flows." *Proceedings of the 21<sup>st</sup> IAHR Congress*, IAHR, Melbourne, Australia, Vol. 3.

## **APPENDIX A: MODEL RESULTS**

This appendix presents the statistical properties and plots of the depth-averaged velocity distributions predicted by the models developed in this document (Equation 2.9 and Equation 4.3). Table A.1 and Figure A.1 – Figure A.34 present the statistical properties and velocity distributions of the general and CV models for the calibration data sets. Table A.2, Figure A.35, and Figure A.36 present similar information for validation data.



**Table A.1. Depth-averaged velocity distribution statistics for calibration data**

Series	Test	Optimized Model Coefficients				Number of Observations	General Model		CV Model	
		$a_1$	$a_2$	$a_3$	$a_4$		$R^2$	$s$ (m/s)	$R^2$	$s$ (m/s)
S-03*	221	0.810	1.880	6.042	0.581	54	0.992	0.012	0.952	0.031
S-03	224	0.697	1.535	5.594	0.653	54	0.989	0.012	0.967	0.022
S-03	227	0.583	2.309	7.631	0.721	55	0.985	0.013	0.976	0.016
S-03	230	0.507	2.158	7.294	0.769	55	0.980	0.013	0.976	0.015
FCF-01	10201	1.041	1.756	8.776	0.343	48	0.989	0.015	0.987	0.018
FCF-01	10301	0.928	1.675	9.143	0.498	48	0.995	0.009	0.952	0.038
FCF-01	10401	0.842	1.988	8.272	0.612	49	0.994	0.010	0.900	0.050
FCF-01	10501	0.657	2.454	9.796	0.728	48	0.994	0.010	0.800	0.063
FCF-01*	10601	0.476	1.589	16.591	0.800	48	0.984	0.011	0.773	0.056
FCF-01*	10701	0.335	2.882	4.162	0.909	48	0.963	0.013	0.470	0.053
FCF-02	20201	0.904	1.257	7.822	0.361	35	0.992	0.016	0.983	0.025
FCF-02	20301	0.842	1.283	7.260	0.455	35	0.990	0.015	0.988	0.017
FCF-02	20401	0.767	1.306	7.612	0.535	35	0.992	0.013	0.990	0.015
FCF-02	20501	0.652	1.325	8.294	0.629	35	0.983	0.016	0.978	0.021
FCF-02	20601	0.588	1.351	6.035	0.701	35	0.955	0.025	0.953	0.027
FCF-02	20701	0.450	1.272	2.662	0.820	35	0.948	0.026	0.886	0.040
FCF-02	20801	0.261	0.864	2.683	0.898	36	0.954	0.022	0.503	0.066
FCF-03*	30201	0.837	0.852	10.552	0.256	20	0.990	0.026	0.821	0.105
FCF-03	30301	0.739	0.891	9.192	0.371	20	0.983	0.026	0.827	0.091
FCF-03*	30401	0.691	0.726	9.576	0.424	20	0.973	0.032	0.804	0.092
FCF-03*	30501	0.645	1.054	8.840	0.494	20	0.987	0.020	0.832	0.088
FCF-08	80201	1.035	1.788	6.334	0.320	32	0.989	0.017	0.979	0.027
FCF-08	80301	0.921	1.341	5.844	0.448	32	0.992	0.012	0.985	0.017
FCF-08	80401	0.813	1.959	6.769	0.566	32	0.983	0.017	0.970	0.025
FCF-08	80501	0.672	1.946	7.098	0.669	32	0.976	0.015	0.949	0.032
FCF-08	80601	0.561	2.025	6.405	0.751	32	0.950	0.018	0.914	0.036
FCF-08*	80701	0.267	7.482	17.250	0.895	33	0.862	0.027	0.653	0.058
FCF-10	100201	0.907	1.823	14.262	0.291	34	0.994	0.015	0.944	0.056
FCF-10	100301	0.857	1.349	8.469	0.402	34	0.991	0.017	0.973	0.034
FCF-10	100401	0.751	1.180	7.602	0.516	34	0.987	0.017	0.982	0.022
FCF-10	100501	0.611	1.465	9.947	0.634	34	0.982	0.015	0.980	0.019
FCF-10	100601	0.495	1.665	12.491	0.723	34	0.971	0.016	0.960	0.024
FCF-10	100701	0.309	1.205	14.430	0.847	34	0.890	0.027	0.760	0.043
FCF-10*	100801	0.245	4.314	29.245	0.891	34	0.826	0.030	0.379	0.071

\*Outliers not used in calibration of the CV model.

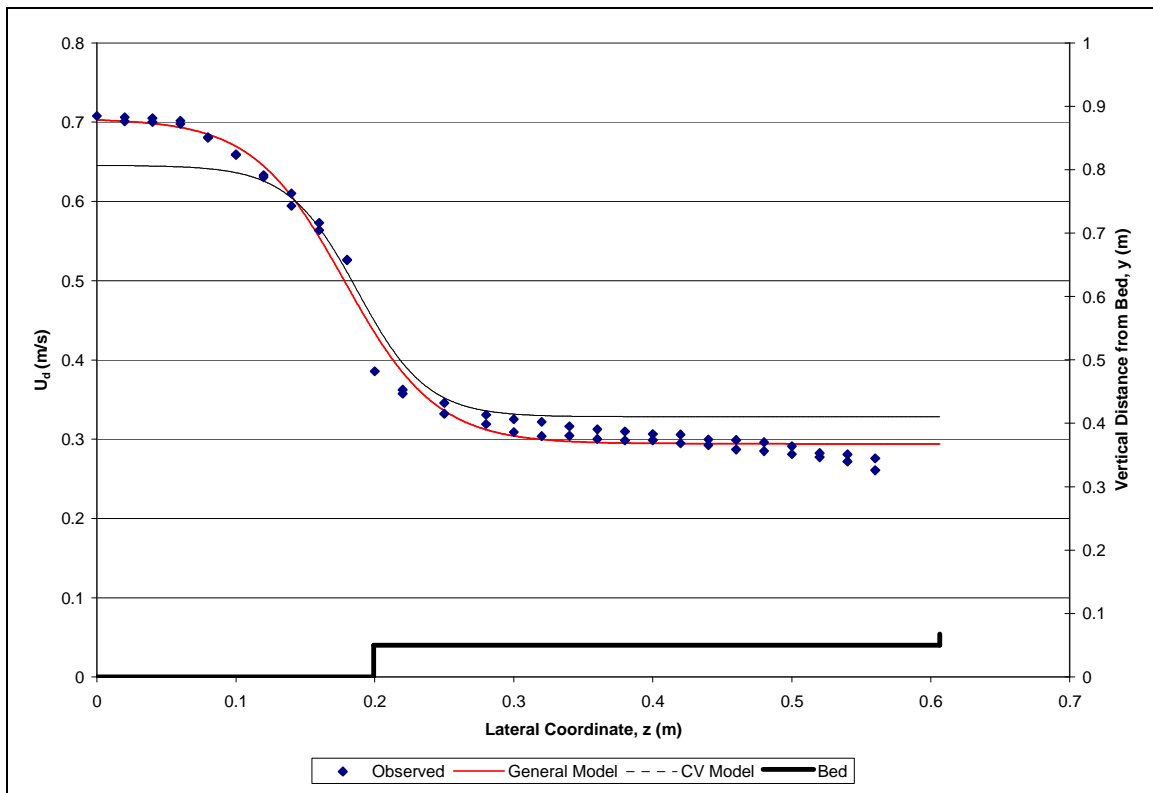


**Figure A.1. Depth-averaged velocity distribution for S-03-221**

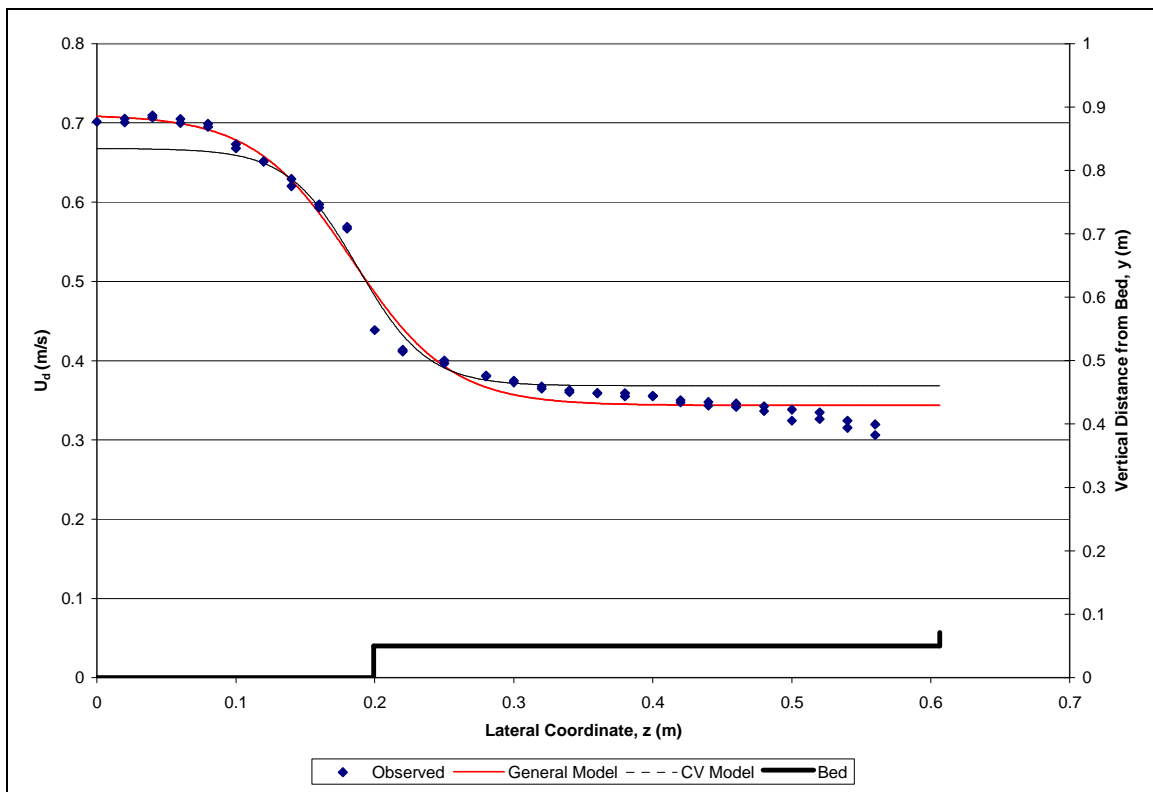


**Figure A.2. Depth-averaged velocity distribution for S-03-224**

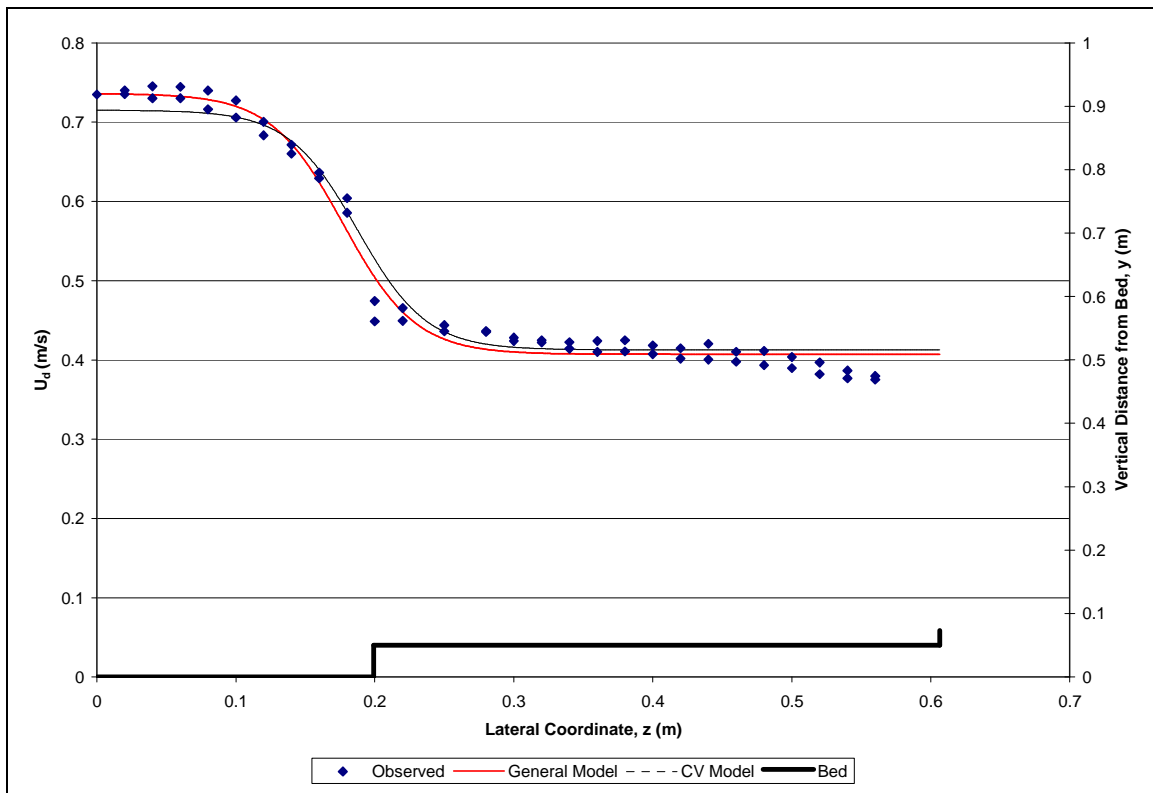


**Figure A.3. Depth-averaged velocity distribution for S-03-227**

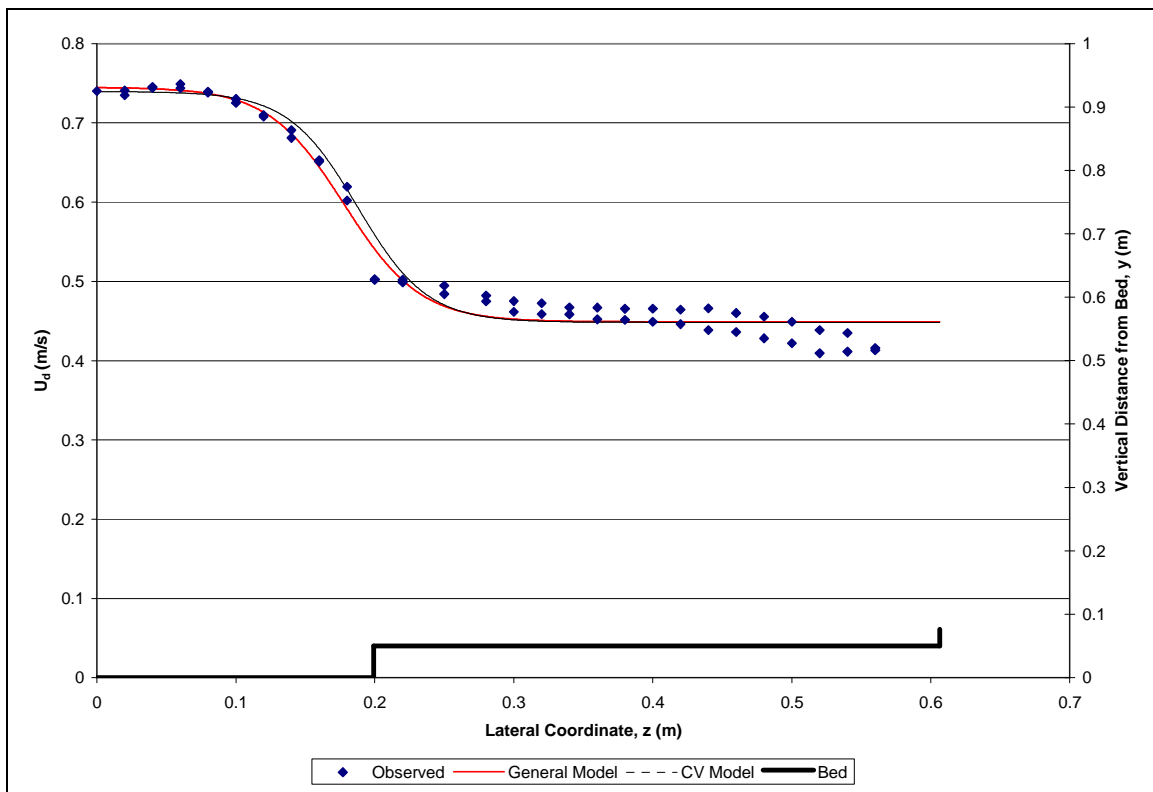


**Figure A.4. Depth-averaged velocity distribution for S-03-230**

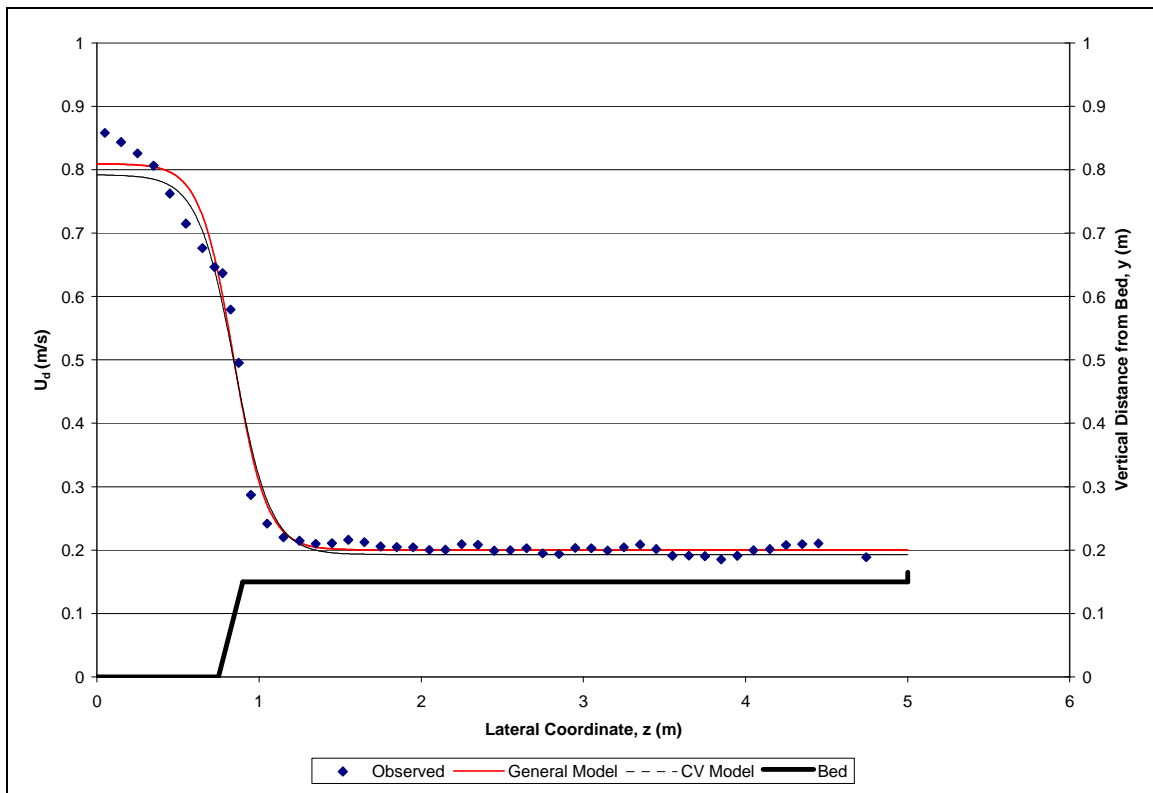


**Figure A.5. Depth-averaged velocity distribution for FCF-010201**

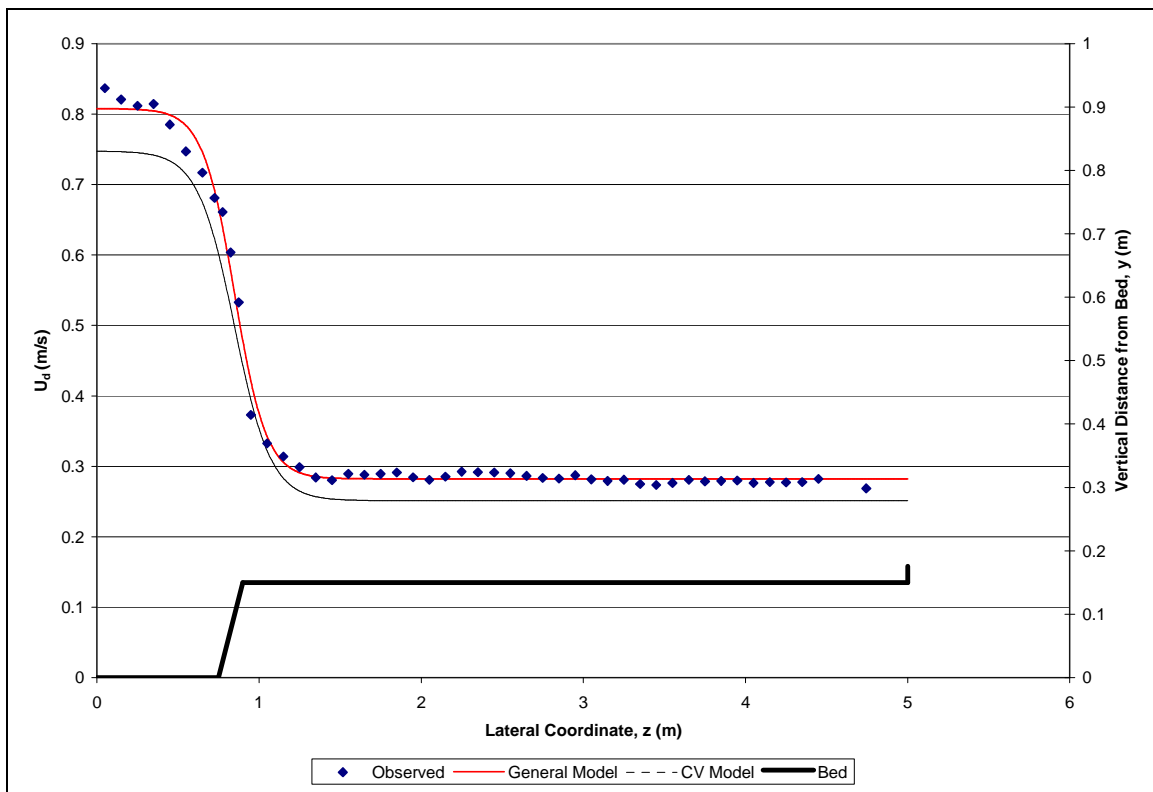


**Figure A.6. Depth-averaged velocity distribution for FCF-010301**

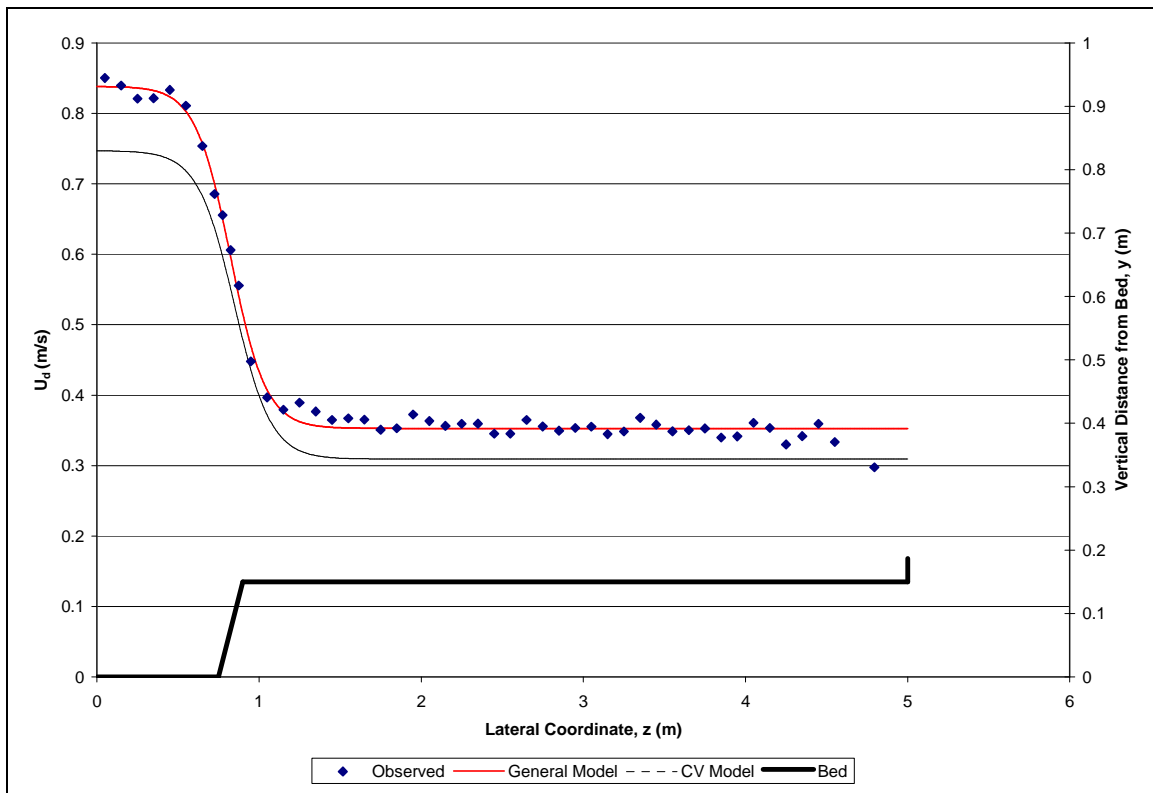


**Figure A.7. Depth-averaged velocity distribution for FCF-010401**

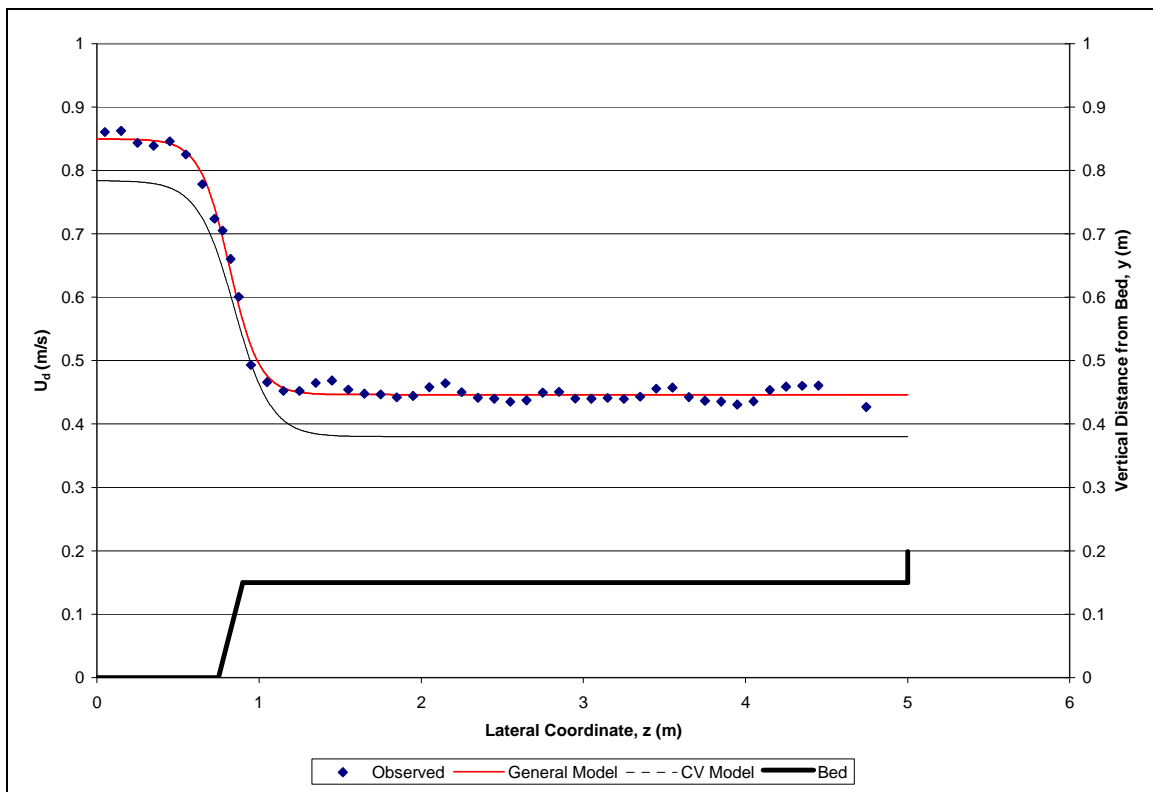


**Figure A.8. Depth-averaged velocity distribution for FCF-010501**

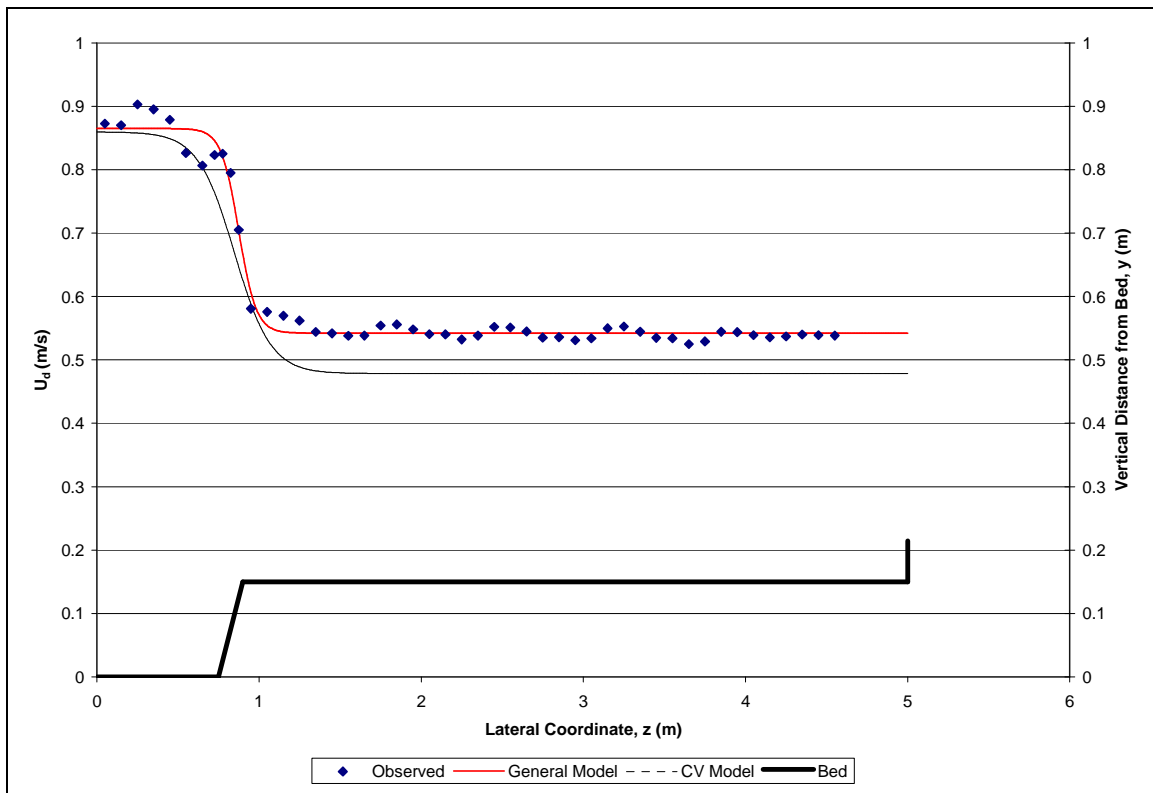


**Figure A.9. Depth-averaged velocity distribution for FCF-010601**

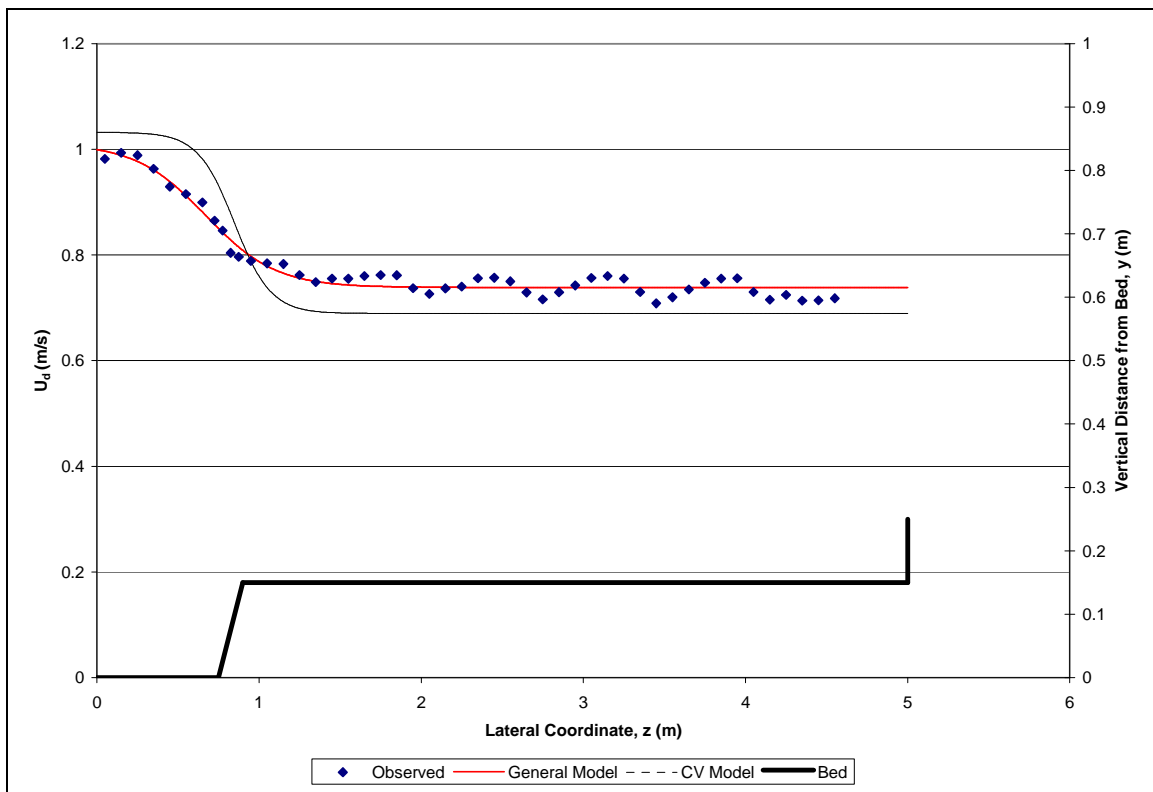


**Figure A.10. Depth-averaged velocity distribution for FCF-010701**

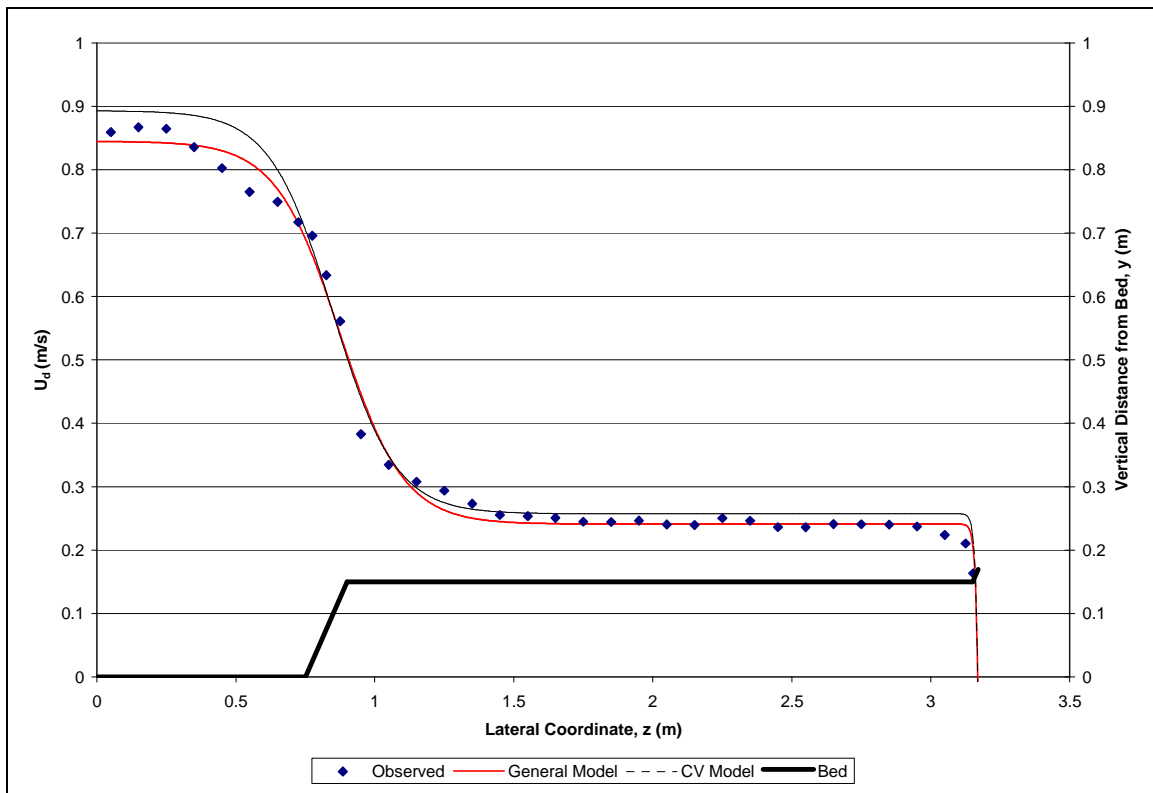


**Figure A.11. Depth-averaged velocity distribution for FCF-020201**

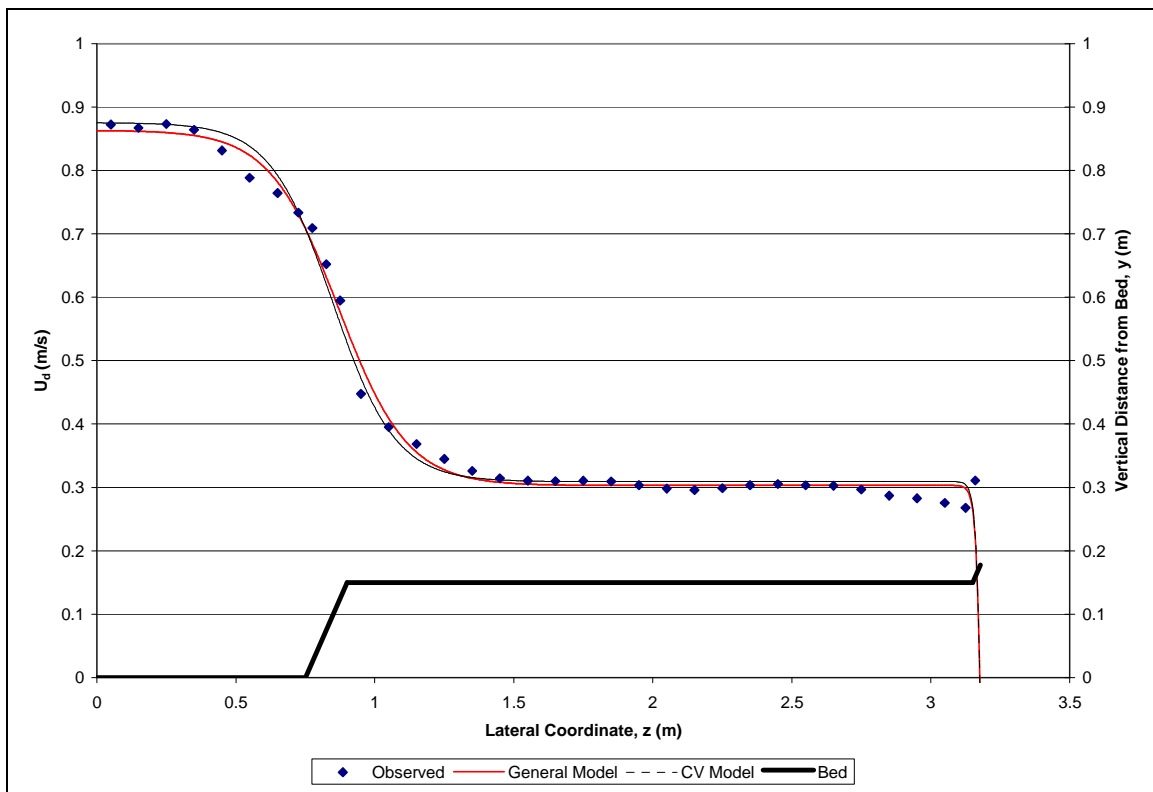


**Figure A.12. Depth-averaged velocity distribution for FCF-020301**

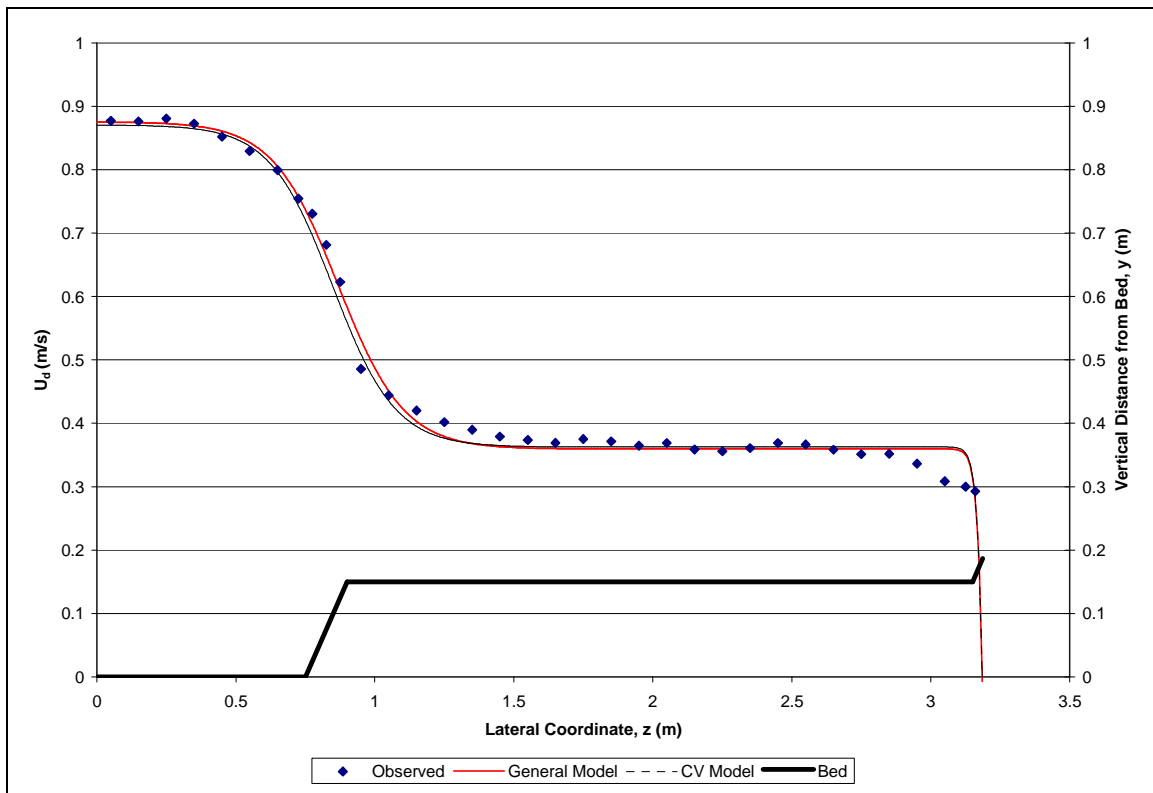


**Figure A.13. Depth-averaged velocity distribution for FCF-020401**

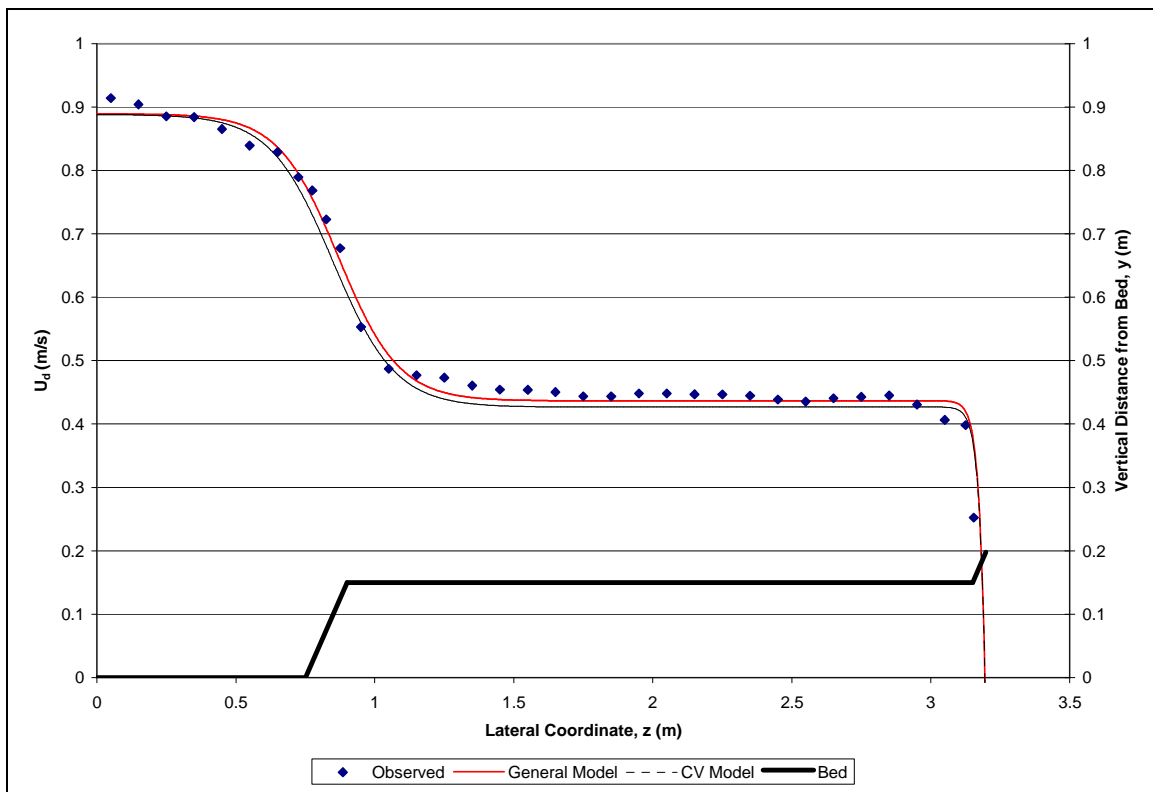


**Figure A.14. Depth-averaged velocity distribution for FCF-020501**



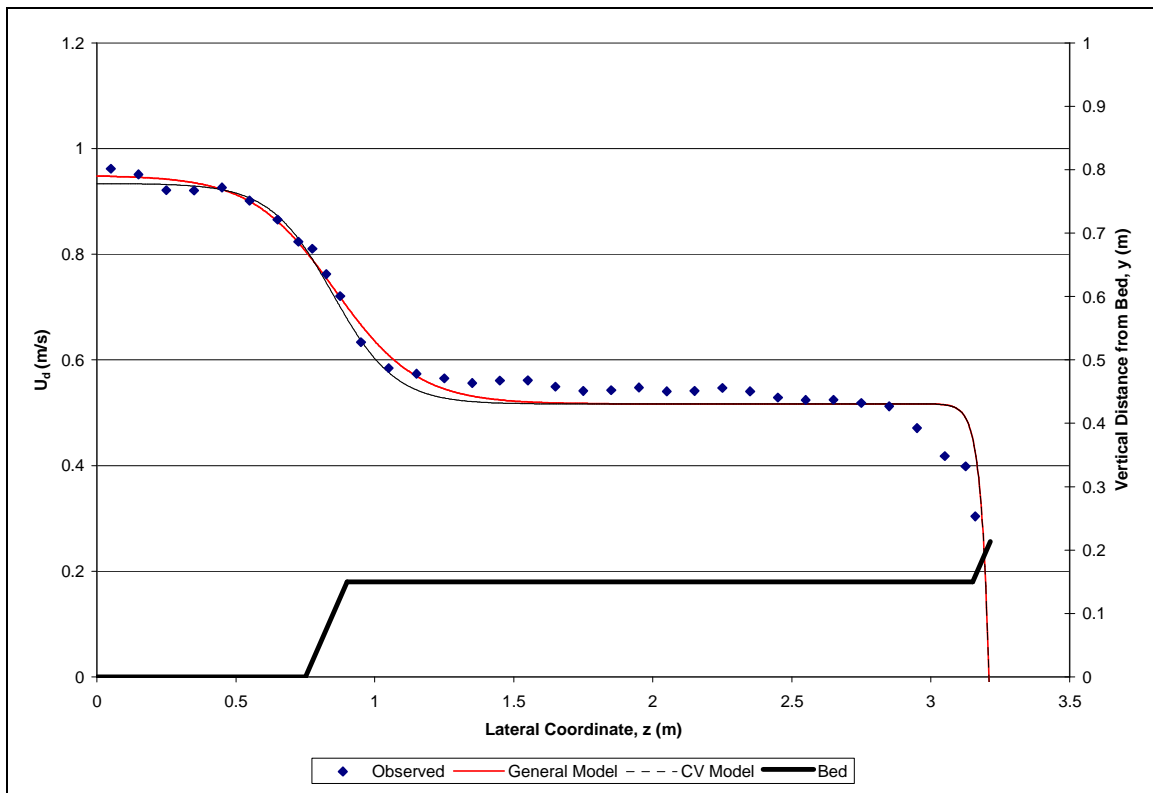


**Figure A.15. Depth-averaged velocity distribution for FCF-020601**

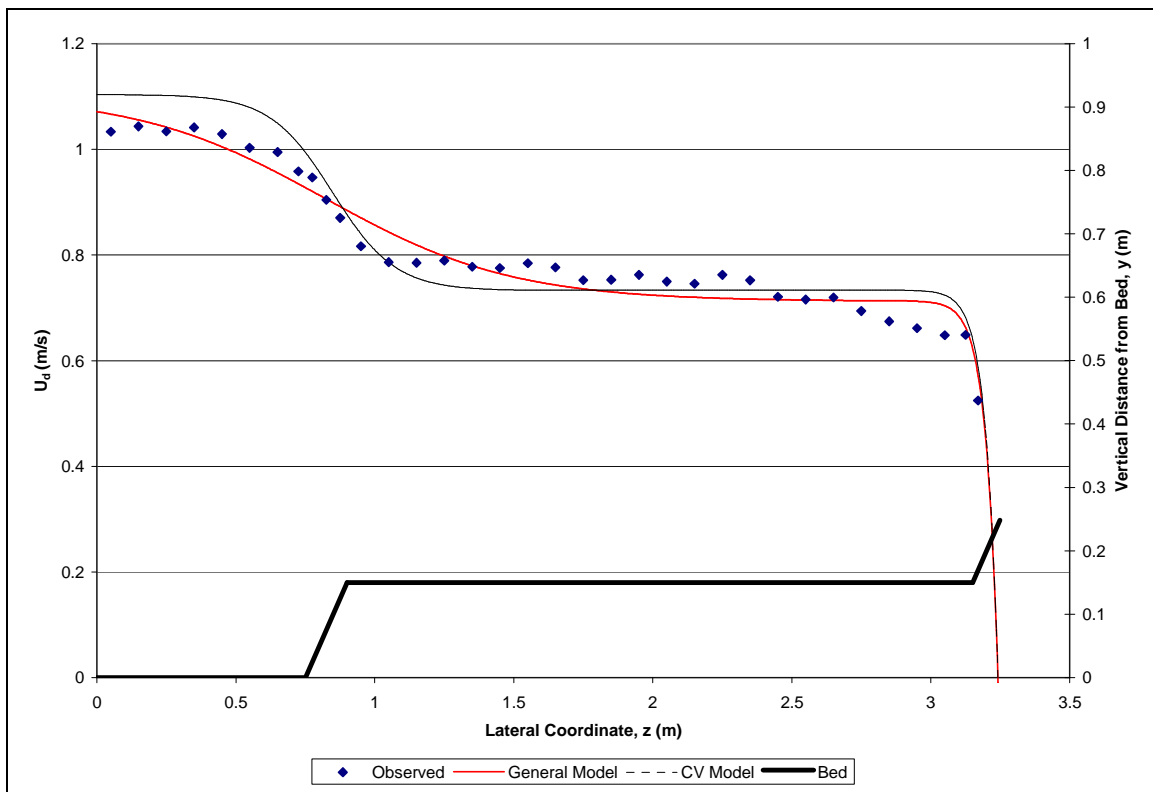


**Figure A.16. Depth-averaged velocity distribution for FCF-020701**

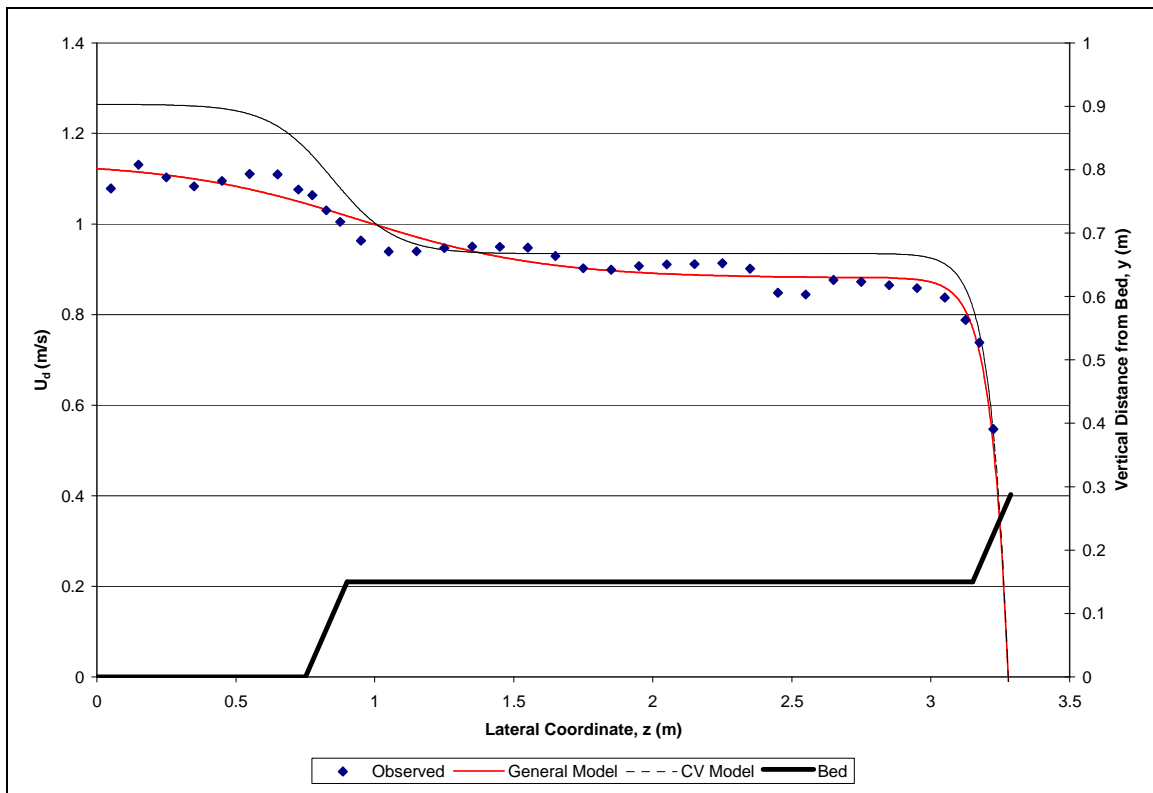


**Figure A.17. Depth-averaged velocity distribution for FCF-020801**

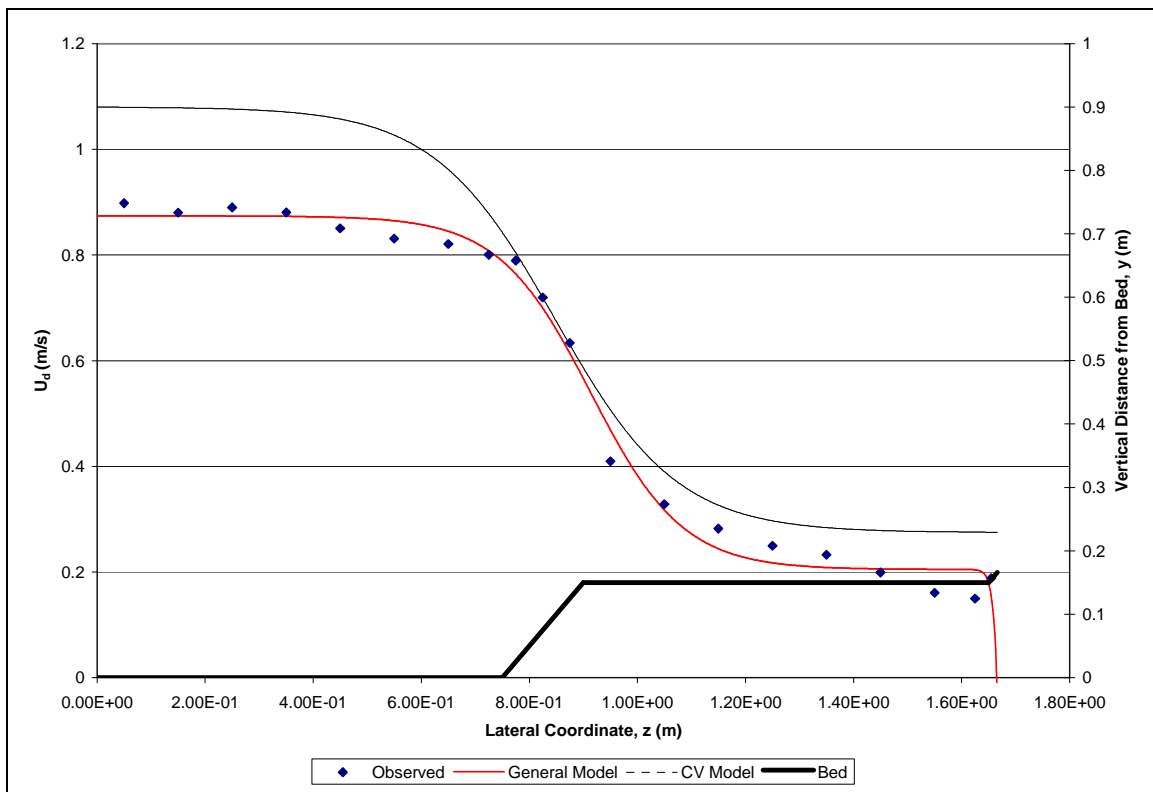


**Figure A.18. Depth-averaged velocity distribution for FCF-030201**

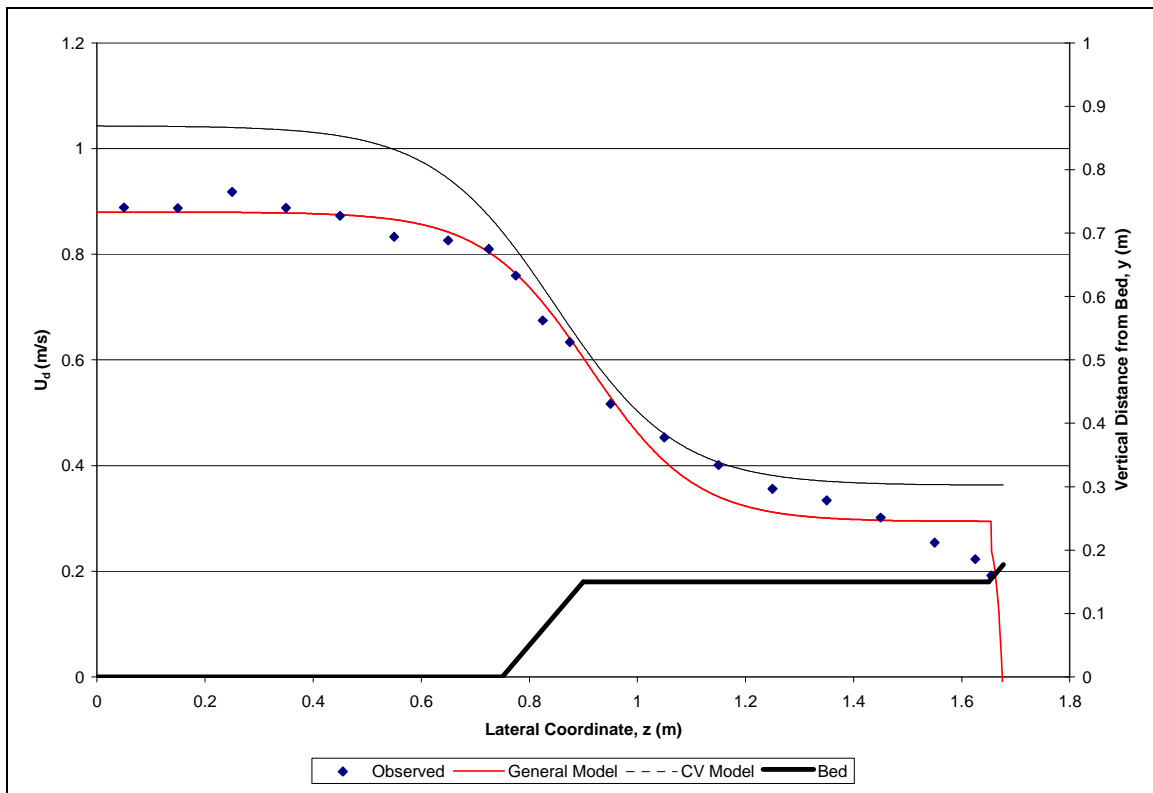


**Figure A.19. Depth-averaged velocity distribution for FCF-030301**

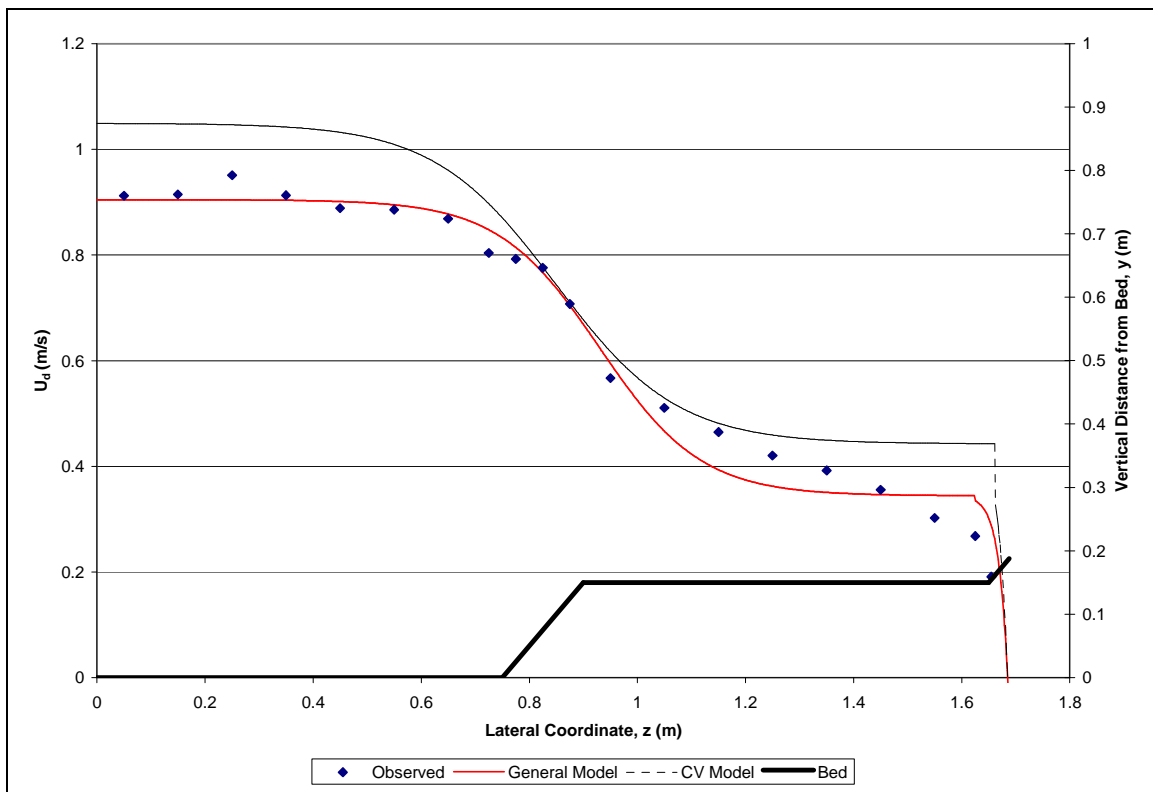


**Figure A.20. Depth-averaged velocity distribution for FCF-030401**

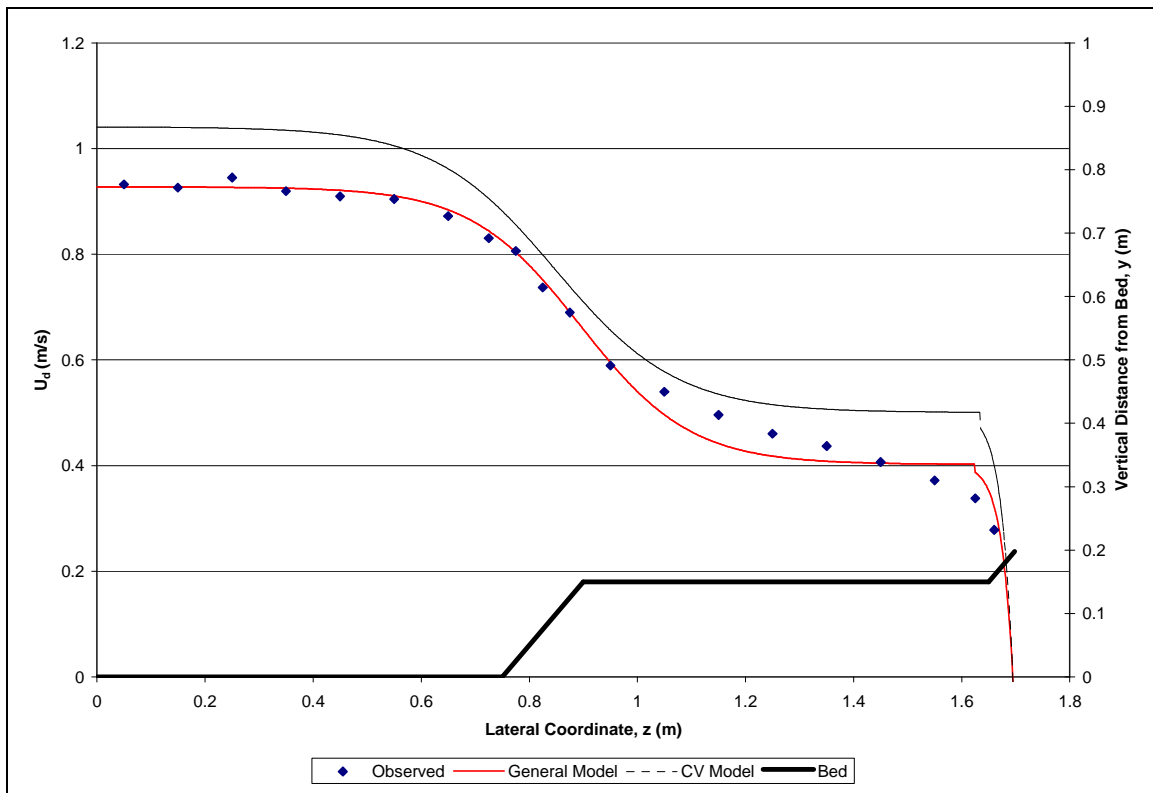


**Figure A.21. Depth-averaged velocity distribution for FCF-030501**

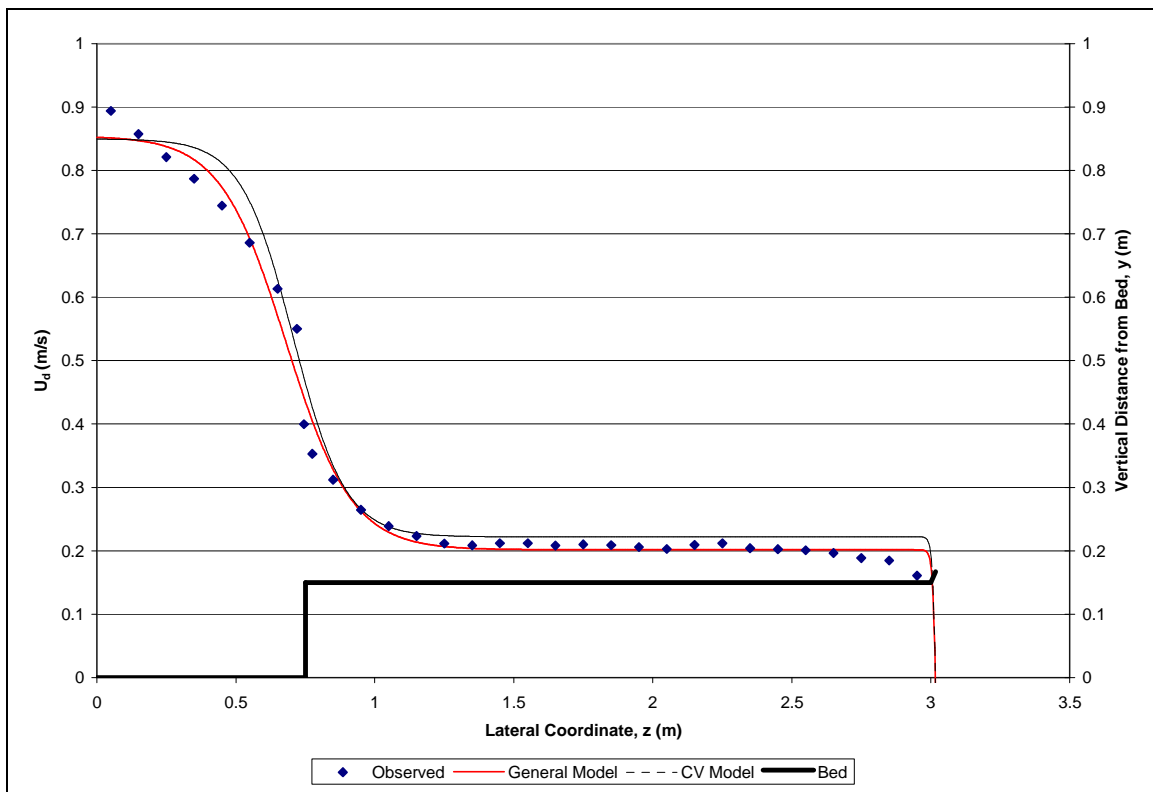


**Figure A.22. Depth-averaged velocity distribution for FCF-080201**

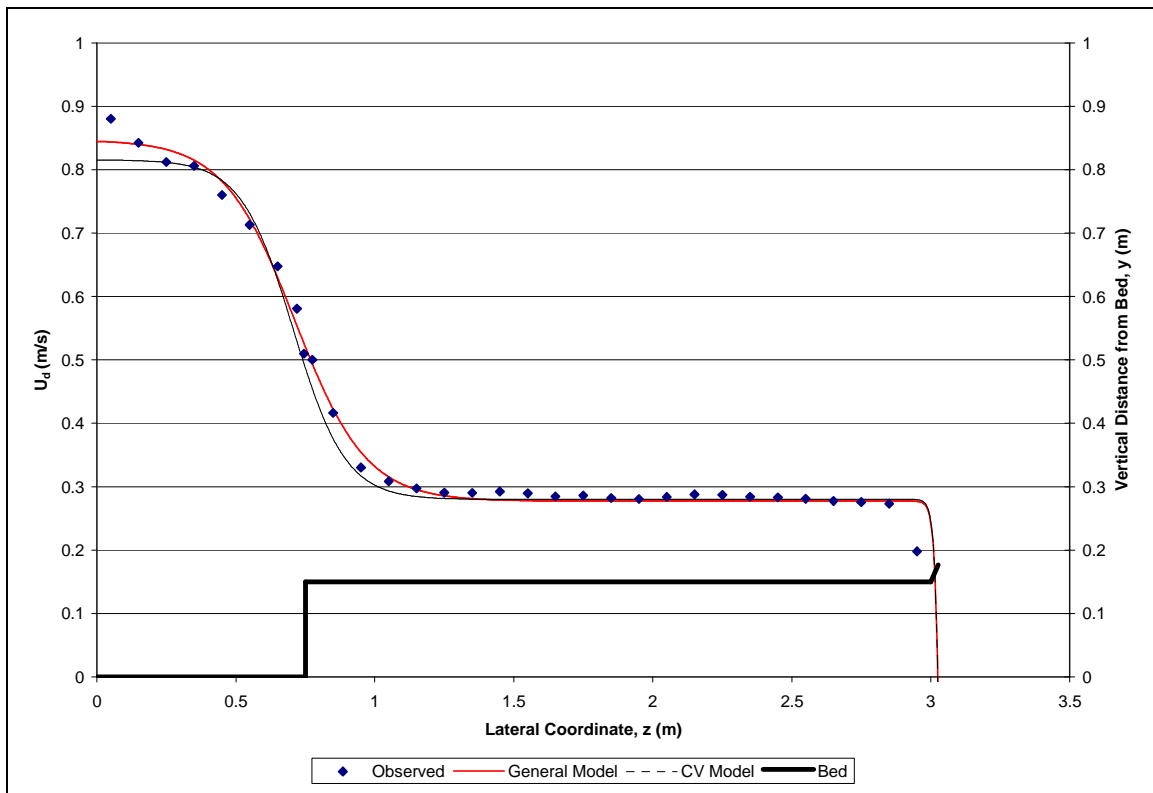


**Figure A.23. Depth-averaged velocity distribution for FCF-080301**

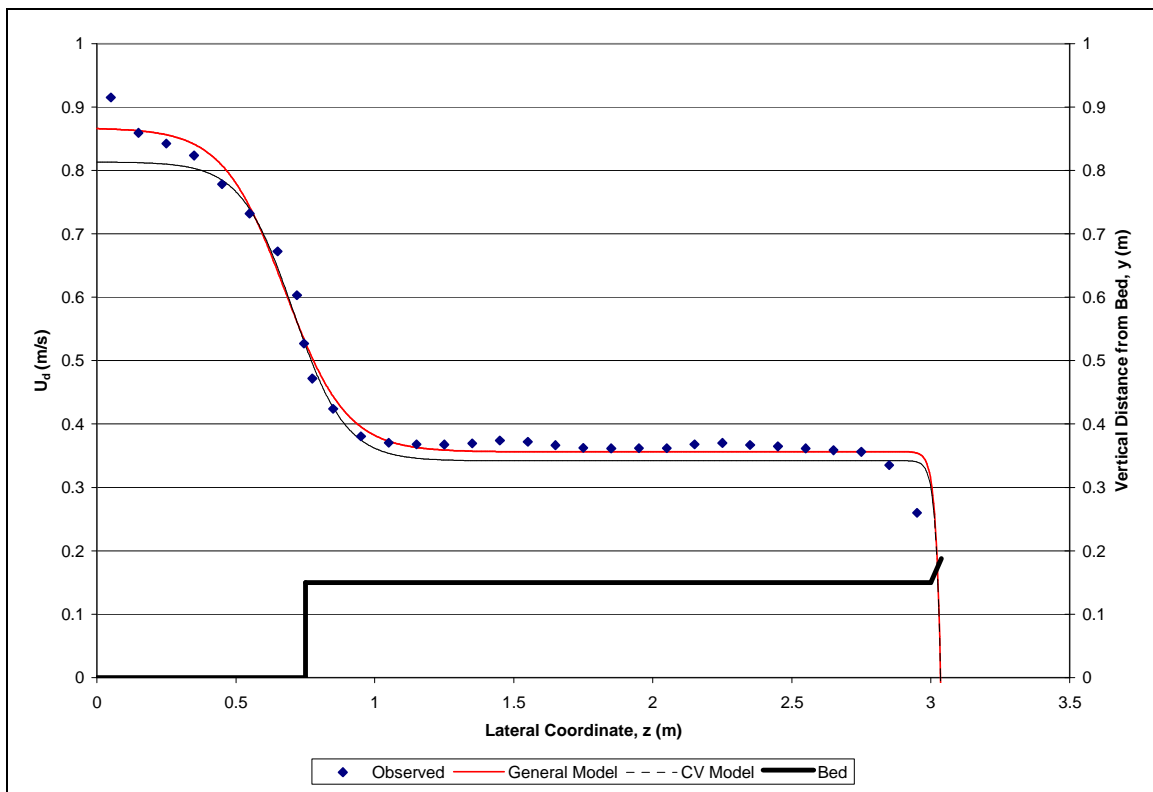


**Figure A.24. Depth-averaged velocity distribution for FCF-080401**

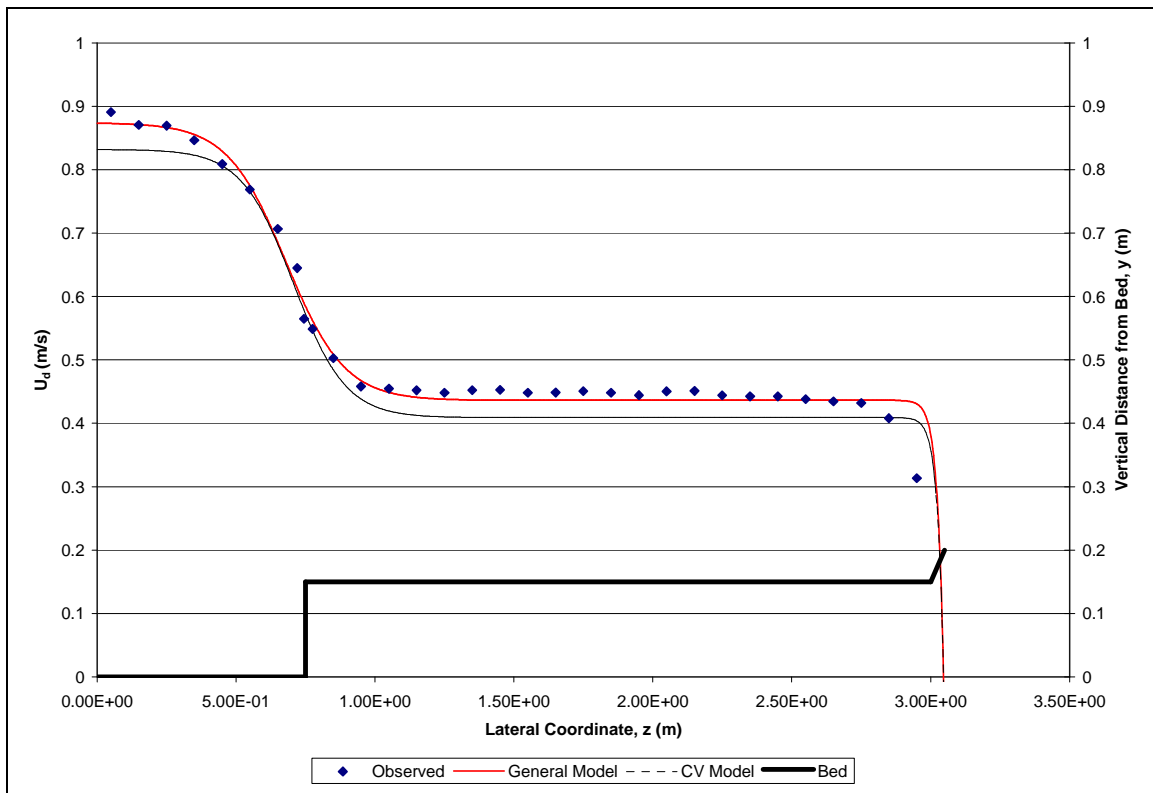


**Figure A.25. Depth-averaged velocity distribution for FCF-080501**

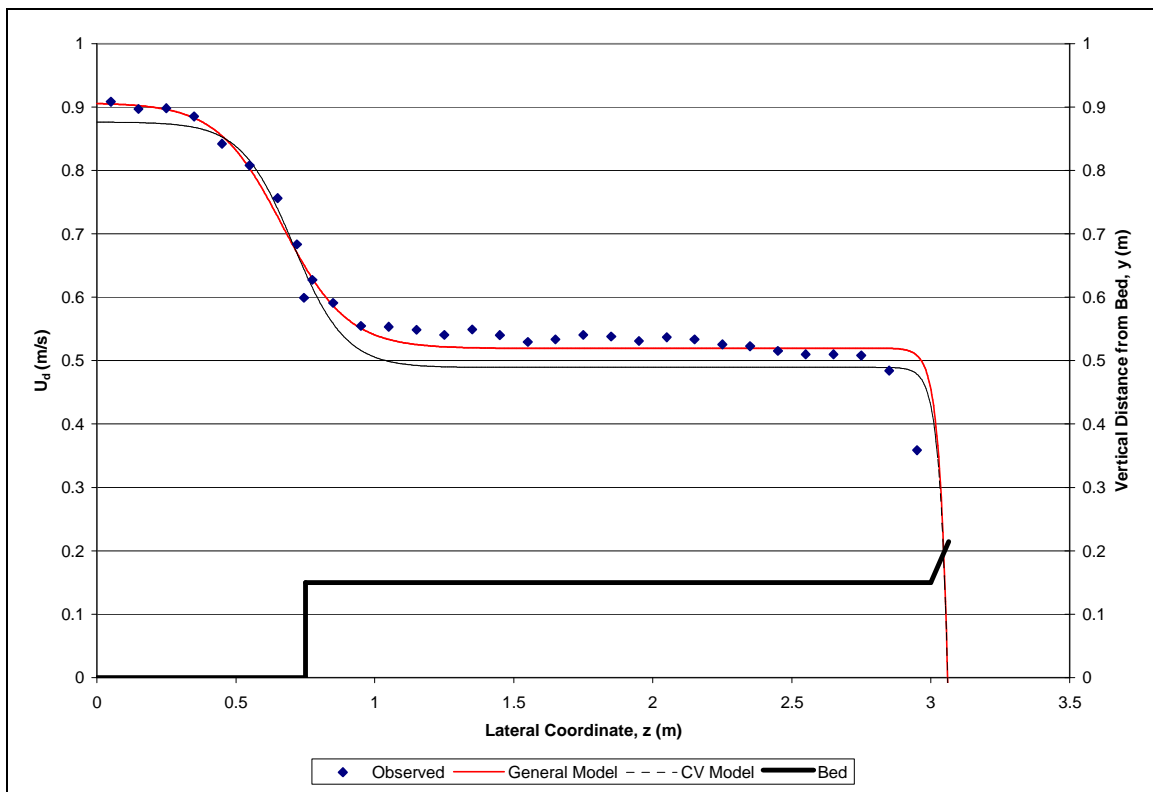


**Figure A.26. Depth-averaged velocity distribution for FCF-080601**

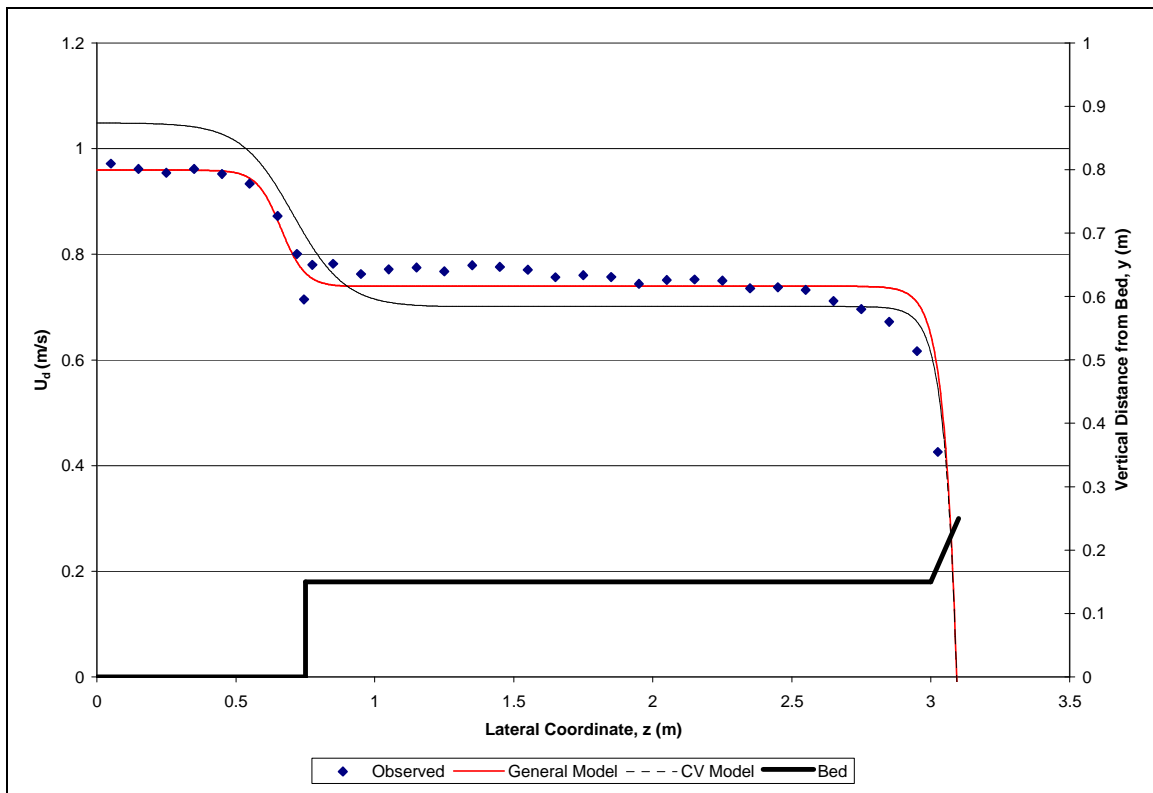


**Figure A.27. Depth-averaged velocity distribution for FCF-080701**

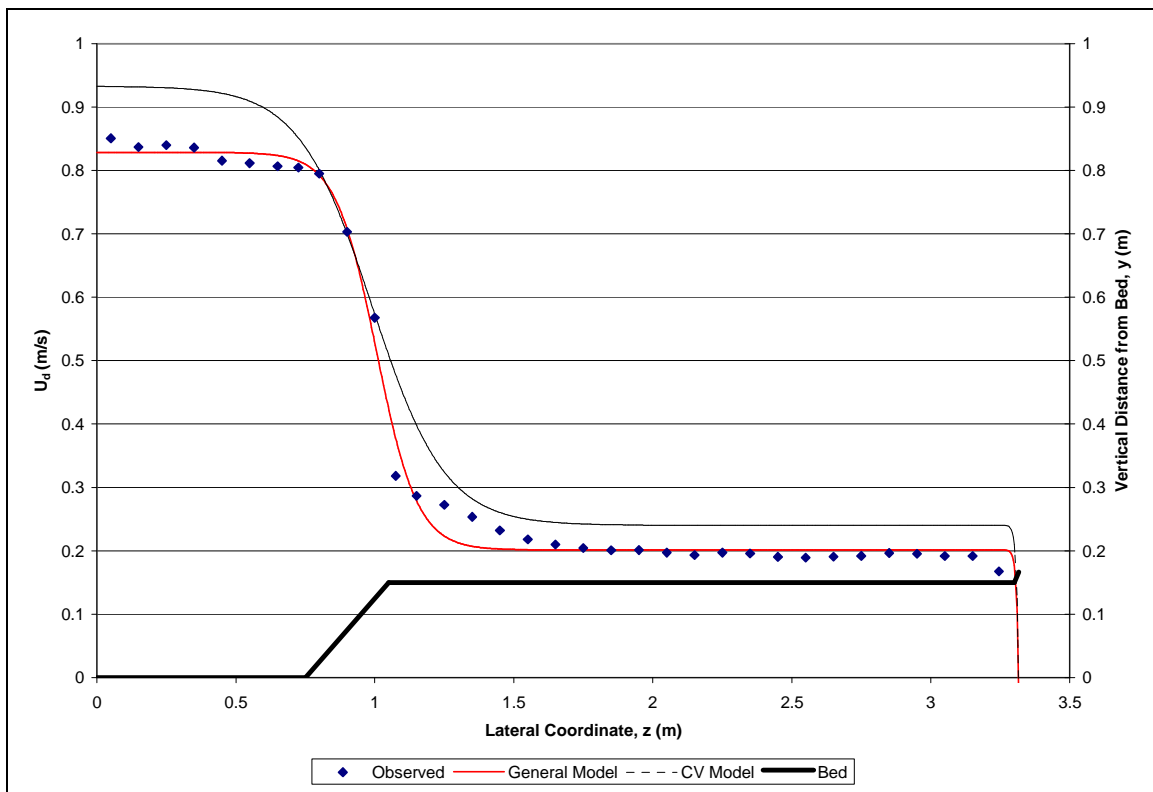


**Figure A.28. Depth-averaged velocity distribution for FCF-100201**

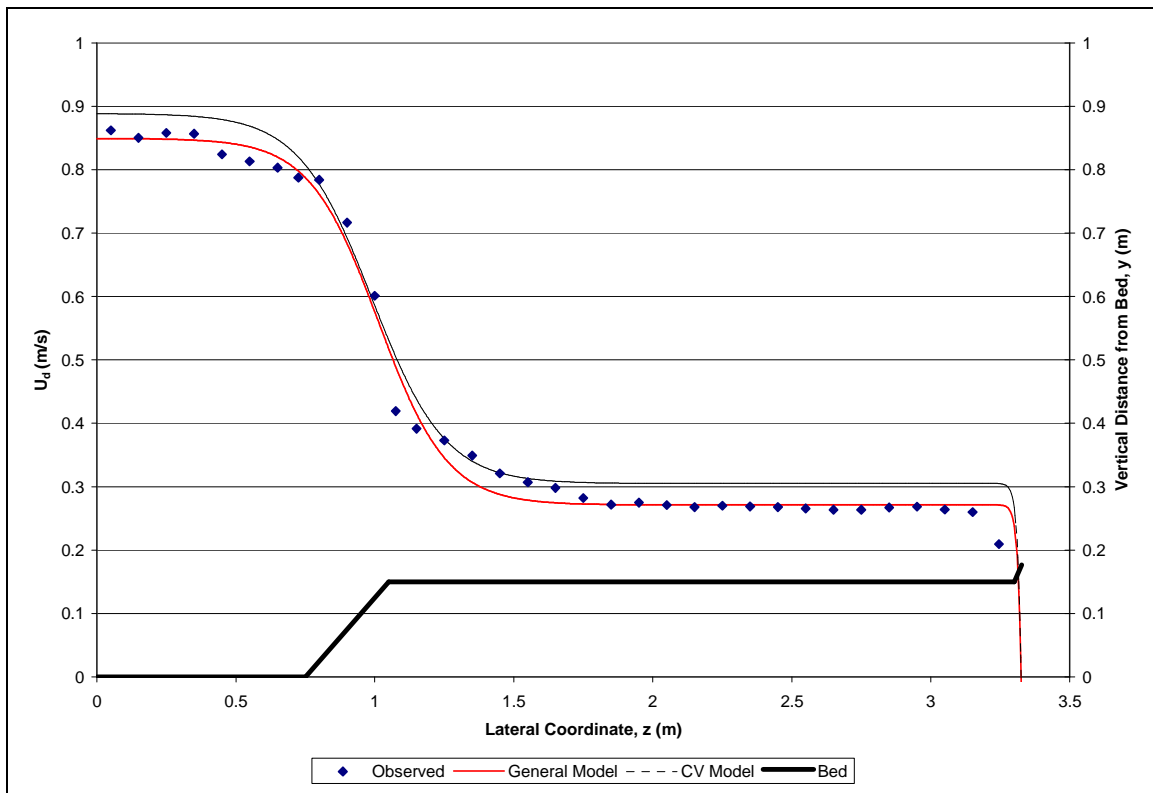


**Figure A.29. Depth-averaged velocity distribution for FCF-100301**

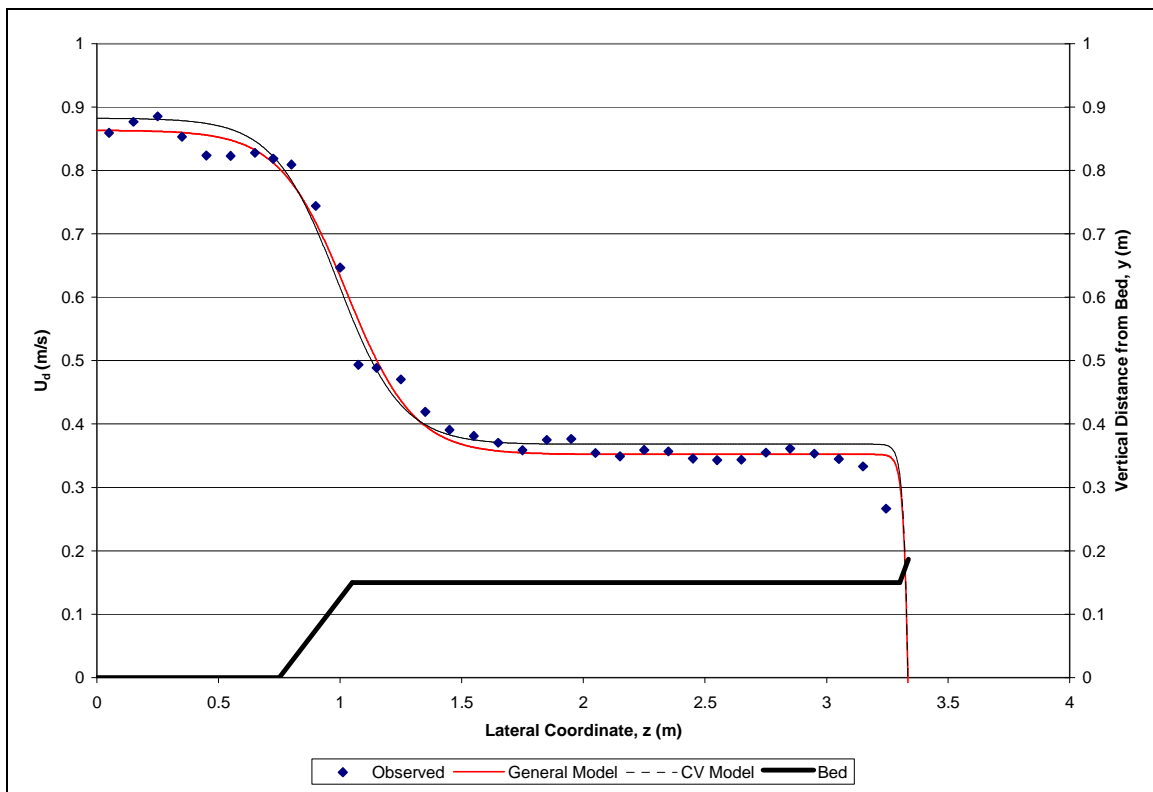


**Figure A.30. Depth-averaged velocity distribution for FCF-100401**



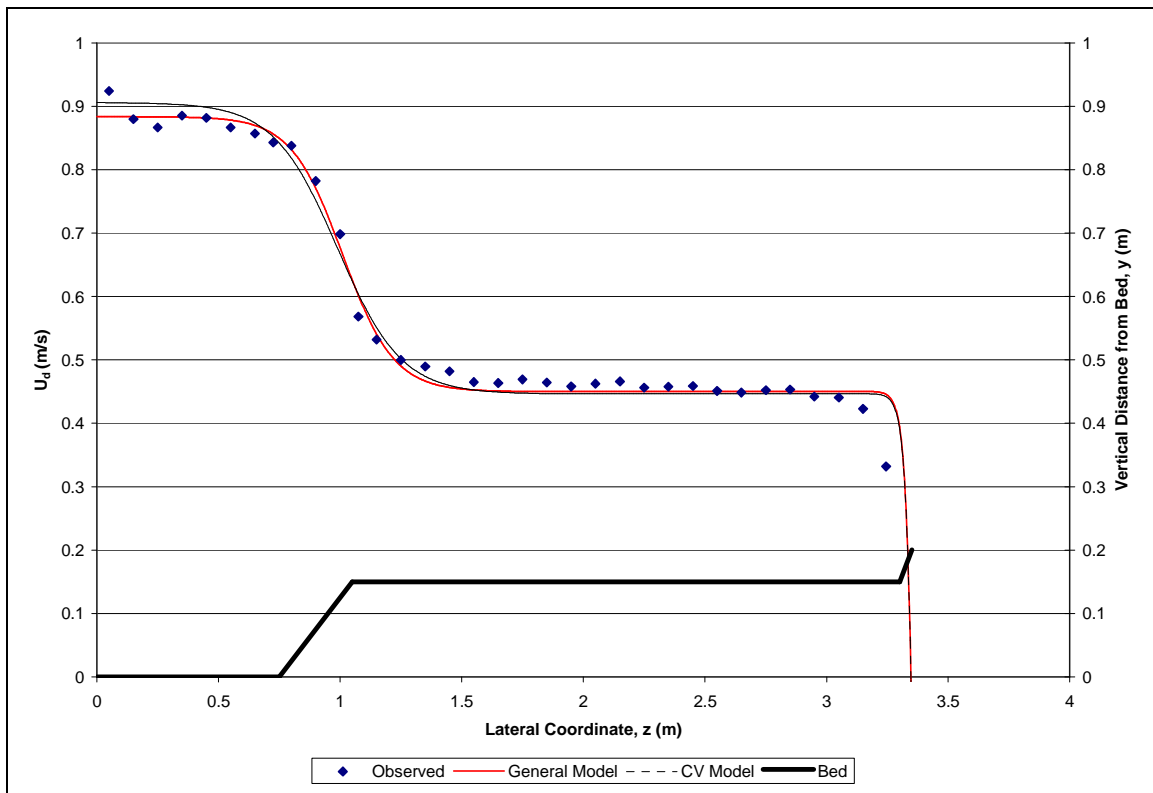


**Figure A.31. Depth-averaged velocity distribution for FCF-100501**

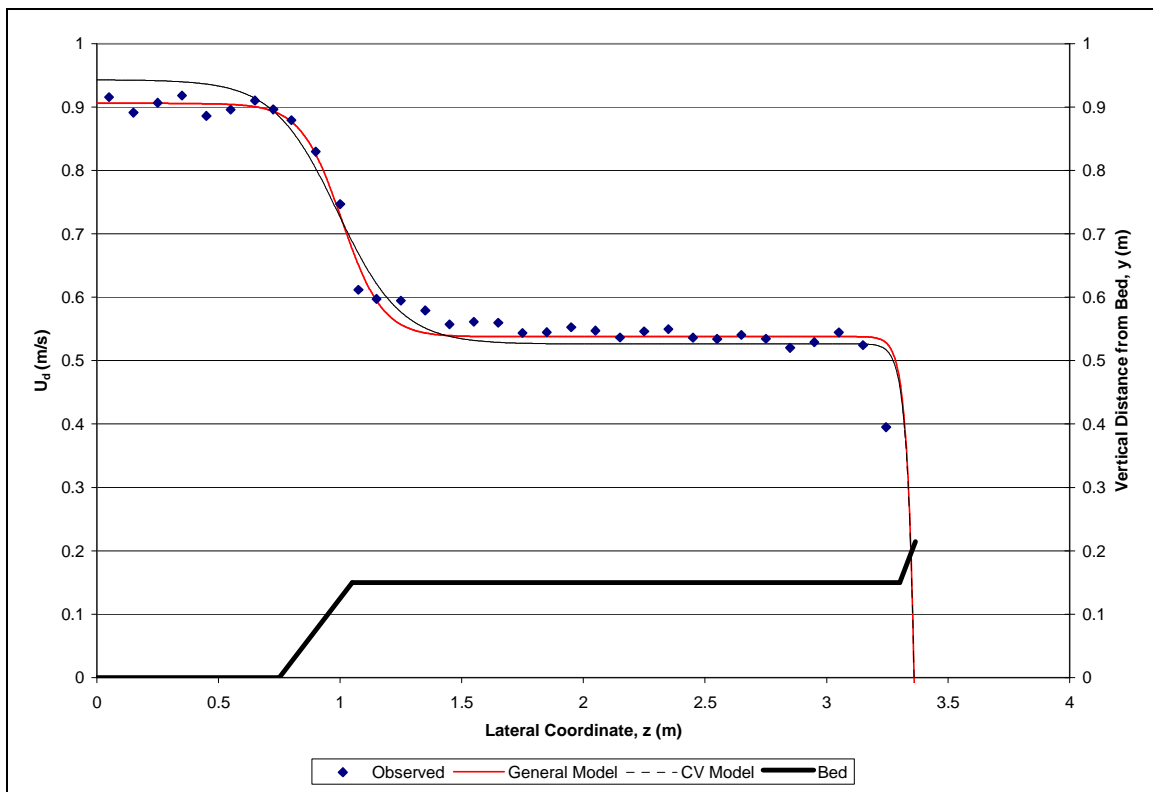


**Figure A.32. Depth-averaged velocity distribution for FCF-100601**

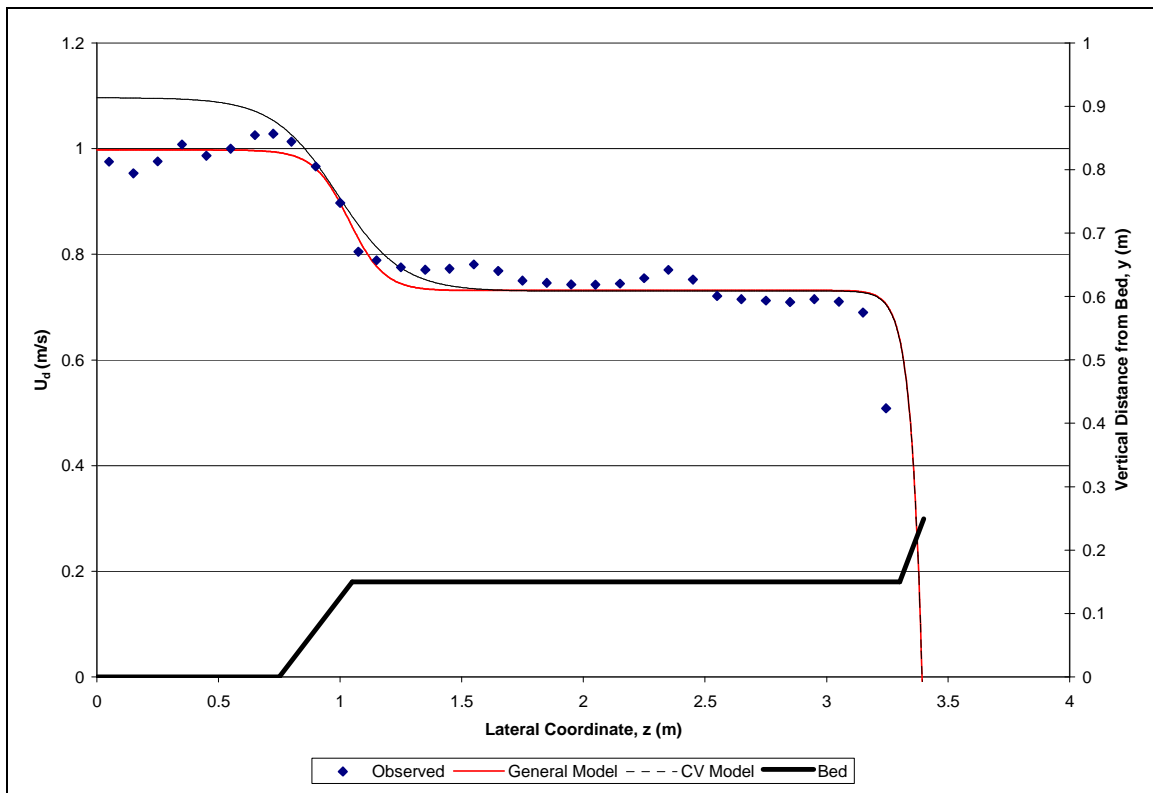


**Figure A.33. Depth-averaged velocity distribution for FCF-100701**

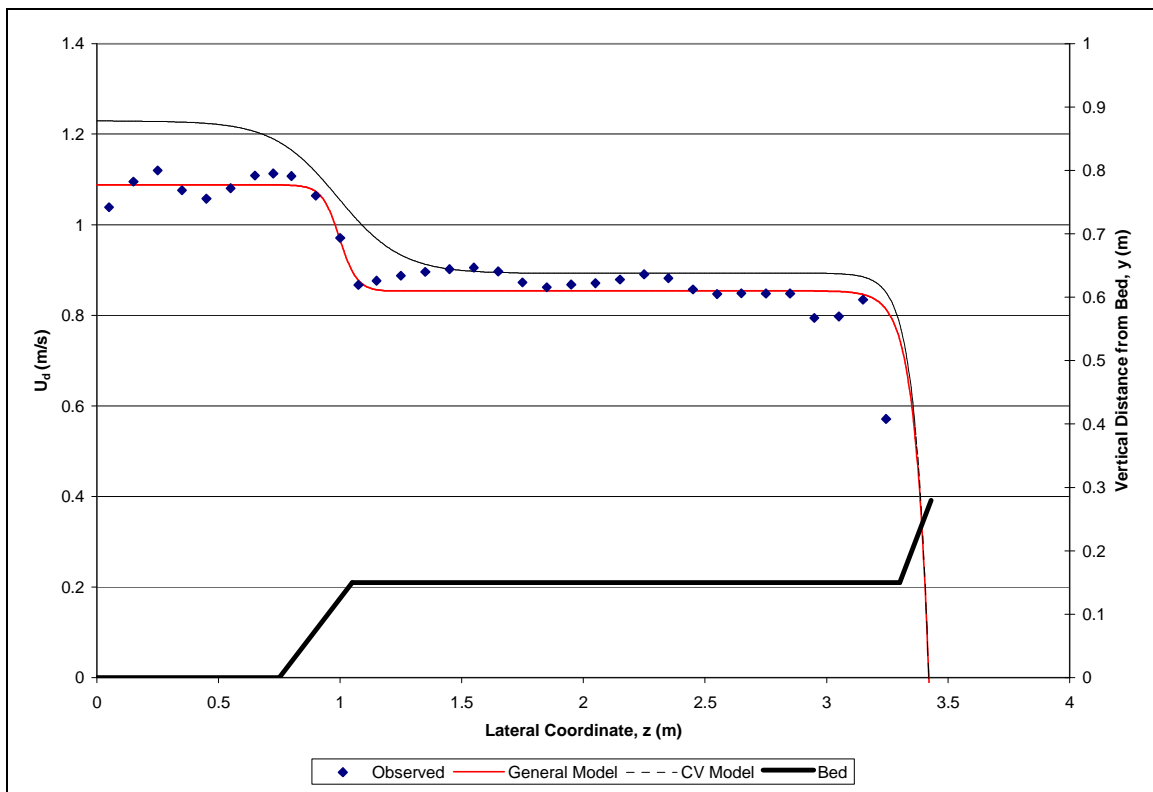


**Figure A.34. Depth-averaged velocity distribution for FCF-100801**

**Table A.2. Depth-averaged velocity distribution statistics for validation data**

Series	Test	Optimized Model Coefficients				Number of Observations	General Model		Continuously Varying Model	
		$a_1$	$a_2$	$a_3$	$a_4$		$R^2$	$s$ (m/s)	$R^2$	$s$ (m/s)
FCF-01	10602	0.492	1.534	15.598	0.811	49	0.972	0.013	0.698	0.067
FCF-02	20402	0.764	1.304	7.597	0.536	35	0.992	0.014	0.990	0.016

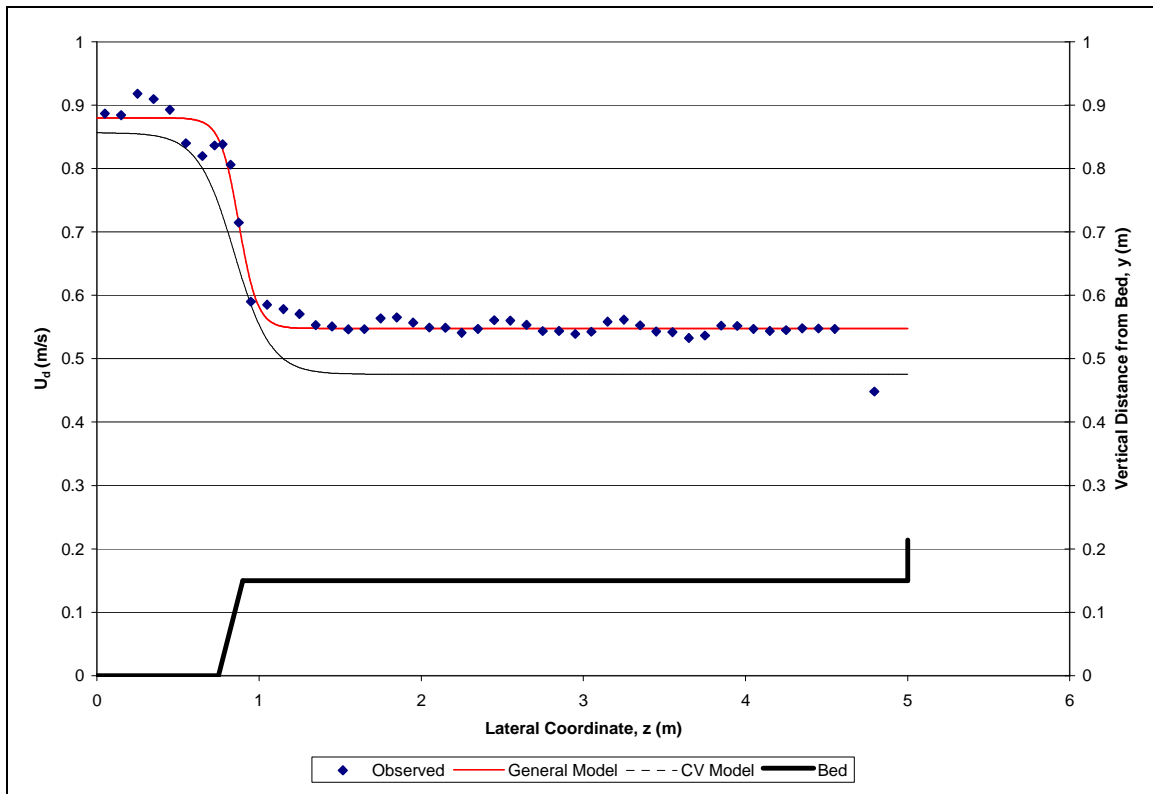


**Figure A.35. Depth-averaged velocity distribution for FCF-010602**

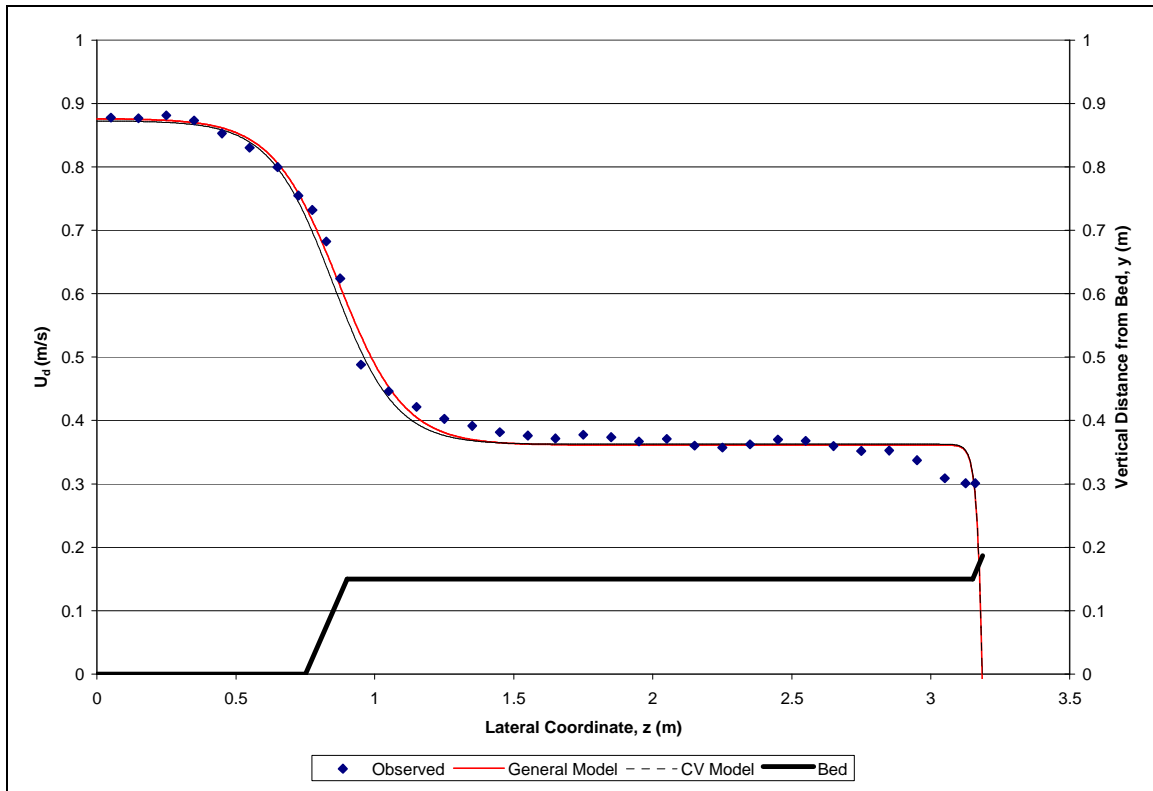


**Figure A.36. Depth-averaged velocity distribution for FCF-020402**